

SYNTHESIS AND CHARACTERIZATION OF WELL-DEFINED DIBLOCK  
COPOLYMERS OF POLY(N-ISOPROPYLACRYLAMIDE) AND POLY(VINYL  
ACETATE)

by

Çimen Özgüç

B.S., Chemistry, Boğaziçi University, 2006

Submitted to the Institute for Graduate Studies in  
Science and Engineering in partial fulfillment of  
the requirements for the degree of  
Master of Science

Graduate Program in Chemistry

Boğaziçi University

2009

*To My Beloved Mother and Father*

## ACKNOWLEDGEMENTS

I would like to express my sincere gratitude to my supervisor Prof. Turgut Nugay for his encouragement and support, for being patient and understanding towards me and for everything that I learned from him related to both chemistry and life.

I would like to thank the members of my committee Prof. İlknur Doğan and Assoc. Prof. Mustafa Demir for giving their valuable time for the reviewing of this thesis and also for their constructive advices.

I am also grateful to Prof. Nihan Nugay for her valuable advices and guidance throughout this project.

I would like to thank Dr. Sinan Şen not only for his help and guidance in terms of AFM and DSC characterizations, but also for his friendship. I would also like to thank Dr. Bilge Gedik Uluocak for ESEM analysis, Dr. Ayla Türkekul and Burcu Selen Çağlayan for NMR analysis and Dr. Mine Memeşa for SEC analysis.

I would especially like to express my gratefulness to my dear friend Görkem Şahin, who never ceased to give her support, friendship and love, even when we were miles away from each other. I would also like to thank my friends in the Chemistry Department, especially to Melis Çağdaş, Burcu Çakır, İlke Uğur, Özgül Gök, Hikmet Karayel, Cem Öztürk and my lab partner Ekmel Helvacıoğlu; also to the most helpful Hülya Metiner and to members of the Chemistry Department.

Finally the greatest thanks go to my mother and father for their love, care and support. I am also grateful to all my dearest friends for standing by me and being so patient with me throughout this extensive work.

This research has been supported by Bogaziçi University (BAP 09B504P)

## ABSTRACT

### **SYNTHESIS AND CHARACTERIZATION OF WELL-DEFINED DIBLOCK COPOLYMERS OF POLY(N-ISOPROPYLACRYLAMIDE) AND POLY(VINYL ACETATE)**

In this study the synthesis of well-defined diblock copolymers of poly(N-isopropylacrylamide) (PNIPAM) and poly(vinyl acetate) (PVA) was performed for the first time by macromolecular design via interchange of xanthates (MADIX) process. In the first stage, methyl (isopropoxycarbonothioyl)sulfanyl acetate (MIPCTSA) was used as chain transfer agent to obtain PVA macro-chain transfer agent. Then, under the same reaction conditions N-isopropylacrylamide (NIPAM) was introduced as the second monomer and block copolymers were synthesized by using PVA macro-chain transfer agent.

Characterizations of the obtained homopolymers and block copolymers were done.  $^1\text{H}$  NMR spectroscopy confirmed the presence of both blocks in the copolymer structure, with the expected composition based on the feed ratio. Kinetic study showed a linear relationship between conversion and reaction time at early stages. Fourier Transform Infrared (FTIR) Spectroscopy showed the characteristic absorptions of both polymer sequences. The Size Exclusion Chromatography (SEC) data were investigated as relative values in spite of the encountered problems. The Differential Scanning Calorimetry (DSC) analysis showed the two glass transition temperature ( $T_g$ ) values belonging to PVA and PNIPAM blocks. The  $T_g$  values were closer to each other with respect to the original values of homopolymers, which indicated that both polymer sequences were well distributed in each other. Scanning Electron Microscopy (ESEM) characterization showed that the composition of the samples influenced the general morphology and density of the block copolymers. Atomic Force Microscopy (AFM) results showed homogeneously distributed phases, which was a very good indication of the block copolymer structure.

## ÖZET

### **POLİ(N-İZOPROPİLAKRİLAMİD) VE POLİ(VİNİL ASETAT) DİBLOK KOPOLİMERLERİNİN SENTEZİ VE KARAKTERİZASYONU**

Bu çalışmada ksantat değişimi yoluyla makromoleküler tasarım (MADIX) yöntemi kullanılarak iyi tanımlanmış poli(vinil asetat) (PVA) ve poli(N-izopropilakrilamid) (PNIPAM) diblok kopolimerlerinin sentezi ilk defa olarak başarıyla gerçekleştirilmiştir. İlk aşamada, zincir transfer ajanı olarak metil (izopropoksikarbonotioyl)sülfanil asetat (MIPCTSA) kullanılması ile PVA macro-zincir transfer ajanı elde edilmiştir. Daha sonra, aynı reaksiyon koşullarında PVA macro-zincir transfer ajanı varlığında N-izopropilakrilamid (NIPAM) ikinci monomer olarak eklenerek blok kopolimerler yapılarına ulaşılmıştır.

Elde edilen homopolimerler ve kopolimerlerin karakterizasyonu yapılmıştır.  $^1\text{H}$  NMR spektroskopisi her iki bloğun da blok kopolimer yapısında başlangıçtaki eklenme oranı üzerinden beklenen kompozisyonlarda mevcut olduğunu teyit edilmiştir. Kinetik çalışması reaksiyon zamanı ve dönüşüm yüzdesinin ilk evrelerde doğru orantılı olduğunu göstermiştir. Fourier Transform Kızılötesi (FTIR) Spektroskopisi her iki polimer bloğuna ait karakteristik pik değerlerini ortaya koymuştur. Karşılaşılan problemlere rağmen Büyüklükçe Ayırma Kromatografisi (SEC) verileri görece değerler olarak elde edilmiştir. Diferansiyel Taramalı Kalorimetre (DSC) analizi kopolimer yapısında PVA ve PNIPAM bloklarına ait iki camsı geçiş sıcaklığı ( $T_g$ ) değerini göstermiştir. Bu  $T_g$  değerlerinin homopolimerlerin her birinin  $T_g$  değerlerine göre birbirine yaklaştığı olması her iki polimer dizisinin de birbiri içerisinde iyi dağılım gösterdiğini belirtmektedir. Taramalı Elektron Mikroskopisi (ESEM) analizi elde edilen örneklerdeki kompozisyonunun blok kopolimerlerin genel yapısını ve yoğunluğunu etkilediğini göstermektedir. Atomik Kuvvet Mikroskopisi (AFM) sonuçlarında blok kopolimer yapısının iyi bir göstergesi olan homojen faz dağılımı gözlenmiştir.

## TABLE OF CONTENTS

ACKNOWLEDGEMENTS. . . . .	iv
ABSTRACT . . . . .	v
ÖZET . . . . .	vi
LIST OF FIGURES . . . . .	x
LIST OF TABLES . . . . .	xiv
LIST OF SYMBOLS/ABBREVIATIONS . . . . .	xv
1. INTRODUCTION . . . . .	1
1.1. Controlled/Living Radical Polymerizations. . . . .	1
1.2. RAFT Polymerization. . . . .	3
1.2.1. Mechanism of RAFT Polymerization . . . . .	4
1.2.2. Chain Transfer Agents . . . . .	7
1.2.3. Effect of the Z Group . . . . .	7
1.2.4. Effect of the R Group . . . . .	8
1.2.5. Xanthate Mediated RAFT Polymerization . . . . .	9
1.2.6. Monomers. . . . .	10
1.3. RAFT Polymerization of NIPAM. . . . .	11
1.4. RAFT Polymerization of Vinyl Acetate . . . . .	19
2. OBJECTIVES . . . . .	27
3. EXPERIMENTAL . . . . .	28
3.1. Vacuum System . . . . .	28
3.2. Vacuum Distillation . . . . .	28
3.3. Transferring Distillates . . . . .	29
3.4. The Reagents . . . . .	29
3.5. Purification of Vinyl Acetate. . . . .	30
3.6. Purification of NIPAM . . . . .	30
3.7. Purification of 1,4-Dioxane . . . . .	31
3.8. Purification of Diethyl Ether . . . . .	31
3.9. Synthesis and Purification of Methyl(Isopropoxycarbonothioyl)sulfanyl Acetate . . . . .	31

3.10. RAFT Polymerization of Vinyl Acetate by Using MIPCTSA as Chain Transfer Agent . . . . .	32
3.11. RAFT Polymerization of NIPAM by Using MIPCTSA as Chain Transfer Agent . . . . .	33
3.12. Block Copolymerization of MIPCTSA End Functionalized PVA with NIPAM . . . . .	33
3.13. Preparation of MIPCTSA End Functionalized PVA Stock Solution . . . . .	35
3.14. Kinetic Study of Block Copolymerization of MIPCTSA End Functionalized PVA with NIPAM. . . . .	36
3.15. Characterization. . . . .	37
4. RESULTS AND DISCUSSION . . . . .	41
4.1. Synthesis and Purification of Methyl(Isopropoxycarbonothioyl)sulfanyl Acetate . . . . .	41
4.2. RAFT Polymerization of Vinyl Acetate by Using MIPCTSA as Chain Transfer Agent. . . . .	45
4.2.1. Synthesis of C-PVA1 . . . . .	45
4.2.2. Synthesis of C-PVA2 . . . . .	46
4.2.3. SEC Analysis of C-PVA1 and C-PVA2 . . . . .	50
4.3. RAFT Polymerization of NIPAM by Using MIPCTSA as Chain Transfer Agent. . . . .	52
4.4. Block Copolymerization of MIPCTSA End Functionalized PVA with NIPAM . . . . .	55
4.4.1. Synthesis of C-AN1. . . . .	55
4.4.2. Synthesis of C-AN2 and C-AN3 . . . . .	60
4.4.2.1. Synthesis of C-AN2.. . . .	60
4.4.2.2. Synthesis of C-AN3.. . . .	60
4.4.3. Synthesis of C-AN4 and C-AN5 . . . . .	63
4.4.4. Synthesis of C-AN6 and C-AN7 . . . . .	66
4.4.4.1. Synthesis of C-AN6.. . . .	66
4.4.4.2. Synthesis of C-AN7.. . . .	66
4.5. Kinetic Study . . . . .	69
4.6. Thermal Characterization . . . . .	71
4.7. Morphological Analysis . . . . .	75

4.7.1. ESEM Analysis. . . . .	75
4.7.2. AFM Analysis . . . . .	77
5. CONCLUSIONS . . . . .	81
REFERENCES . . . . .	83



## LIST OF FIGURES

Figure 1.1.	Architecture and functionality in polymers generated by CLRP [3]. . . . .	2
Figure 1.2.	Proposed general mechanism of RAFT polymerization. . . . .	4
Figure 1.3.	Overall reaction in RAFT polymerization . . . . .	6
Figure 1.4.	General structures of RAFT agents and examples of the different functional groups on the Z positions . . . . .	7
Figure 1.5.	Choice of Z group for RAFT agents . . . . .	8
Figure 1.6.	Choice of R group for RAFT agents. . . . .	9
Figure 1.7.	Xanthate mediated controlled radical polymerization (the MADIX process). . . . .	10
Figure 1.8.	N-Isopropylacrylamide (NIPAM). . . . .	11
Figure 1.9.	Poly(N-Isopropylacrylamide) (PNIPAM) . . . . .	11
Figure 1.10.	Conformation of (a) a compact polymer globule and of (b) a polymer coil. . . . .	12
Figure 1.11.	Possible modes of aggregate formation for PNIPAM- <i>b</i> -PAA in aqueous solution in dependence of pH and temperature. . . . .	13
Figure 1.12.	Synthetic Pathway for the Heterobifunctional Y-Shaped Block Copolymers mPEG-Lys- <i>b</i> -PNIPAM-Biotin. . . . .	15
Figure 1.13.	In Situ Synthesis of BSA-Poly(NIPAM) Conjugate by RAFT Polymerization Using a BSA-macro-RAFT Agent. . . . .	16
Figure 1.14.	Synthetic route for PEO-based block copolymer . . . . .	17

Figure 1.15.	Block Copolymer PNIPAM- <i>b</i> -PMAA Synthesized by RAFT . . . . .	18
Figure 1.16.	Preparation of PNIPAM- <i>b</i> -PVim Diblock Copolymers . . . . .	19
Figure 1.17.	Vinyl acetate (VA) . . . . .	19
Figure 1.18.	Poly(vinyl acetate) (PVA) . . . . .	20
Figure 1.19.	Chain-transfer reaction of thiocarbonyl compounds in RAFT process. .	21
Figure 1.20.	Dithiocarbamate-mediated RAFT polymerization process . . . . .	22
Figure 1.21.	MADIX agents used for the polymerization of VA . . . . .	24
Figure 1.22.	Star-shaped xanthates used as RAFT agent . . . . .	25
Figure 1.23.	Monofunctional and multifunctional xanthates used as RAFT agent . . .	26
Figure 3.1.	Purification of 1,4-dioxane. . . . .	38
Figure 3.2.	Synthesis of MIPCTSA . . . . .	38
Figure 3.3.	C-PVA1 in sealed reactor . . . . .	39
Figure 3.4.	Schlenck type reactor . . . . .	39
Figure 3.5.	C-PVA1 after freeze-dry process . . . . .	40
Figure 3.6.	PVA- <i>b</i> -PNIPAM after freeze-dry process . . . . .	40
Figure 4.1.	Synthesis of MIPCTSA . . . . .	41
Figure 4.2.	<sup>1</sup> H NMR spectrum of MIPCTSA . . . . .	43
Figure 4.3.	<sup>13</sup> C NMR spectrum of MIPCTSA . . . . .	44
Figure 4.4.	Polymerization of vinyl acetate via RAFT process. . . . .	45
Figure 4.5.	<sup>1</sup> H NMR spectrum of C-PVA1 . . . . .	47

Figure 4.6.	FTIR spectrum of C-PVA1 . . . . .	48
Figure 4.7.	$^1\text{H}$ NMR spectrum of C-PVA2 . . . . .	49
Figure 4.8.	SEC curve of C-PVA1 . . . . .	50
Figure 4.9.	SEC curve of C-PVA2 . . . . .	51
Figure 4.10.	Polymerization of NIPAM via RAFT process. . . . .	52
Figure 4.11.	$^1\text{H}$ NMR spectrum of C-PNIPAM. . . . .	53
Figure 4.12.	FTIR spectrum of C-PNIPAM . . . . .	54
Figure 4.13.	Block copolymerization of MIPCTSA end functionalized PVA with NIPAM . . . . .	55
Figure 4.14.	$^1\text{H}$ NMR spectra of C-PVA1 (I), C-PNIPAM (II), C-AN1 (III) . . . .	56
Figure 4.15.	FTIR spectrum of C-AN1 . . . . .	57
Figure 4.16.	SEC curve of C-AN1 . . . . .	59
Figure 4.17.	$^1\text{H}$ NMR spectrum of C-AN2. . . . .	61
Figure 4.18.	$^1\text{H}$ NMR spectrum of C-AN3. . . . .	62
Figure 4.19.	SEC curve of C-AN4 . . . . .	64
Figure 4.20.	SEC curve of C-AN5 . . . . .	64
Figure 4.21.	$^1\text{H}$ NMR spectrum of C-AN6. . . . .	67
Figure 4.22.	$^1\text{H}$ NMR spectrum of C-AN7. . . . .	68
Figure 4.23.	Variation of conversion as function of time. . . . .	70
Figure 4.24.	DSC curves of C-AN1, C-PNIPAM and C-PVA . . . . .	73

Figure 4.25.	DSC curves of (1 PVA:1 PNIPAM), (2 PVA:1 PNIPAM) and (1 PVA:2 PNIPAM) . . . . .	74
Figure 4.26.	High magnification SEM images of (a) C-AN2, (b) C-AN1 and (c) C-AN3. . . . .	76
Figure 4.27.	Proposed model for morphologies of polymer samples . . . . .	78
Figure 4.28.	AFM wave images of (a) C-AN2, (b) C-AN1 and (c) C-AN3 . . . . .	79
Figure 4.29.	AFM phase images of (a) C-AN2, (b) C-AN1 and (c) C-AN3 . . . . .	80

## LIST OF TABLES

Table 1.1.	Dithiocarbamates used as RAFT agent for the polymerization of VA. . .	23
Table 3.1.	Properties of reagents used in all experiments. . . . .	30
Table 3.2.	Block copolymerization of MIPCTSA end functionalized PVA with NIPAM. . . . .	34
Table 3.3.	Kinetic study of block copolymerization of MIPCTSA end functionalized PNIPAM with vinyl acetate . . . . .	36
Table 4.1.	SEC analysis data of C-PVA1 and C-PVA2 . . . . .	50
Table 4.2.	SEC analysis data of C-AN1 . . . . .	59
Table 4.3.	The ratio of CTA and initiator . . . . .	63
Table 4.4.	SEC analysis data of C-AN4 and C-AN5. . . . .	65
Table 4.5.	Variation of conversion as function of time. . . . .	69
Table 4.6.	Glass transition temperatures of obtained polymers . . . . .	71
Table 4.7.	Composition of samples for morphological analysis . . . . .	75

## LIST OF SYMBOLS/ABBREVIATIONS

Bp	Boiling Point
DP <sub>n</sub>	Degree of Polymerization
g	Gram
h	Hour
k <sub>add</sub>	Rate of Addition
k <sub>-add</sub>	Rate of Fragmentation
k <sub>β</sub>	Rate of Fragmentation
k <sub>-β</sub>	Rate of Addition
k <sub>i</sub>	Rate of Initiation
k <sub>p</sub>	Rate of Propagation
k <sub>re-in</sub>	Rate of Re-initiation
k <sub>tc</sub>	Rate Termination by Combination
k <sub>tp</sub>	Rate of Termination by Disproportionation
min	Minute
ml	Millilitre
μm	Micrometer
mmHg	Millimeter of Mercury
M <sub>n</sub>	Number Average Molecular Weight
M <sub>p</sub>	Melting Point
M <sub>w</sub>	Weight Average Molecular Weight
M <sub>w</sub> /M <sub>n</sub>	Polydispersity Index
MW	Molecular Weight
T <sub>c</sub>	Critical Temperature
T <sub>g</sub>	Glass Transition Temperature
v	Volume

AFM	Atomic Force Microscopy
AIBN	2,2'-azoisobutyronitrile

ATRP	Atom Transfer Radical Polymerization
-b-	Block copolymer
Biotin-BMCC	1-biotinamido-4-[4'-(maleimidomethyl) cyclohexanecarboxamido] butane
BSA	Bovine serum albumin
CDCl <sub>3</sub>	Deuterated chloroform
CLRP	Controlled/Living Radical Polymerization
CTA	Chain Transfer Agent
DSC	Differential Scanning Calorimetry
DMF	N,N-dimethylformamide
DMP	2-Dodecylsulfanylthiocarbonylsulfanyl-2-methyl propionic acid
EA	Ethyl acrylate
ESEM	Scanning Electron Microscope
ESR	Electron Spin Resonance
FTIR	Fourier Transform Infrared Spectroscopy
LCST	Lower Critical Solution Temperature
Lys	L-Lysine
MADIX	Macromolecular Design via Interchange of Xanthates
MIPCTSA	Methyl(Isopropoxycarbonothioyl)sulfanyl acetate
NIPAM	N-Isopropylacrylamide
NMP	Nitroxide Mediated Polymerization
NMR	Nuclear Magnetic Resonance Spectroscopy
PAA	Poly(acrylic acid)
PEG	Poly(ethylene glycol)
PEO	Poly(ethylene oxide)
PMAA	Poly(methacrylic acid)
PNIPAM	Poly(N-Isopropylacrylamide)
PVA	Poly(vinyl acetate)
PVAL	Poly(vinyl alcohol)
PVim	Poly(N-vinylimidazole)
RAFT	Reversible Addition-Fragmentation Chain Transfer
SEC	Size Exclusion Chromatography

THF	Tetrahydrofuran
St	Styrene
VA	Vinyl acetate
Vim	N-vinylimidazole



## 1. INTRODUCTION

### 1.1. Controlled/Living Radical Polymerizations

Controlled/Living Radical Polymerization (CLRP) is one of the most rapidly developed areas of polymer science. The advantages of this technique over the conventional free radical polymerization could be regarded to be the reason of its increased popularity throughout the years.

Conventional free radical polymerization has been a very important commercial process for preparing high molecular weight polymers, since it could be used for the polymerization of many vinyl monomers under mild reaction conditions and over a wide temperature range. In addition, copolymerization of many monomers could be conducted via a radical route. However, the conventional radical systems have important limitations concerning the control of chain architecture, composition, end functionality, molecular weight and polydispersity. Anionic and cationic living polymerization processes could be applied to obtain well-defined polymers with controlled structural properties. However, the monomers that are suitable for the ionic living polymerizations are limited and the reaction conditions are rather strict. Thus, emergence of CLRP has enabled the generation of well-defined architectures in polymers with relatively mild reaction conditions. CLRPs offer a possible solution to synthesizing distinctive homo and copolymers on a large scale economically [1, 2].

General features of CLRPs include the following:

- Pseudo-first order kinetics
- Linear evolution of the number average molecular weight with conversion
- Narrow molecular weight polydispersities,  $M_w/M_n$
- Ability of the chains to grow after the initial monomer charge is exhausted

One of the most important and appealing properties of CLRP systems is their ability to continue adding monomer units, which enables the structural design of the polymers. Because of the ability of the dormant chains to add additional monomer units, CLRPs allow the relatively facile synthesis of copolymers, by addition of a second monomer after the charge of the first monomer has been exhausted. This presents the possibility of synthesizing a broad range of architectures with different chemical and material properties [2], as shown in Figure 1.1.

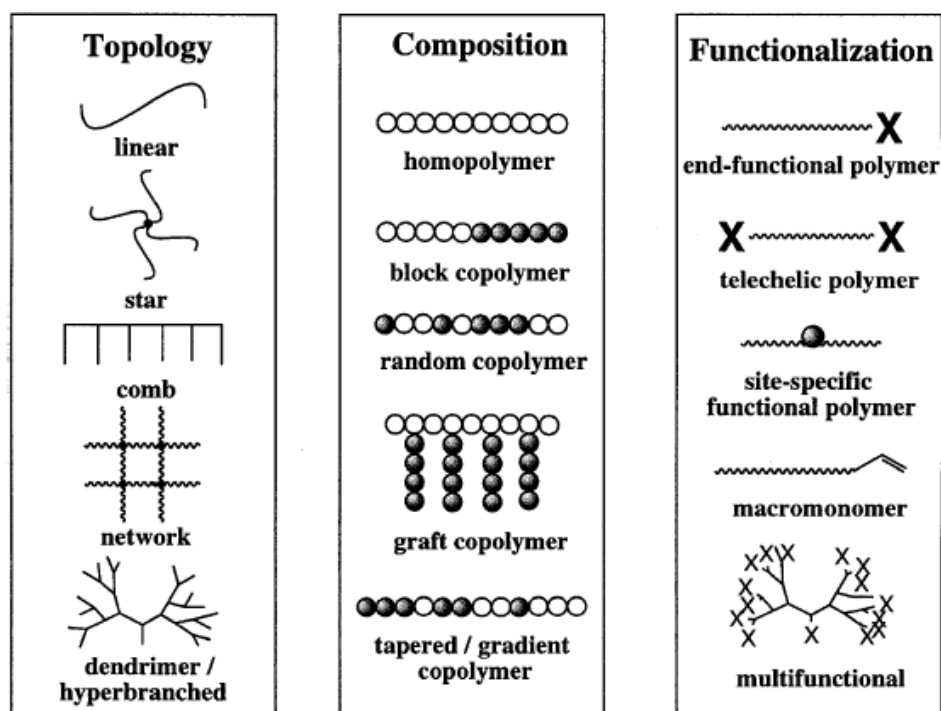


Figure 1.1. Architecture and functionality in polymers generated by CLRP [3]

CLRPs can be listed as the following:

- Nitroxide mediated polymerization
- Atom transfer radical polymerization
- Degenerative transfer
  - Reversible addition-fragmentation chain transfer (RAFT) process
  - Macromolecular design via interchange of xanthates (MADIX)
  - (Reversible) Iodine transfer polymerization [(R)ITP]
  - Initiator-transfer agent-terminator (Iniferter) process

Among the CLRP methods, reversible addition-fragmentation chain transfer (RAFT) polymerization is the most commonly used technique for producing living polymers via reversible transfer [4].

## 1.2. RAFT Polymerization

Recently, the synthesis of polymers via reversible addition-fragmentation chain transfer (RAFT) polymerization has gained importance due to its great versatility, its compatibility with a wide range of monomers, the control on the molecular weights and the low polydispersities of the synthesized polymers [5]. It also offers all advantages of a conventional free radical polymerization; e.g. the same range of temperatures, monomers, initiators, and solvents can be applied [6, 7]. The polymerization is carried out in the presence of thiocarbonylthio compounds of general structure  $Z-C(=S)-S-R$  that act as reversible addition-fragmentation chain transfer agents and results in the formation of end-functionalized polymers [8].

The process is performed by adding a suitable chain transfer agent to an otherwise conventional free radical polymerization mixture, and it provides living polymers of predetermined molecular weight and of narrow polydispersity (usually  $M_w/M_n < 1.2$ ) [5].

RAFT process consists of the introduction of a small amount of dithioester (1) (Figure 1.2) [4] as chain transfer agent (CTA) in a conventional free-radical system, which contains monomer and initiator. The transfer of the CTA between growing radical chains, present at a very low concentration, and dormant polymeric chains, present at a higher concentration, will control the growth of the molecular weight and limit the termination reactions.

### 1.2.1. Mechanism of RAFT Polymerization

The mechanism of RAFT polymerization, as it is generally accepted, is shown in Figure 1.2 [4, 6, 9, 10].

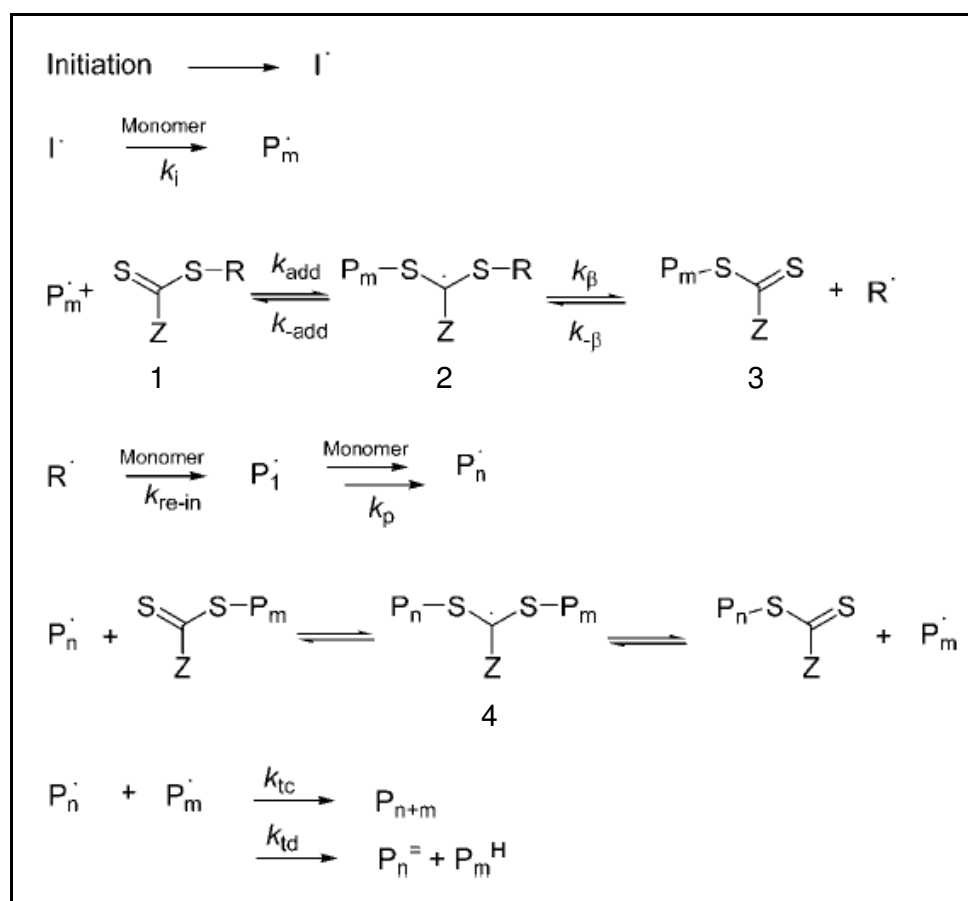


Figure 1.2. Proposed general mechanism of RAFT polymerization

The radical species formed by the decomposition of the radical initiator reacts with the monomer ( $k_i$ ). This growing polymer chain rapidly adds to the reactive C=S bond of the CTA (1) ( $k_{add}$ ) to form a radical intermediate (2) (Figure 1.2). The radical initiator may add directly onto the CTA, before reacting with any monomer. The fragmentation of the intermediate occurs reversibly either toward the initial growing chain ( $k_{add}$ ) or to free the re-initiating group (R) and a macro chain-transfer agent (macro-CTA; 3) ( $k_{\beta}$ ) (Figure 1.2). The R group may react back on the macro-CTA ( $k_{\beta}$ ). On the other hand, re-initiation may

take place by the reaction of the R group with the monomer ( $k_{\text{re-in}}$ ), which would start the propagation of a new polymer chain ( $k_p$ ). Once the initial CTA has been entirely consumed, only the macro-CTA agent is present in the reaction medium. The macro-CTA then enters the main equilibrium to give the intermediate radical (4) (Figure 1.2). A rapid exchange between active and dormant chains, the latter being capped with the thiocarbonylthio compound, ensures equal probability for all chains to grow. As a result, the production of polymers with narrow molecular weight distribution is accomplished.

The Commonwealth Scientific and Industrial Research Organization (CSIRO) group observed the intermediate radicals (2) and (4) (Figure 1.2) for the first time via electron spin resonance (ESR) [11] and their presence have since been confirmed by many other research groups [11-15].

A variety of side reactions may take place during polymerization due to the involvement of radical intermediates, which includes termination with a propagating polymeric chain. There are unavoidable reactions of termination present in all free-radical polymerizations, which take place by either combination ( $k_{tc}$ ) or disproportionation ( $k_{td}$ ). However, as the termination reactions are kept to a minimum, the final product consists of a large majority of polymeric chains showing the re-initiating group (R) at one end and the thiocarbonylthio group at the other.

The mechanism of RAFT differs from mechanisms of atom transfer radical polymerization (ATRP) or nitroxide mediated polymerization (NMP), which are in the form of monomolecular reactions of reversible radical capping. In the RAFT system, the chain growth is based on bimolecular reactions consisting of the cooperative chain transfer between polymeric chains.

The degenerative chain transfer is triggered by the source of radicals, which enables the growth of polymeric chains. An increase in the radical concentration will increase the rate of polymerization. However, this will also increase the probability of chain termination, which leads the formation of polymers with higher polydispersities [4].

The majority of the polymeric chains are initiated by the CTA re-initiating group (R group) and terminated by the thiocarbonylthio group (Figure 1.3) [4].

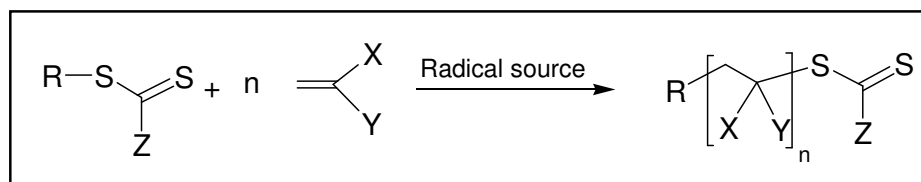


Figure 1.3. Overall reaction in RAFT polymerization

The molecular weight increases linearly with conversion. If it is assumed that all CTAs have reacted and if the chains initiated by the source of radicals are neglected, the molecular weight can be predicted by Equation 1.1.

$$M_{n,\text{theo}} = \frac{[\text{Monomer}]}{[\text{CTA}]} \times \text{FW(M)} \times c + \text{FW(CTA)} \quad (1.1)$$

Here  $M_{n,\text{theo}}$  is the theoretical number average molecular weight; [Monomer] and [CTA] are the concentrations of the monomer and CTA, respectively; FW(M) and FW(CTA) are the monomer and CTA formula weights, respectively; and c is the fractional conversion [4].

### 1.2.2. Chain Transfer Agents

CTAs can be categorized into four classes, depending on their activating Z group (Figure 1.4) [4]: dithioesters, xanthates, trithiocarbonates and dithiocarbamates.

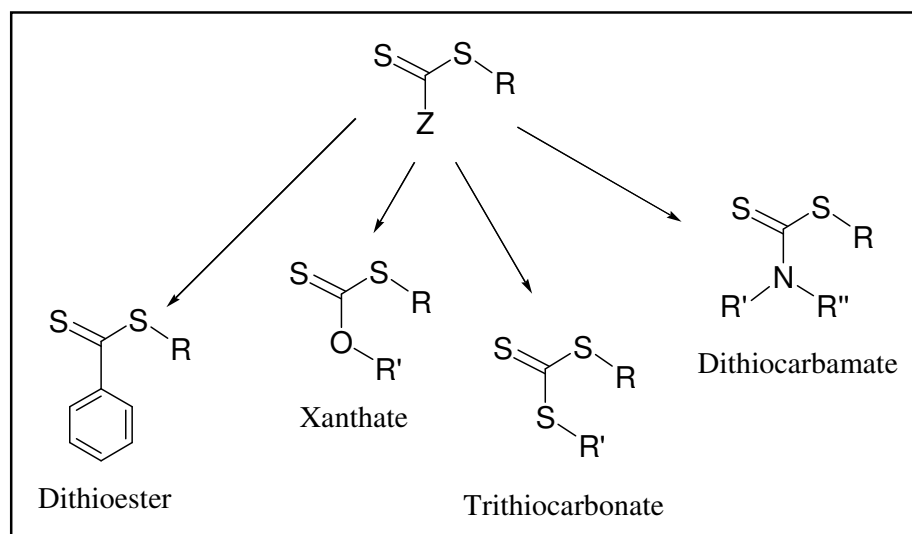


Figure 1.4. General structures of RAFT agents and examples of the different functional groups on the Z positions

### 1.2.3. Effect of the Z Group

The stability of the thiocarbonylthio radical intermediate, (8) and (10) (Figure 1.2), is strongly influenced by the Z group (Figure 1.3) [4]. Therefore, strong stabilizing groups will favor the formation of the intermediate and as a result enhance the reactivity of the  $\text{C}=\text{S}$  bond toward radical addition. However, the stability of the intermediate should be finely tuned, so that its fragmentation will also be favored and hence the reinitiating group ( $\text{R}\cdot$ ) will be freed [16]. The effect of the Z group on the polymerization of a variety of monomers have been studied by several groups [7, 17-20].

A general classification of Z groups that allow good control over the majority of monomers is as follows:

dithiobenzoates > trithiocarbonates ~ dithioalkanoates > dithiocarbamates (where the nonbonded electron pair on N is conjugated with another electron-withdrawing group) > xanthates > dithiocarbamates.

The polymerization of methacryloyl derivatives is better controlled by dithiobenzoates, whereas the polymerization of vinyl acetate and derivatives is better controlled by xanthates. Experimental data [7, 17-19, 20-22] and *ab initio* calculations [23] provide the following guideline (Figure 1.5) [4] for the selection of a CTA Z group:

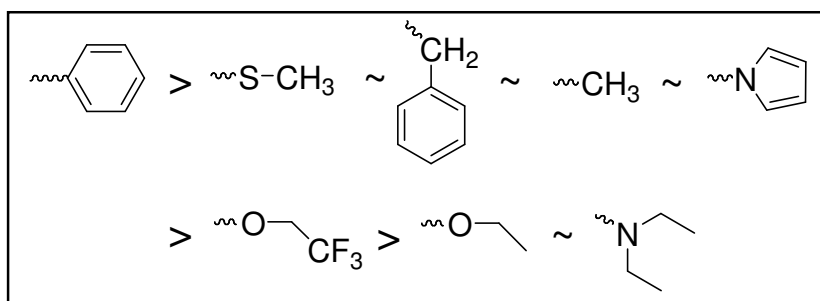


Figure 1.5. Choice of Z group for RAFT agents

#### 1.2.4. Effect of the R Group

The R group (Figure 1.3) [4] must be a good leaving group with respect to the growing polymeric chain and a good re-initiating species toward the monomer that is used. It also contributes toward the stabilization of the radical intermediate, although the stabilization is mainly provided by the Z group. When choosing an appropriate R group, parameters such as the stability of the expelled radical, steric bulk and polarity need to be considered. Previous studies have shown the importance of this group when monomers are polymerized with a high rate of propagation [5, 24-26].



Experimental data and *ab initio* calculations [23] suggest the following guideline [Figure 1.6] for R group selection for a CTA [4]:

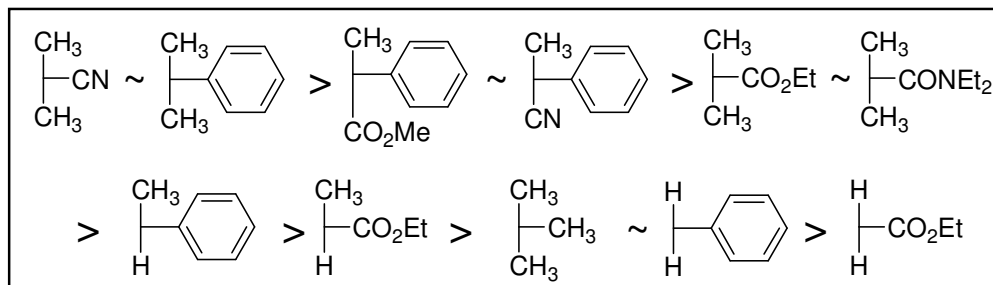


Figure 1.6. Choice of R group for RAFT agents

### 1.2.5. Xanthate Mediated RAFT Polymerization

The xanthate mediated reversible addition fragmentation polymerization has been termed MADIX (macromolecular design via interchange of xanthates) by its inventors [18, 27]. When the reaction mechanisms are considered, the RAFT and MADIX processes are identical (Figure 1.7). However, MADIX solely refers to the use of xanthates, whereas RAFT is used for thiocarbonylthio compounds  $Z-C(=S)-S-R$  in general.

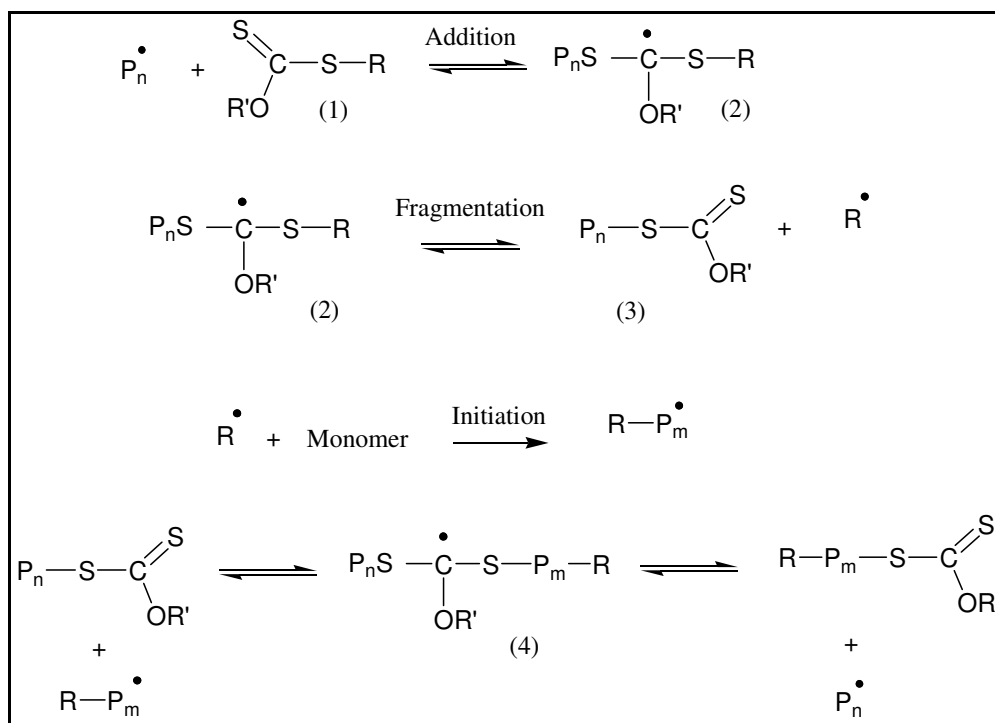


Figure 1.7. Xanthate mediated controlled radical polymerization (the MADIX process)

Highly reactive propagating radical species such as the vinyl acetate radical have a tendency to add swiftly to activated double bonds, such as the carbon-sulfur double bonds of RAFT agents. As a result the addition products or the macro-RAFT radicals (2) and (4) (Figure 1.7) will be relatively stable and the tendency to fragment will be small [27]. Two strategies could be taken into account in order to enable the fragmentation process: destabilizing the intermediate radical center (2) and increasing the stability of RAFT agent species (3) (Figure 1.7). In order to fulfill these criteria, different RAFT agents may be designed by varying the R or Z groups, as discussed in section 1.2.3 and also to obtain linear and predictable evolution of molecular weight and polydispersity index, PDI, by the polymerization process.

### 1.2.6. Monomers

The RAFT process has been applied successfully to all the monomers used in conventional free radical polymerization [4].

### 1.3. RAFT Polymerization of NIPAM

N-Isopropylacrylamide (NIPAM) is an extremely important nonionic acrylamido monomer, which is soluble in water (Figure 1.8). Due to many fascinating properties exhibited by its polymer, NIPAM has been the subject of intensive research over the years [28-39].

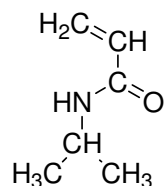


Figure 1.8. N-Isopropylacrylamide (NIPAM)

Poly(N-Isopropylacrylamide) (PNIPAM) (Figure 1.9) displays a coil-to-globule transition (Figure 1.10) [29] at 32 °C in water, which is defined as the lower critical solution temperature (LCST). This property is considered to be due to a balance of hydrogen bonding and hydrophobic interactions influencing polymer-solvent and polymer-polymer interactions [30].

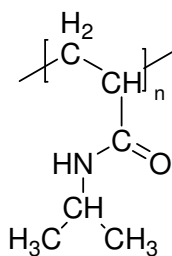


Figure 1.9. Poly(N-Isopropylacrylamide) (PNIPAM)

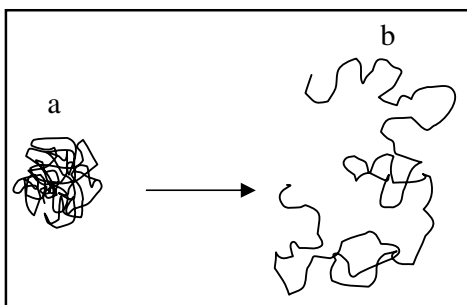


Figure 1.10. Conformation of (a) a compact polymer globule and of (b) a polymer coil

Below the LCST, the amide functionality of the molecule enables the absorption of water molecules via hydrogen bonding, which provides water solubility and surface activity. However, the hydrogen bonds are broken as the temperature is raised above the LCST and the interaction between NIPAM units becomes stronger. As a result, the polymer expels water molecules and undergoes a coil-to-globule transition, thereby precipitating to form particles [31].

The thermoresponsive behavior of PNIPAM has applications in fields such as surface modification, drug delivery, reaction catalysis, stabilization and functionalization of metal nanoparticles [32-39]. Many studies have been done concerning the effect of copolymerization of NIPAM with suitable comonomers.

The traditional way of preparing NIPAM copolymers by free radical polymerization leads to polymers with high polydispersity and with poorly defined end-group chemistries. These disadvantages limit the possibility of synthesizing well-defined and also end-functionalized block copolymers that may be used in further applications. High polydispersity is also undesirable due to its influence on the varying results regarding the effect of chain length on the LCST of PNIPAM [32].

Reversible addition-fragmentation chain transfer (RAFT) polymerization is an exceptionally versatile tool for the synthesis of polymers of narrow molecular weight distributions. This technique has created new possibilities for the synthesis of various NIPAM copolymers and the incorporation of different monomers has been investigated in many studies.

Copolymerization with a pH-sensitive comonomer yields NIPAM copolymers in which the phase transition can be triggered by a change in the pH at specific temperature [33, 34].

Schilli et al. [33] synthesized poly(N-isopropylacrylamide)-b-poly(acrylic acid) (PNIPAM-b-PAA) by RAFT polymerization, for the first time, with low polydispersity. The block copolymerization was performed using poly(acrylic acid) as a macromolecular chain transfer agent.

The solubility of the PAA block in aqueous solutions depends on the pH of the medium. Therefore, the combination of pH-responsive poly(acrylic acid) (PAA) and thermoresponsive poly(N-isopropylacrylamide) (PNIPAM) in a block copolymer leads to a system that responds to both pH and temperature. As a result, the double-responsive block copolymers form micelles in aqueous solutions depending on these two variables (Figure 1.11) [33].

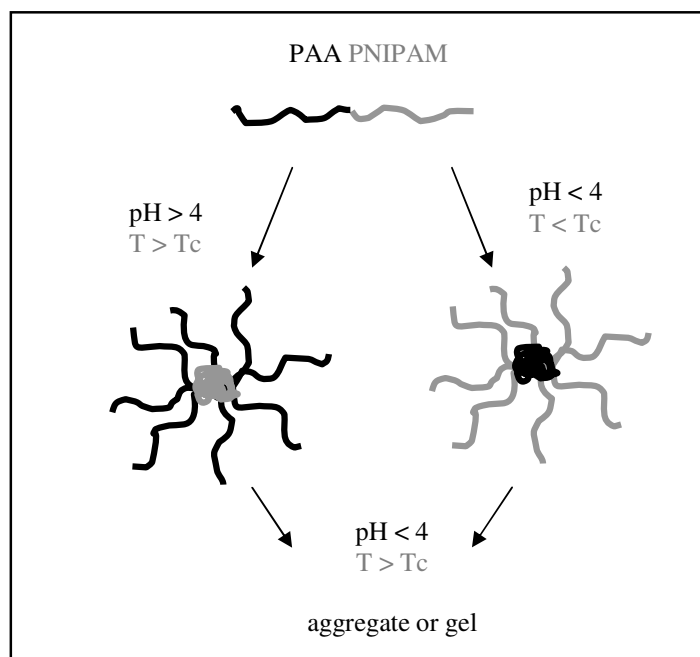


Figure 1.11. Possible modes of aggregate formation for PNIPAM-b-PAA in aqueous solution in dependence of pH and temperature.

PNIPAM has been investigated also for biomedical applications owing to the fact that its LCST is close to human body temperature (37 °C), which can be further tuned by variation in comonomer content. Many studies have been done concerning protein conjugation and preparation of delivery systems for drugs and genes [32, 35, 36].

You et al. [32] synthesized Y-shaped heterobifunctional block copolymers of poly(ethylene glycol) (PEG) and poly(N-isopropylacrylamide) (PNIPAM) by RAFT polymerization of NIPAM using a macromolecular trithiocarbonate PEG-based chain transfer agent (Figure 1.12).

The synthesized block copolymers contained a carboxylic acid group from L-lysine at the focal point, which enables the attachment of these copolymers to the surfaces of particles and a variety of substrates. The trithiocarbonate functionality at the terminus of the PNIPAM block was converted into a thiol group and used for conjugation of biotin, also known as vitamin H or B<sub>7</sub>.

The copolymers showed temperature-dependent association behavior in aqueous solution with a phase transition of 32 °C, which gives rise to the possibility of usage in a variety of biomedical applications in which stimulus-controlled presentation of ligands is desired [32].

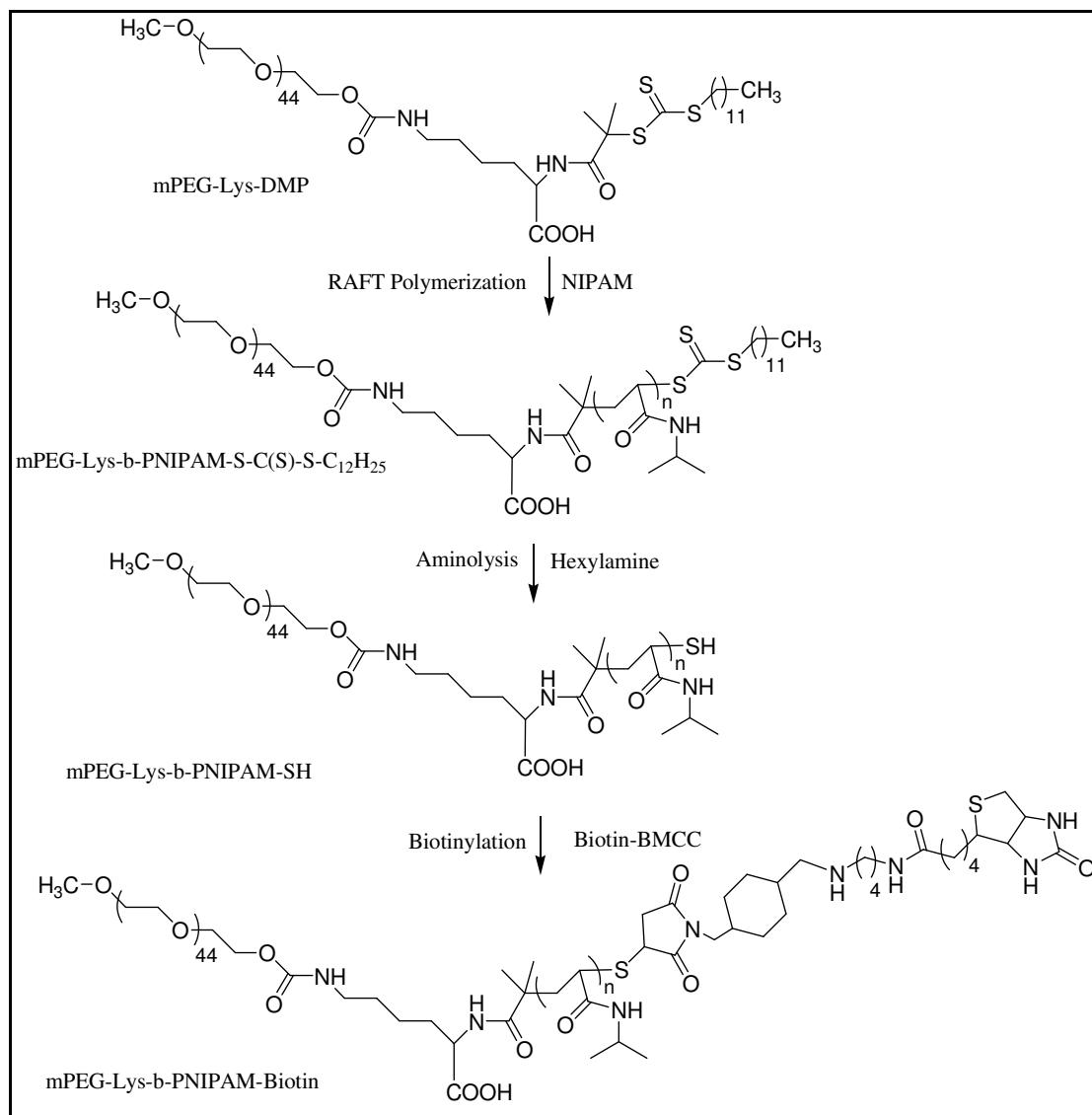


Figure 1.12. Synthetic Pathway for the Heterobifunctional Y-Shaped Block Copolymers mPEG-Lys-b-PNIPAM-Biotin

Boyer et al. [35] reported the in situ synthesis of protein-polymer conjugates via RAFT polymerization process. A water soluble RAFT agent was conjugated to a model protein, bovine serum albumin (BSA). The obtained BSA-macro-RAFT agent was then used to control the polymerization of NIPAM (Figure 1.13). BSA-poly(NIPAM) conjugates showed hybrid temperature-dependent phase separation and aggregation behavior. The lower critical solution temperature values of the conjugates were found to

increase with the decrease in molecular weight of poly(NIPAM) block conjugated to BSA [35].

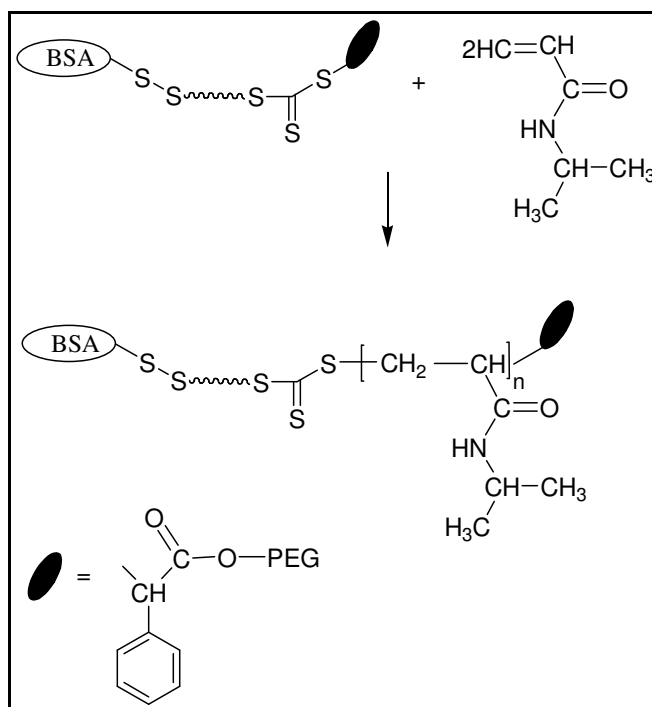


Figure 1.13. In Situ Synthesis of BSA-Poly(NIPAM) Conjugate by RAFT Polymerization Using a BSA-macro-RAFT Agent

The thermoresponsive behavior of PNIPAM has further applications in the functionalization of metal nanoparticles. In this field of research, especially gold nanoparticles have attracted great interest during the past decade due to their various potential applications as biomedical, electronic, and optical materials as well as in catalysis. Recently, environmentally responsive polymers which show different behaviors as a result of changes in temperature or pH have also been used to stabilize gold nanoparticles. [37, 38]

Jeon et al. [37] reported the synthesis of amphiphilic block copolymers by RAFT polymerization of N-isopropylacrylamide (NIPAM) using poly(ethylene oxide) (PEO)-based xanthate-type of RAFT agent (Figure 1.14).



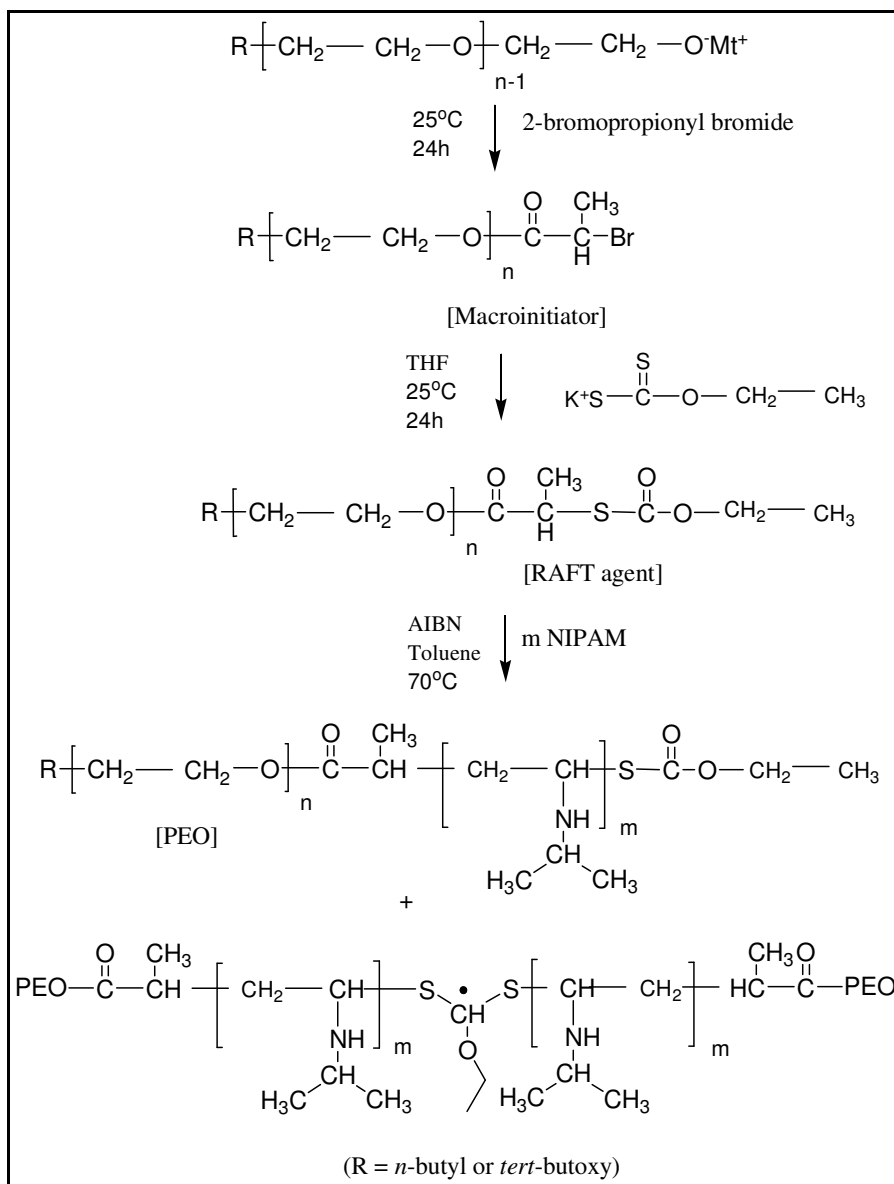


Figure 1.14. Synthetic route for PEO-based block copolymer

The different molecular weights of the poly(*N*-isopropylacrylamide) (PNIPAM) fragments of poly(ethylene oxide-*b*-*N*-isopropylacrylamide) had an important role to exhibit different thermoresponsive behaviors. The resulting block copolymers were used as polymeric stabilizers to prepare water-soluble nano-sized gold particles [37].

In another study, Nuopponen et al. [38] prepared gold nanoparticles protected with poly(methacrylic acid)-b-poly(N-isopropylacrylamide) (PMAA-b-PNIPAM) (Figure 1.15), which was synthesized using the RAFT technique.

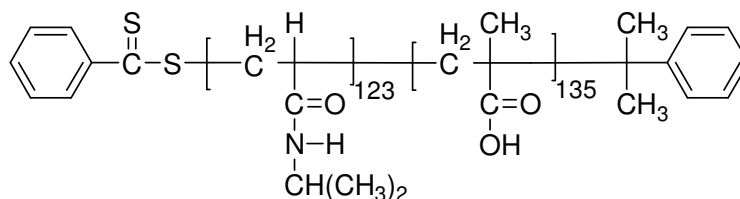


Figure 1.15. Block Copolymer PNIPAM-b-PMAA Synthesized by RAFT Polymerization [19]

The gold nanoparticles were coated with block copolymers, with the thermosensitive PNIPAM block bound to the particle surface and pH-sensitive PMAA as an outer block form stimuli-sensitive aggregates in water. Block copolymers made it possible to protect particles in a way that the outer layer colloidally stabilizes the aggregates while the inner layer modulates the polarity of the immediate surroundings of the gold core [38].

The incorporation of PNIPAM in polymer catalyst systems has also been investigated. Ge et al. [39] synthesized well-defined diblock copolymers of poly(N-isopropylacrylamide)-b-poly(N-vinylimidazole) (PNIPAM-b-PVim) via RAFT process.

PVim is well-known to be able to catalyze esterolysis reactions. In order to obtain the target diblock copolymers, first NIPAM was polymerized by using a xanthate based RAFT agent and the obtained polymer was then employed as the polymeric macro-chain transfer agent for the polymerization of N-vinylimidazole (Vim) (Figure 1.16) [39].

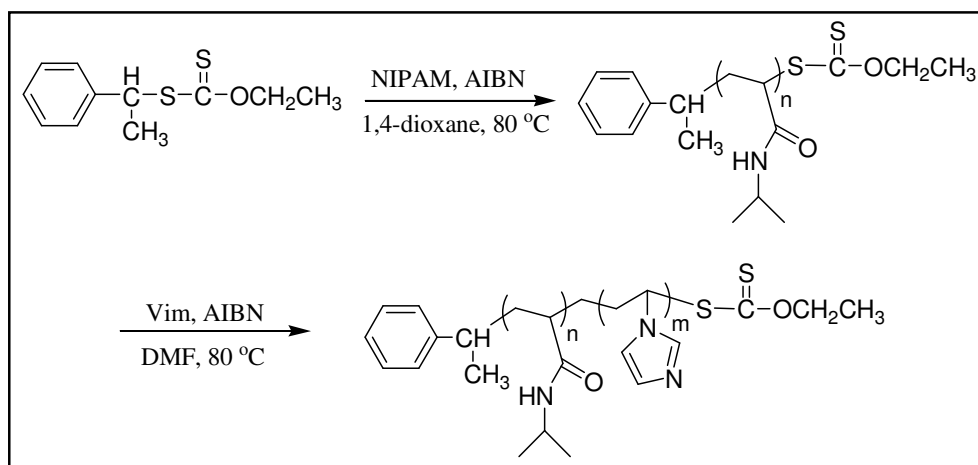


Figure 1.16. Preparation of PNIPAM-b-PVim Diblock Copolymers

The imidazole-containing diblock copolymers molecularly dissolved at low temperatures in water, but at elevated temperatures above the phase transition temperature of PNIPAM block or in a proper mixture of methanol/water, PNIPAM block became hydrophobic and stable micelles formed with a dense core consisting of hydrophobic PNIPAM block and a polar shell formed by PVim block. It was observed that double hydrophilic block copolymer micelles of PNIPAM-b-PVim could serve as self-catalyzing nanoreactors. Moreover, the catalytic activities were determined to be tunable with external temperatures or solvent compositions [39].

#### 1.4. RAFT Polymerization of Vinyl Acetate

Vinyl acetate (VA) is a highly important monomer (Figure 1.17) and its polymers have application areas ranging from adhesives, paints, concrete additives to pharmaceuticals [40].

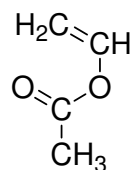


Figure 1.17. Vinyl acetate (VA)

Another major property of this monomer is that partial or complete hydrolysis of poly(vinyl acetate) (PVA) (Figure 1.18) is used as a precursor to poly(vinyl alcohol) (PVAL), which makes the controlled polymerization of VA extremely desirable [40].

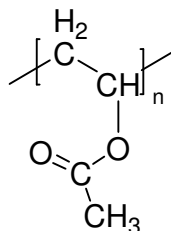


Figure 1.18. Poly(vinyl acetate) (PVA)

Vinyl acetate is one of the most important monomers that can be polymerized only via a radical mechanism. The lack of a conjugating substituent in the structure of VA, which creates a difference from monomers like acrylates and styrene, causes the propagating radical of VA to be highly reactive and, in other words, less stable. This radical tends to undergo chain transfer and termination reactions in particular. This mostly results in products showing broad molecular distributions and a poor control of chain end functionality, the latter preventing the synthesis of block copolymers [41].

Throughout the years, several attempts have been done in order to determine a suitable technique to perform the polymerization of VA, which would enable control over the process and lead to the formation of well defined products. The polymerization has been proved to be difficult to control via NMP and ATRP or using standard dithioester RAFT agents [42].

In the case of RAFT process, the standard dithioesters actually inhibit polymerization. It is thought that, since the vinyl acetate propagating radical is a poor homolytic leaving group, the fragmentation of the RAFT-adduct radical (3) is thus very slow (Figure 1.19) [42].

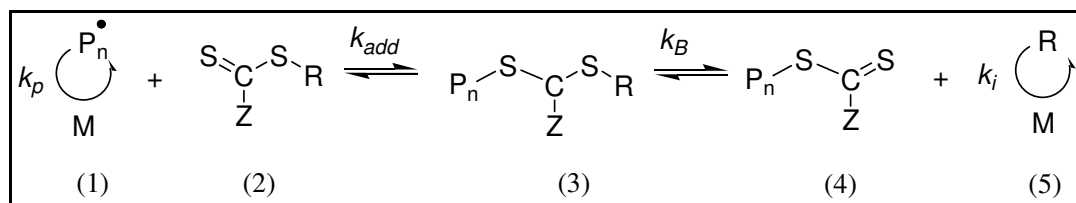


Figure 1.19. Chain-transfer reaction of thiocarbonyl compounds in RAFT process

However, controlled polymerization of VA has been achieved using either dithiocarbamates or xanthates as RAFT agents [17, 40, 43]. It has been suggested that dithiocarbamates and xanthates are successful because they increase the electron density at the radical center (i.e. the intermediate macro RAFT radical), which causes the destabilization of the RAFT adduct radical relative to normal dithioester substituents, such as methyl and phenyl. As a result, the fragmentation rate increases [40, 42]. The electron-donating OR and NR<sub>2</sub> substituents as the Z group are also thought to stabilize the thiocarbonyl product (4) of fragmentation (Figure 1.19) [42] through their conjugation with the C=S double bond [18, 19].

Destarac et al. [17] worked on N,N-disubstituted and cyclic dithiocarbamates to show the effect of the nature of the substituents on the control of the polymerization of VA, ethyl acrylate (EA) and styrene (St).

It was reported that, for a thiocarbonylthio compound to be a good RAFT agent, the following criteria must be fulfilled: firstly, the rate of addition to the C=S double bond and fragmentation of the intermediate radical B (Figure 1.20) must be rapid relative to propagation. Secondly, the expelled radical (R•) must be capable of reinitiating polymerization, preferably with a rate at least equal to that of propagation to avoid retardation [7, 17].

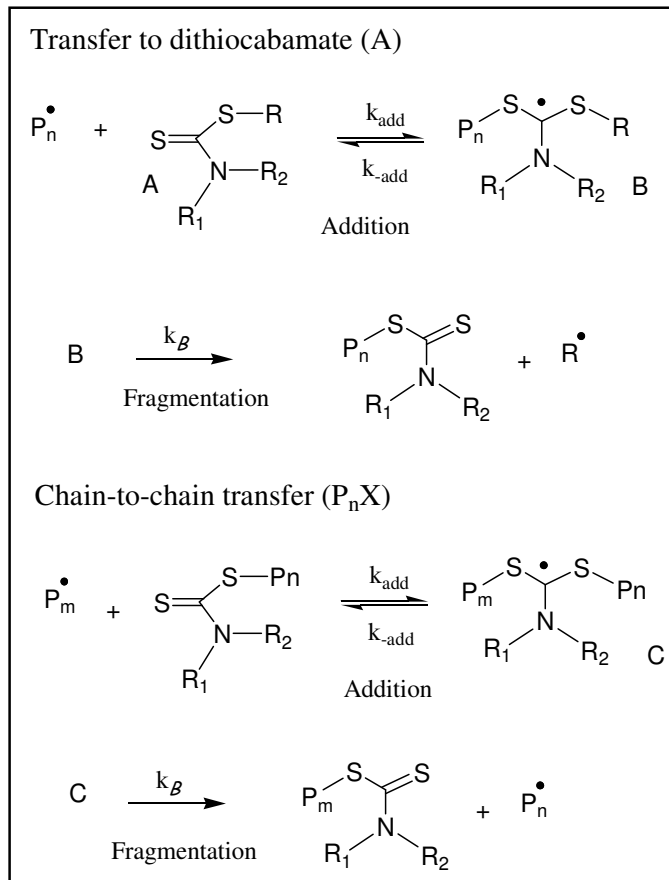
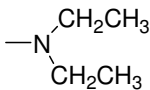
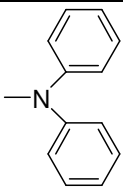
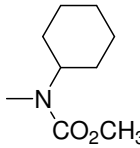
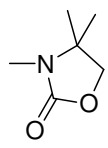


Figure 1.20. Dithiocarbamate-mediated RAFT polymerization process

The research showed that, unlike dithioesters, dithiocarbamates do control the polymerization of vinyl acetate (VA). The results indicated that dithiocarbamates A<sub>1</sub> and A<sub>3</sub> (Table 1.1) [17] which are known to be relatively inert towards styrene and methacrylates were efficient RAFT agents in the case of VA. On the other hand, the most active dithiocarbamates, A<sub>5</sub> and A<sub>10</sub> (Table 1.1), of the series for St and EA strongly retardate polymerization. It was explained that for the latter case, the intermediate radical C (Figure 1.20) is more stabilized than the ones derived from A<sub>1</sub> and A<sub>3</sub>, which causes its fragmentation to be more difficult.

Table 1.1. Dithiocarbamates used as RAFT agent for the polymerization of VA

$\begin{array}{c} \text{S}-\text{R} \\ \diagup \\ \text{S}=\text{C} \\ \diagdown \\ \text{R}' \end{array}$				
	A <sub>1</sub>	A <sub>3</sub>	A <sub>5</sub>	A <sub>10</sub>
R	(CH <sub>3</sub> CH <sub>2</sub> O <sub>2</sub> C) <sub>2</sub> HC	(CH <sub>3</sub> CH <sub>2</sub> O <sub>2</sub> C) <sub>2</sub> HC	(CH <sub>3</sub> CH <sub>2</sub> O <sub>2</sub> C) <sub>2</sub> HC	(CH <sub>3</sub> CH <sub>2</sub> O <sub>2</sub> C) <sub>2</sub> HC
R'				

Another important point was that; in order to favor the transfer reaction, the lone pair of electrons of the nitrogen atom must be conjugated with carbonyl or aromatic groups. This feature shows the importance of the effect of the nature of the substituents on the control of polymerization, especially for VA [17].

Stenzel et al. worked on xanthates for the RAFT polymerization of VA [40]. In the mentioned study, eight different xanthates (Figure 1.21) were synthesized in order to examine the influence of the Z-group on the kinetics of MADIX agent mediated VA bulk polymerization.

Of the eight MADIX agents investigated (Figure 1.21) [40], D to G were found to be suitable for the successful living polymerization of vinyl acetate. The MADIX agent H did not allow any polymerization to proceed and showed total inhibition. The intermediate radicals, (2) and (4) (Figure 1.7), generated by the MADIX agents A to C were relatively stable and thus did not allow effective fragmentation, making the main equilibrium too slow to compete with the relatively fast VA radical propagation. On the other hand, the intermediate radicals formed by the compounds D, E, F and G performed fragmentation fast enough because of their relative instability, which enabled an effective reversible addition fragmentation reaction.

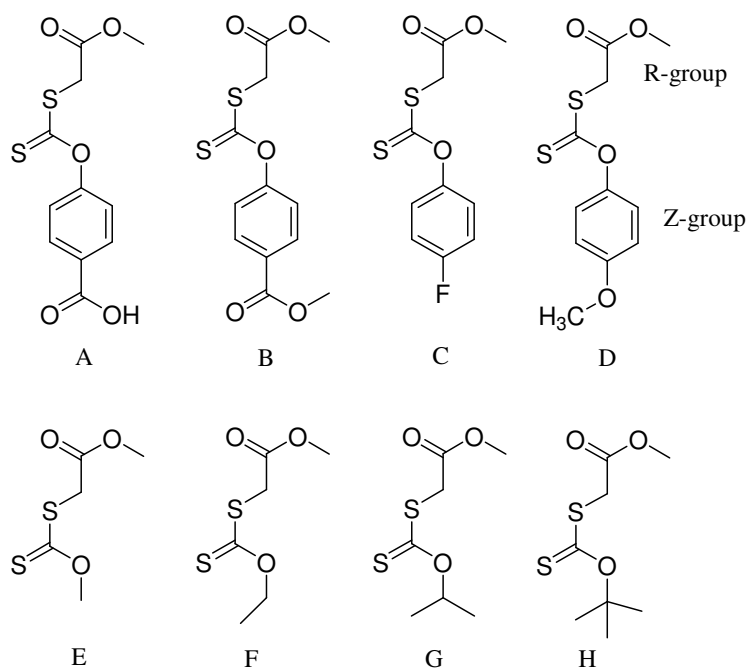


Figure 1.21. MADIX agents used for the polymerization of VA

These MADIX agents; methyl(4-methoxyphenoxy)carbonothioylsulfanyl acetate D, methyl(methoxycarbonothioyl)sulfanyl acetate E, ethyl(ethoxycarbonothioyl)sulfanyl acetate F, methyl(isopropoxycarbonothioyl)sulfanyl acetate G yielded very good molecular weight control and low polydispersities. The ability of these compounds to control VA polymerization can be correlated with the electron density on the central carbon atom of the xanthate. The observed inhibition times and moderate rate retardation may be attributed to slow fragmentation of the intermediate RAFT radicals, (2) and (4) (Figure 1.7), in possible conjunction with termination processes [40].

Boschmann et al. [44] designed three novel tetra-functional xanthate based RAFT agents for the synthesis of poly(vinyl acetate) and poly(vinyl propionate) star polymers (Figure 1.22). The agents were designed to contain the stabilizing Z group at the core and the influence of the leaving R-group on the control that is exerted on polymerization was investigated.



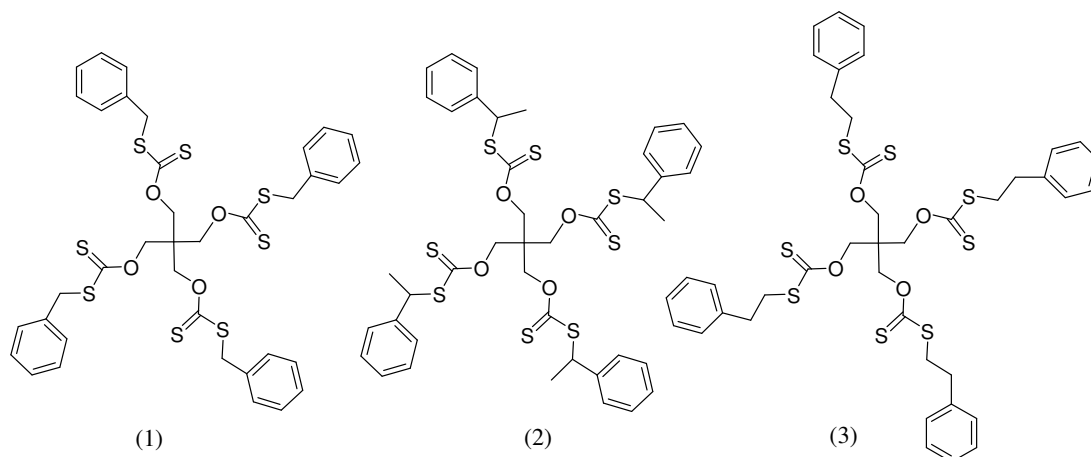


Figure 1.22. Star-shaped xanthates used as RAFT agent

The results showed that destabilization of the expelled leaving group radical in (3) (Figure 1.22) [44], a 2-phenyl ethyl leaving group, did not induce any control in VA polymerization. When RAFT agent (2) (Figure 1.22) was used, total inhibition up to ten hours of reaction time with no polymer production was observed. This was explained by the decreased reinitiation ability of the more stable 1-phenyl ethyl radical, as the leaving R group of (2), toward the relatively unreactive VA monomer. However, employment of RAFT agent (1) (Figure 1.22), tetrakis(benzyl-sulfanyl-carbothioyl-oxymethyl)methane, lead to a successful polymerization process, with control over molecular weight and relatively narrow polydispersities, depending on the concentration of the initial RAFT agent [44].

In another study, Fleet et al. [45] prepared new multiarmed (MADIX)/RAFT agents for VA polymerization. The chain transfer ability of the five synthesized agents to induce living characteristics in free radical polymerization of vinyl acetate was investigated with respect to molar mass control and kinetic behavior.

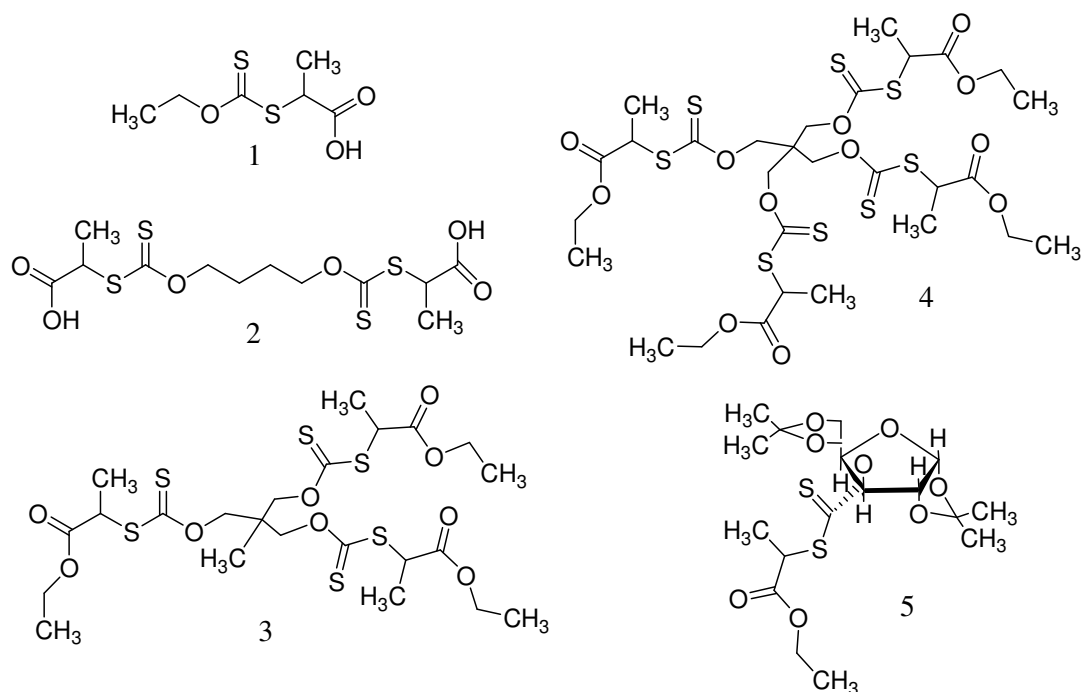


Figure 1.23. Monofunctional and multifunctional xanthates used as RAFT agent

These five compounds (Figure 1.23) [45], S-sec propionic acid O-ethyl xanthate 1, 1,4 di(S-sec propionic acid xanthate) butane 2, 1,1,1 tri(S-sec ethyl propionoate O-methylene xanthate) ethane 3, 1,1,1,1 tetra(S-sec ethyl propionoate O-methylene xanthate) methane 4 and 1,2:5,6-Di-Oisopropylidene- α-D-glucofuranose -3 -(S-sec ethyl propionoate) xanthate 5 were identified as suitable MADIX/RAFT agents, yielding linear and star shaped polyvinyl acetate with low polydispersities.

## **2. OBJECTIVES**

The aim of this study is to synthesize well-defined diblock copolymers of poly(N-isopropylacrylamide) and poly(vinyl acetate) via MADIX process and to perform spectroscopic, thermal and morphological characterizations.

### **3. EXPERIMENTAL**

#### **3.1. Vacuum System**

All synthesis reactions were carried out in a system which is totally isolated from the external atmosphere. The vacuum system is equipped with a pump that is capable of reducing the pressure to  $10^{-3}$  mmHg. Additionally, nitrogen gas is used in order to create an inert atmosphere for the reactions. Since nitrogen gas might be containing impurities such as oxygen, water vapor and peroxides; it is passed through traps containing molecular sieves and active materials like calcium hydride in order to prevent possible undesired effects on the reactions.

#### **3.2. Vacuum Distillation**

The vacuum distillation apparatus is connected to the main vacuum line with the pressure decreasing to  $10^{-3}$  mmHg. This process provides fresh and highly pure distillate in a relatively shorter period of time.

Initially, the vacuum apparatus is evacuated and the glassware is flamed. This is done before any material is added inside in order to remove moisture that might be present on the inner surface of the glass. Nitrogen gas is introduced into the system after the glassware cools down. The material to be purified is transferred into the system via syringe or capillary technique. Prior to distillation, the round bottom flask containing the impure material is immersed into liquid nitrogen for cooling and then evacuated. Then the part where the distillate will be collected is flamed again and the system is evacuated again until bubbling is observed. This step is carried out several times in order to recover any evaporated material by condensing it back and also to remove nitrogen dissolved inside. Then the collection flask is immersed into a Dewar cup filled with liquid nitrogen in order to create a pressure difference between the two parts which will enable the distillation process. The distillate is collected on the glass surface of the collection flask in solid state. The vacuum distillation is completed with the introduction of nitrogen gas to the system.

### 3.3. Transferring Distillates

Capillary technique is used for the transfer of liquid reagents and mainly distillates. The steel capillary to be used is flamed under nitrogen gas flow before transfer process in order to remove impurities that might be present in it. During the process, one end of the capillary is connected to the flask containing the material to be transferred and with nitrogen gas flowing inside; the other end is inserted into a previously evacuated and nitrogen gas filled flask. When the capillary is plunged into the liquid material, the pressure difference between the flasks enables the transfer of the material through the capillary. At the end of transfer process, the material is kept under nitrogen atmosphere.

### 3.4. The Reagents

All the reagents used in the experiments are listed in Table 3.1.

Potassium hydroxide, 2-propanol, carbon disulfide, methyl bromoacetate, n-hexane, ethyl acetate, methanol and benzene were used as received without purification.

The initiator, 2,2'-azobisisobutyronitrile (AIBN), was recrystallized from methanol.

Table 3.1. Properties of reagents used in all experiments

Name	Formula	MW (g/mol)	Supplier	Bp (°C)	Density (g/ml)
Potassium hydroxide	KOH	56.11	Merck	Mp:360	2.04
2-propanol	C <sub>3</sub> H <sub>8</sub> O	60.10	Merck	82	0.785
Carbon disulfide	CS <sub>2</sub>	76.14	Allied Chemical	46	1.260
Methyl bromoacetate	C <sub>3</sub> H <sub>5</sub> BrO <sub>2</sub>	152.98	Acros	51	1.616
Vinyl acetate	C <sub>4</sub> H <sub>6</sub> O <sub>2</sub>	86.09	Merck	72	0.934
AIBN	C <sub>8</sub> H <sub>12</sub> N <sub>4</sub>	164.21	Acros	Mp:99	-
n-Hexane	C <sub>6</sub> H <sub>14</sub>	86.18	Merck	69	0.652
Ethyl acetate	C <sub>4</sub> H <sub>8</sub> O <sub>2</sub>	86.105	Merck	77	0.857
Methanol	CH <sub>3</sub> OH	32.04	Merck	65	0.791
NIPAM	C <sub>6</sub> H <sub>11</sub> NO	113.16	Acros	Mp:62	0.877
Benzene	C <sub>6</sub> H <sub>6</sub>	78.11	Merck	80	0.874
1,4-Dioxane	C <sub>4</sub> H <sub>8</sub> O <sub>2</sub>	88.11	Merck	100	1.034
Diethyl ether	C <sub>4</sub> H <sub>10</sub> O	74.12	Merck	34.6	0.706

### 3.5. Purification of Vinyl Acetate

Vinyl acetate was filtered before utilization through a column of basic aluminum oxide. The yellow liquid collected was further purified by vacuum distillation procedure in section 3.2.

### 3.6. Purification of NIPAM

NIPAM was purified by recrystallization from a mixture of benzene and n-hexane (3/7, v/v).

### 3.7. Purification of 1,4-Dioxane

The required amount of 1,4-dioxane was transferred into the distillation apparatus. Then, two teaspoons of solid benzophenone and a few peaces of sodium metal were added and the mixture was stirred with magnetic stirrer. In sufficient time, sodium metal reacts with benzophenone and forms a complex that acts as a water and oxygen scavenger. The formation of persistent dark blue color indicates purification (Figure 3.1). The solution was stirred and vacuum distillation procedure (3.2) was followed. During the process, distillation was aided by warming the reactor part of the apparatus by hair dryer machine.

### 3.8. Purification of Diethyl Ether

The required amount of diethyl ether was transferred into distillation apparatus. Then, two teaspoons of solid benzophenone and a few peaces of sodium metal were added. The mixture was stirred with magnetic stirrer to allow sodium metal to react with benzophenone and form a complex that acts as a water and oxygen scavenger. The flask was heated and ether was allowed to reflux for a period of time. Afterwards it was distilled and collected in a separate flask.

### 3.9. Synthesis and Purification of Methyl(Isopropoxycarbonothioyl)sulfanyl Acetate

A 100 ml round bottom flask equipped with a magnetic stirrer was previously evacuated, flamed and then filled with nitrogen gas. 2.84 g of potassium hydroxide ( $5 \times 10^{-2}$  mol) and 20 ml of 2-propanol was transferred into the reactor. The system was evacuated and recharged with nitrogen gas. The mixture was stirred and occasionally heated with hair dryer. The reaction was carried out for 3 h until a clear solution was obtained. Then, 10 ml of carbon disulfide ( $1.7 \times 10^{-1}$  mol) was added dropwise under nitrogen atmosphere during 1 h and the mixture was stirred for 5 h. In the next step, 4.9 ml of methyl bromoacetate was added dropwise under nitrogen atmosphere. The reaction mixture was stirred overnight and a light yellow-green solution was obtained (Figure 3.2). The solution was filtered via

vacuum filtration to remove the white precipitate of potassium bromide and afterwards the solvent was evaporated.

The light yellow-green xanthate Methyl(Isopropoxycarbonothioyl)sulfanyl acetate (MIPCTSA) was purified by column chromatography on silica gel (Kieselgel-60) with hexane/ethyl acetate (4/1, v/v) as eluent and obtained with 80 % yield.

$^1\text{H}$  NMR ( $\text{CDCl}_3$ ):  $\delta$ = 1.4 (d, 6H,  $\text{CH}(\text{CH}_3)_2$ ), 3.8 (s, 3H,  $\text{CO}_2\text{CH}_3$ ), 3.9 (s, 2H,  $\text{CH}_2$ ), 5.7 ppm (s, 1H,  $\text{CH}(\text{CH}_3)_2$ ).

$^{13}\text{C}$  NMR ( $\text{CDCl}_3$ ):  $\delta$ = 21.2 ( $\text{CH}(\text{CH}_3)_2$ ), 37.4 ( $\text{CH}_2$ ), 52.6 ( $\text{CO}_2\text{CH}_3$ ), 78.7 ( $\text{CH}(\text{CH}_3)_2$ ), 168.2 ( $\text{C}=\text{O}$ ), 211.4 ppm ( $\text{C}=\text{S}$ ).

### 3.10. RAFT Polymerization of Vinyl Acetate by Using MIPCTSA as Chain Transfer Agent

The reactor equipped with a magnetic stirrer and a rubber septum was thoroughly dried by flaming before the reaction.

MIPCTSA (0.2864 g, 1.4 mmol) and 2,2'-azoisobutyronitrile (AIBN) (0.1044 g, 0.64 mmol) were added into the reactor. The reactor was evacuated and charged with nitrogen. Then, freshly distilled vinyl acetate (10 ml, 0.1086 mol) was transferred into the reactor via syringe. The reactor was degassed by three freeze-thaw cycles and sealed under vacuum. Subsequently, it was placed in a constant temperature oil bath at 60 °C. The reaction was carried out for 16 h. At the end of the process, the polymer was quenched by shock cooling in liquid nitrogen (Figure 3.3). The sealed top of the reactor was broken and connected to vacuum. The polymer was heated in water bath to remove any unreacted vinyl acetate monomer. Poly(vinyl acetate) which was end functionalized with MIPCTSA was obtained with 96 per cent yield and named as C-PVA1.



The same experimental procedure was followed for the synthesis of MIPCTSA end functionalized PVA with the temperature raised to 65 °C. The product C-PVA2 was purified by freeze-dry method and obtained with 94 per cent yield.

### 3.11. RAFT Polymerization of NIPAM by Using MIPCTSA as Chain Transfer Agent

The reactor equipped with a magnetic stirrer and a rubber septum was thoroughly dried by flaming before the reaction.

MIPCTSA (0.2665 g, 0.001281 mol), NIPAM monomer (3.5073 g, 0.03104 mol) and AIBN (0.0115 g, 0.07012 mmol) were added into the flask. 10 ml freshly distilled 1,4-dioxane was transferred into the flask via syringe under nitrogen atmosphere. The flask was degassed by three freeze-thaw cycles and sealed under vacuum. The reaction was carried out at 75 °C for 21 h. At the end of the process, the polymer was quenched by shock cooling in liquid nitrogen. The sealed top of the reactor was broken and the polymer was dissolved in 10 ml 1,4-dioxane. Subsequently, it was precipitated in diethyl ether non-solvent, filtered and dried in vacuum oven. MIPCTSA end functionalized poly(NIPAM) in white solid form was obtained with 98 per cent yield.

$^1\text{H}$  NMR ( $\text{CDCl}_3$ ):  $\delta$  = 1.1 (s, 6H,  $\text{CH}(\text{CH}_3)_2$ ), 1.6-1.9 (d, 2H,  $\text{CH}_2\text{CH}$ ), 2.3 (s, 1H,  $\text{CH}_2\text{CH}$ ), 4.0 ppm (s, 1H,  $\text{NHCH}(\text{CH}_3)_2$ ).

FTIR: 3293.57 (N-H), 2971.54 ( $-\text{CH}_3$ ), 1638.80 (C=O), 1541.92 (N-H), 1386.50–1366.58  $\text{cm}^{-1}$  ( $-\text{CH}_3$ ).

### 3.12. Block Copolymerization of MIPCTSA End Functionalized PVA with NIPAM

Seven sets of polymerization reactions were carried out with different amounts/compositions of PVA, NIPAM and AIBN, as shown in Table 3.2. The reaction flasks equipped with magnetic stirrers and rubber septums had been prepared by evacuating, flaming and charging with nitrogen. MIPCTSA end functionalized PVA,

NIPAM monomer, and AIBN were introduced into the flasks. Freshly distilled 1,4-dioxane was transferred into the flasks via syringe under nitrogen atmosphere in case of necessity. The mixtures were stirred to allow complete dissolution. Then the systems were degassed by three freeze-thaw cycles and sealed under vacuum. The polymerizations were carried out at 75 °C. At the end of the processes, the colorless and viscous materials obtained were quenched by shock cooling in ice. The product C-AN1 was precipitated in diethyl ether, subsequently filtered with sintered glass and dried in vacuum oven. The products C-AN2 to C-AN7 were purified by freeze-dry technique. Poly(vinyl acetate)-b-poly(NIPAM) diblock copolymers were obtained in white solid form (Figure 3.6).

$^1\text{H}$  NMR ( $\text{CDCl}_3$ ):  $\delta$ = 1.1 (s, 6H,  $\text{CH}(\text{CH}_3)_2$ ), 1.6-1.9 (m, 2H,  $\text{CH}_2\text{CH}$  ; 2H,  $\text{CH}_2\text{CHO}$ ), 2.0 (s, 3H,  $\text{CO}_2\text{CH}_3$ ), 2.3 (s, H,  $\text{CH}_2\text{CH}$ ), 4.0 ppm (s, 1H,  $\text{NHCH}(\text{CH}_3)_2$ ), 4.8-5.0 ppm (s, 1H,  $\text{CH}_2\text{CHO}$ ).

FTIR: 3292.56 (N–H), 2969.92 ( $-\text{CH}_3$ , PNIPAM), 1737.67 (C=O, PVA), 1644.55 (C=O, PNIPAM), 1538.74 (N–H), 1367.77 ( $-\text{CH}_3$ , PVA), 1238.84 and 1022.17  $\text{cm}^{-1}$  (C–O).

Table 3.2. Block copolymerization of MIPCTSA end functionalized PVA with NIPAM

Name	PVA (mol/10 <sup>-2</sup> )	NIPAM (mol/10 <sup>-2</sup> )	AIBN (mol/10 <sup>-4</sup> )	Time (h)
C-AN1	1.817	1.827	1.079	19
C-AN2	1.770	0.888	1.177	24
C-AN3	1.770	3.552	1.177	24
C-AN4	1.771	1.772	1.116	24
C-AN5	1.771	1.771	0.567	24
C-AN6	1.771	0.885	0.573	24
C-AN7	1.771	3.542	0.585	24

### 3.13. Preparation of MIPCTSA End Functionalized PVA Stock Solution

After RAFT polymerization process described in section 3.11, MIPCTSA end functionalized PVA (C-PVA1) was stuck on the glass surface of the reactor tube (Figure 3.3). The tube was broken and a small amount of PVA was taken to be used in block copolymerization reaction of C-AN1, as explained in section 3.12. The rest was dissolved using 1,4-dioxane to be separated from the glass surface. Excess solvent was evaporated and the material was precipitated in diethyl ether. However, the polymer could not be collected due to incomplete phase separation. Therefore the material was once again dissolved in 1,4-dioxane and purified by freeze-dry technique (Figure 3.5). At the end of the process, small samples were taken from the flask for analysis.

$^1\text{H}$  NMR ( $\text{CDCl}_3$ ):  $\delta$ = 1.6-1.9 (d, 2H,  $\text{CH}_2\text{CHO}$ ), 2.0 (s, 3H,  $\text{CO}_2\text{CH}_3$ ), 4.8-5.0 ppm (s, 1H,  $\text{CH}_2\text{CHO}$ ).

FTIR: 1729.57 (C=O), 1370.38 ( $-\text{CH}_3$ ), 1225.59 and 1018.16  $\text{cm}^{-1}$  (C–O).

Since it was still difficult to remove PVA from the glass surface (Figure 3.5), the rest of the material was dissolved in determined amount of 1,4-dioxane. The stock solution of MIPCTSA end functionalized PVA was obtained (0.088 mol PVA in 109 ml 1,4-dioxane). Samples from this stock solution were used for the polymerization reactions which yield the products C-AN2 and C-AN3.

C-PVA2 was dissolved in 1,4-dioxane also for preparation of PVA stock solution (0.2172 mol PVA in 187 ml 1,4-dioxane). The block copolymers C-AN4 to C-AN7 were synthesized by using samples of this stock solution

### 3.14. Kinetic Study of Block Copolymerization of MIPCTSA End Functionalized PVA with NIPAM

The polymerization reaction was carried out in Schlenck type reactor (Figure 3.4) with the determined quantities of PVA, NIPAM monomer and AIBN as shown in Table 3.3. AIBN and NIPAM were added into the reaction flask. The medium was degassed and purged with nitrogen gas. Determined amount of MIPCTSA end functionalized PVA stock solution in 1,4-dioxane (C-PVA2) was transferred into the flask via syringe under nitrogen atmosphere. The mixture was stirred to allow dissolution. Then, small amount sample was taken at room temperature as original reaction mixture sample. The flask was inserted into oil bath at constant temperature of 75 °C. Samples were taken from the reaction medium via capillary method at specific time intervals. Afterwards they were quenched by shock cooling in liquid nitrogen and stored for analysis. The final products were also shock cooled in liquid nitrogen. Except the original reaction mixture, all samples were purified by freeze-dry technique after initial analysis by  $^1\text{H}$  NMR spectroscopy.

Table 3.3. Kinetic study of block copolymerization of MIPCTSA end functionalized PNIPAM with vinyl acetate

Name	PVA (mol/10 <sup>-2</sup> )	NIPAM (mol/10 <sup>-2</sup> )	AIBN (mol/10 <sup>-4</sup> )	Time (h)
C-KAN	1.771	1.771	0.579	5.4

### 3.15. Characterization

The microstructures of the polymers were determined by  $^1\text{H}$  and  $^{13}\text{C}$  nuclear magnetic resonance (NMR) spectroscopy using Varian Gemini 400 MHz spectrometer.

Fourier Transform Infrared (FTIR) analysis was performed on Thermo Nicolet, FTIR 380 Spectrometer, using the diamond ATR accessory.

Size Exclusion Chromatography (SEC) was carried out in tetrahydrofuran (THF) using a Waters Isocratic HPLC Pump with Waters Refractive Index Detector and Styragel column. Polystyrene standards were used for the calibration of the instrument. Additional analysis were performed for samples C-AN1, C-AN2, C-AN3 and C-PVA1 by using N,N-dimethylformamide (DMF) as eluent by using another Waters SEC instrument.

Thermal behavior of samples were investigated by Differential Scanning Calorimetry (DSC) measurements on dry polymer samples performed using TA Instruments Q200, under nitrogen atmosphere. The samples of about 0.0035g in aluminium pans were heated from -60 to 200 °C at a rate of 10 °C/min, then cooled back to -60 °C and reheated to 200 °C again at a rate of 10 °C/min. The glass transition temperatures ( $T_g$ ) were always determined from the second heating scan.

The morphology of the polymer samples were examined by Scanning Electron Microscopy (ESEM), by ESEM-FEG/EDAX Philips XL-30 instrument.

Atomic Force Microscopy (AFM) was also performed by using Quesant-Ambios Universal Scanning Probe Microscope (USPM). Polymer samples were dissolved in chloroform and spin-coated onto glass surface for the preparation of thin films for the analysis.

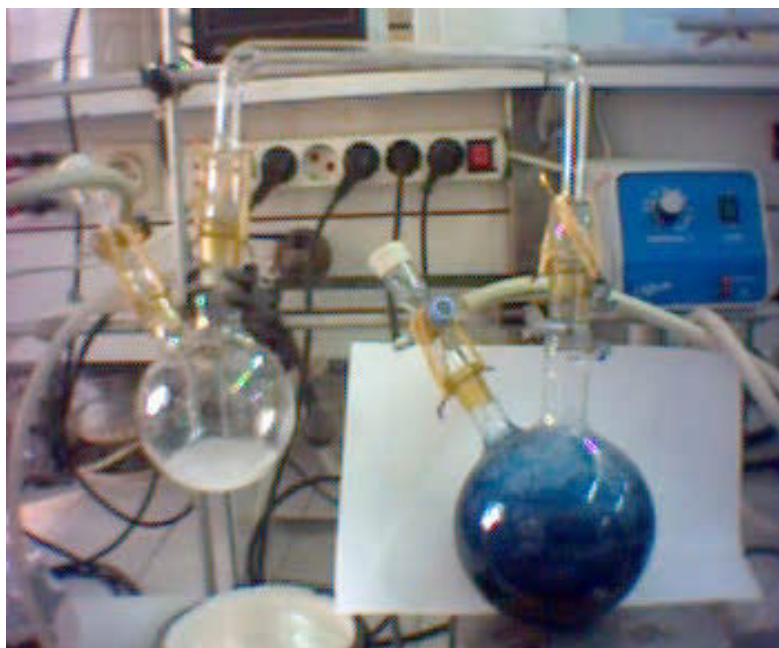


Figure 3.1. Purification of 1,4-dioxane



Figure 3.2. Synthesis of MIPCTSA



Figure 3.3. C-PVA1 in sealed reactor



Figure 3.4. Schlenk type reactor



Figure 3.5. C-PVA1 after freeze-dry process



Figure 3.6. PVA-b-PNIPAM after freeze-dry process



## 4. RESULTS AND DISCUSSION

### 4.1. Synthesis and Purification of Methyl(Isopropoxycarbonothioyl)sulfanyl Acetate

The synthesis of MIPCTSA was done using literature procedure [46] with the reactions indicated in Figure 4.1.

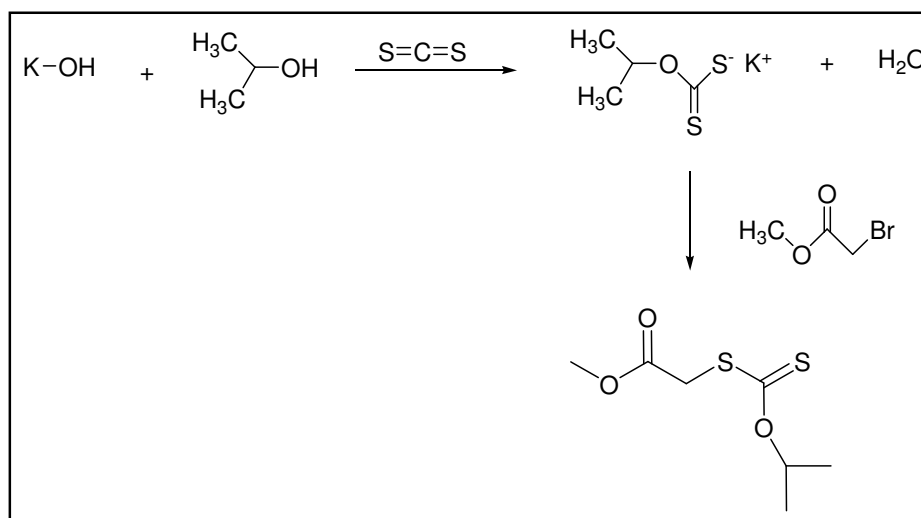


Figure 4.1. Synthesis of MIPCTSA

After the addition of methyl bromoacetate the reaction became slightly exothermic, the temperature of the flask was measured to be around 30 °C. At the end of the process, the light yellow-green xanthate (MIPCTSA) was purified by column chromatography. The purity of the final product was investigated using thin layer chromatography (TLC). One spot corresponding to the final product was observed at  $R_f = 0.6$ , with no further spots, as indicated in the literature procedure [46]. After purification, the xanthate was obtained with 80 % yield.

The  $^1\text{H}$ -NMR spectrum of MIPCTSA (Figure 4.2) shows methyl protons of isopropoxy group at 1.4 ppm, methoxy protons at 3.8 ppm, methylene protons at 3.9 ppm and methine proton at 5.7 ppm.

The  $^{13}\text{C}$ -NMR spectrum of MIPCTSA (Figure 4.3) shows methyl peak of isopropoxy group at 21.2 ppm, methylene carbon peak at 37.4 ppm, methoxy carbon peak at 52.6 ppm, methine carbon peak at 78.7 ppm, carbonyl peak at 168.2 ppm and carbon disulfide peak at 211.4 ppm.

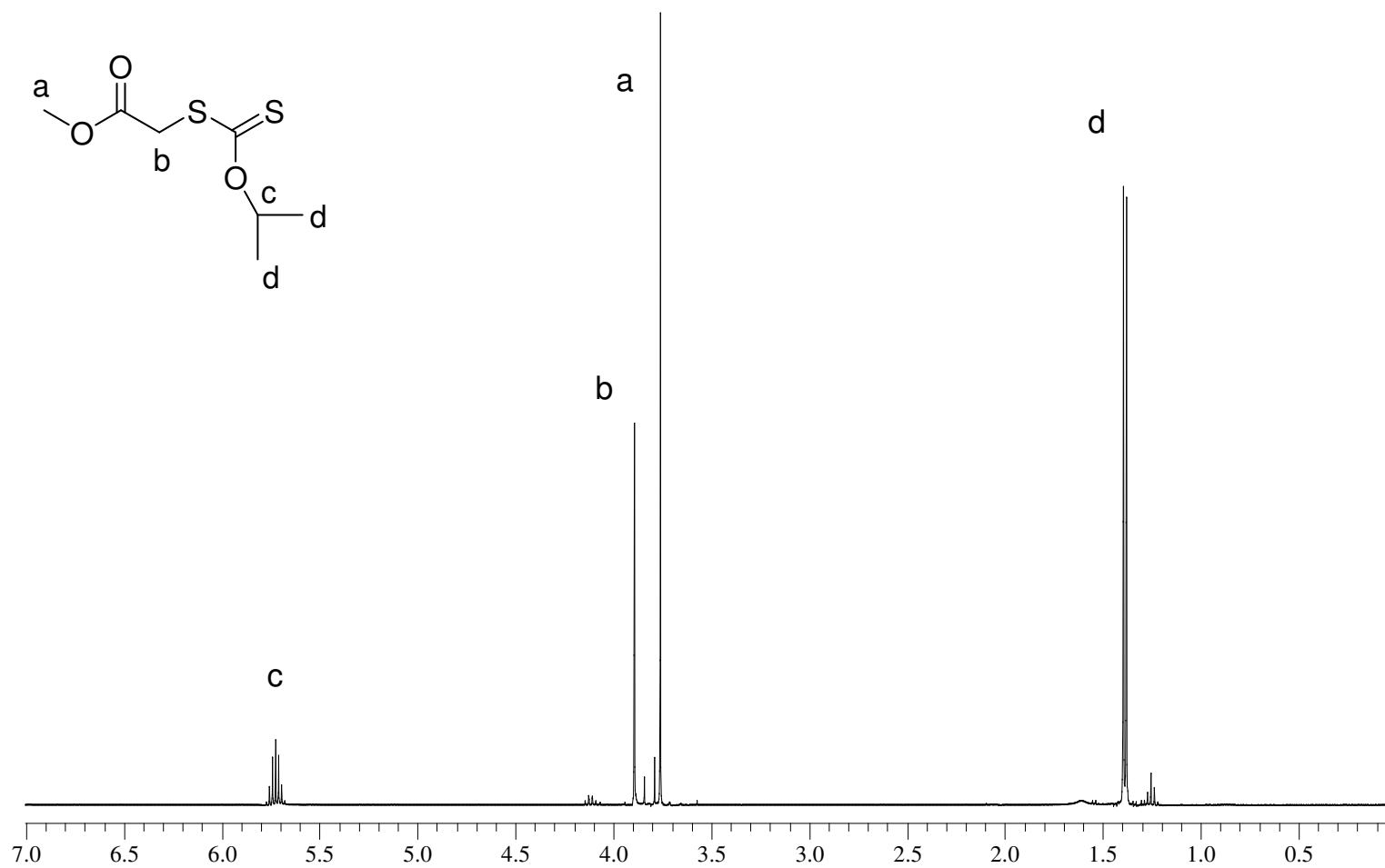


Figure 4.2.  $^1\text{H}$  NMR spectrum of MIPCTSA

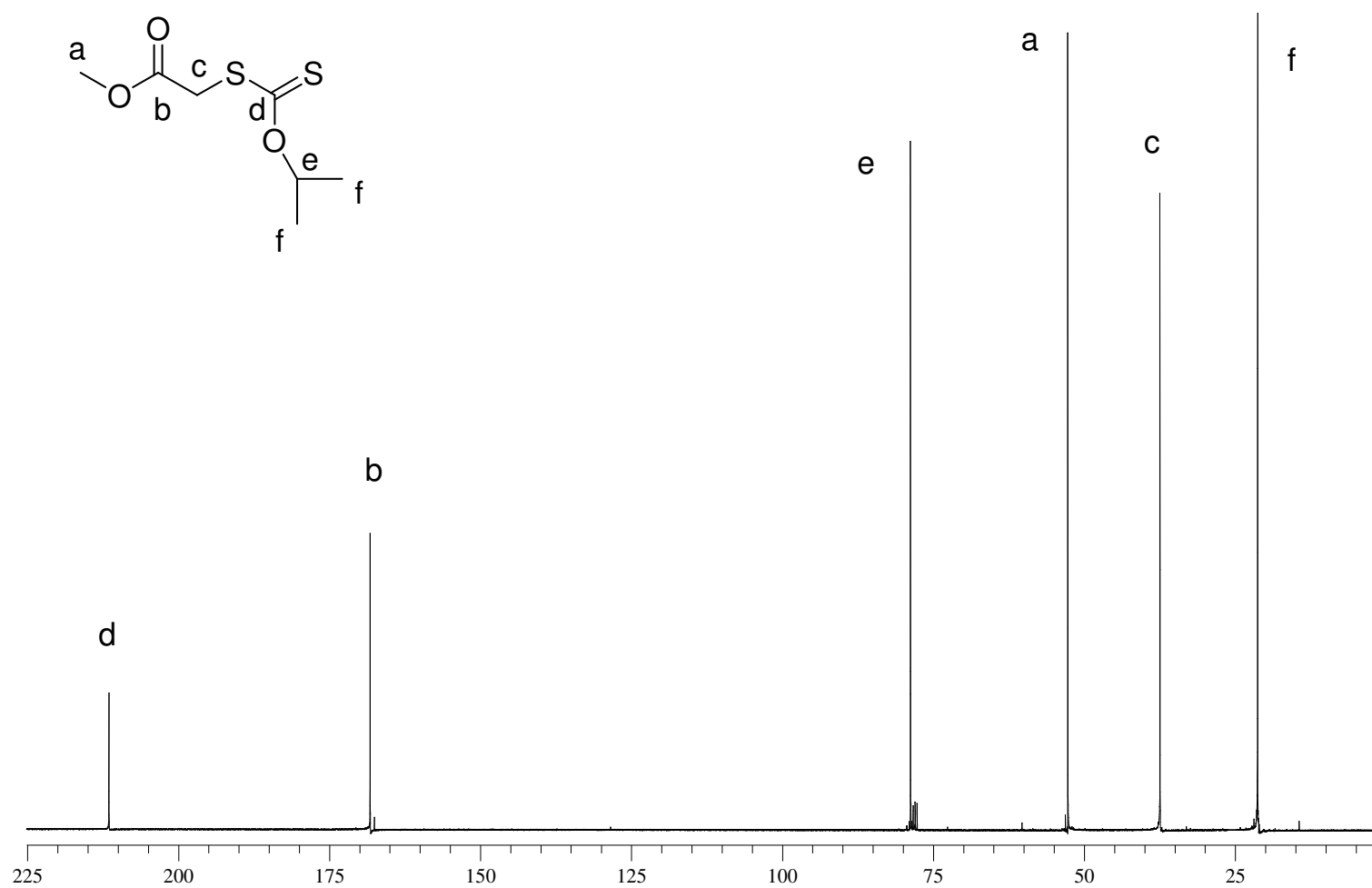


Figure 4.3.  $^{13}\text{C}$  NMR spectrum of MIPCTSA

## 4.2. RAFT Polymerization of Vinyl Acetate by Using MIPCTSA as Chain Transfer Agent

### 4.2.1. Synthesis of C-PVA1

Vinyl acetate was polymerized via RAFT process by using MIPCTSA as chain transfer agent (CTA) as described in literature procedure [46]. The reaction regarding the process is indicated in Figure 4.4.

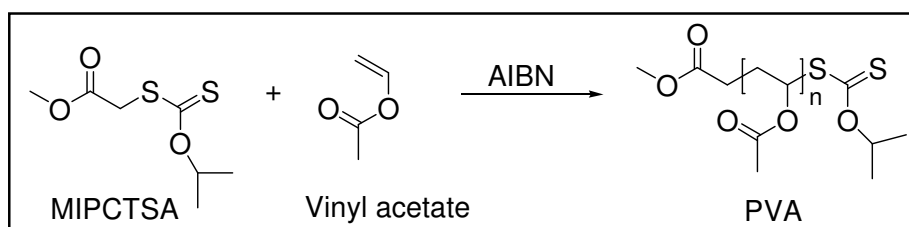


Figure 4.4. Polymerization of vinyl acetate via RAFT process

The <sup>1</sup>H NMR spectrum of C-PVA1 (Figure 4.5) shows methylene protons between 1.6 and 1.9 ppm, methyl protons at 2.0 ppm and methine proton between 4.8 and 5.0 ppm. The peak around 9.78 ppm belongs to the methine proton of the terminal vinyl acetate unit of the polymer chain, which is attached to the sulfur atom of the chain transfer agent. This indicates that the polymer chains are terminated with the chain transfer agent, becoming macro-chain transfer agents (macro-CTA) that could be further polymerized with suitable monomers to form block copolymers.

Traces of unreacted monomer could be observed at 4.6, 5.9 and 7.2 ppm, belonging to vinyl protons of vinyl acetate and the conversion was calculated as 96 %. From the relative intensities of the peaks at 4.8-5.0 ppm and 9.78 ppm, the DP<sub>n</sub> of PVA macro-CTA was calculated as 142.

The FTIR spectrum of the polymer (Figure 4.6) shows the dominant peaks of the carbonyl stretch at  $1729.57\text{ cm}^{-1}$  and the C-O single bond stretch of the acetate group at  $1225.59\text{ cm}^{-1}$ . Also the methyl deformation at  $1370.38\text{ cm}^{-1}$  and the C-O single bond stretch of the polymer backbone carbons at  $1018.16\text{ cm}^{-1}$  are observed.

#### **4.2.2. Synthesis of C-PVA2**

The second polymerization trial of vinyl acetate was carried out with the same molar ratios of monomer, CTA and initiator. The reaction temperature was elevated to  $65\text{ }^{\circ}\text{C}$  in order to investigate the effect of decomposition of AIBN on the molecular weight distribution.

The  $^1\text{H}$  NMR spectrum of C-PVA2 (Figure 4.7) shows the same peaks as C-PVA1, as indicated in section 4.2.1. The conversion was calculated as 94 % and the  $\text{DP}_n$  as 125, by using the same calculation method in section 4.2.1.

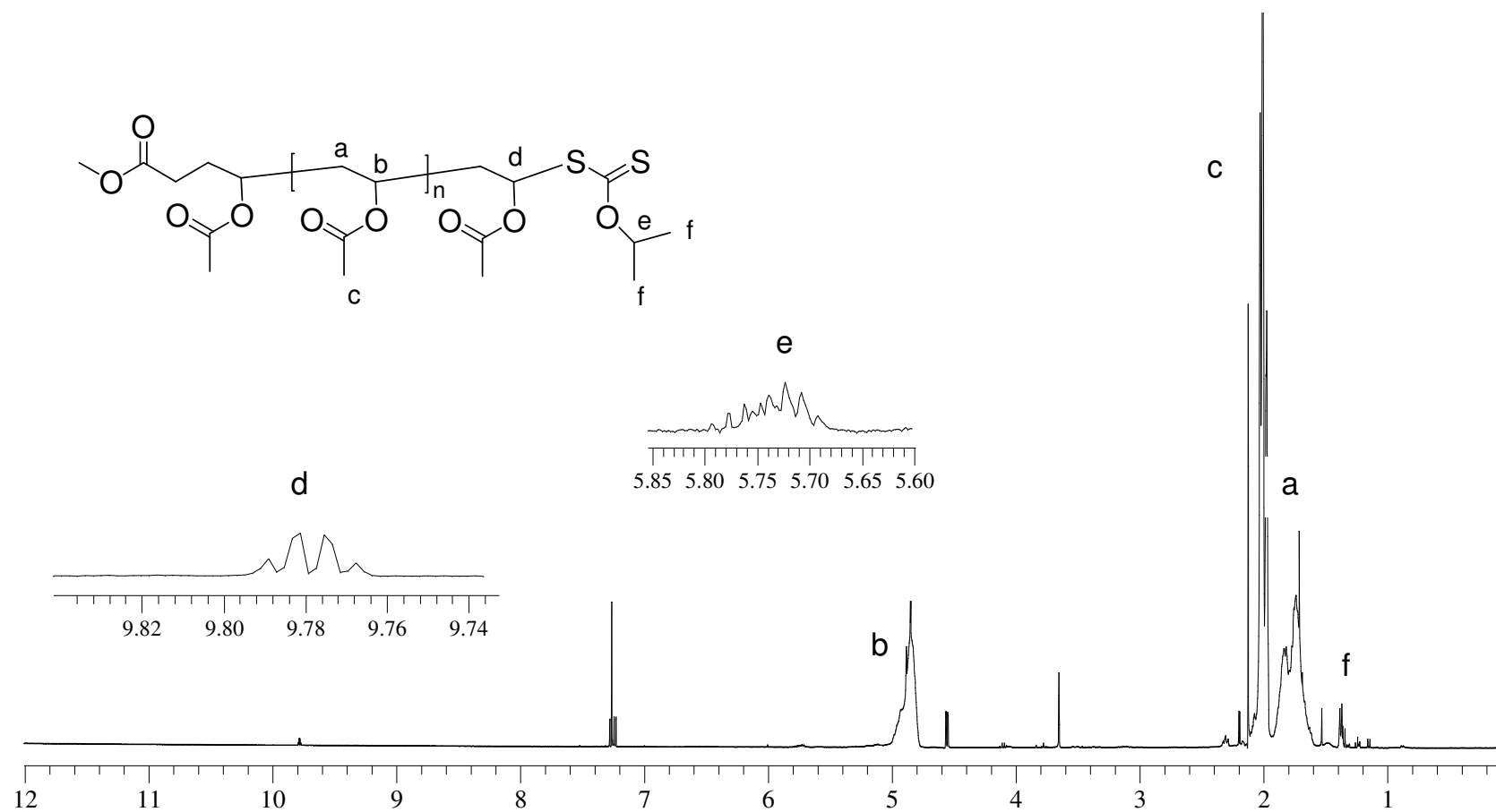


Figure 4.5.  $^1\text{H}$  NMR spectrum of C-PVA1

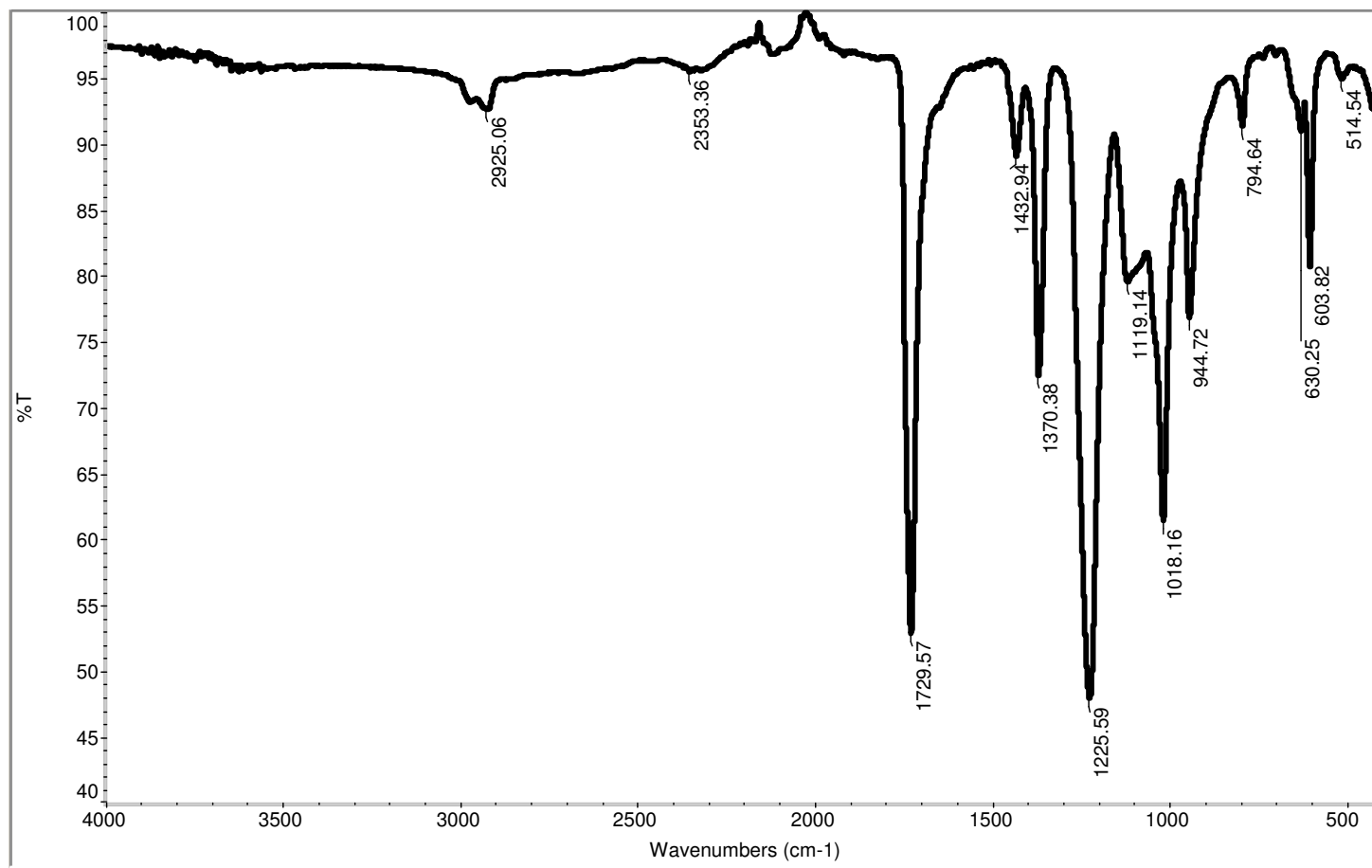


Figure 4.6. FTIR spectrum of C-PVA1



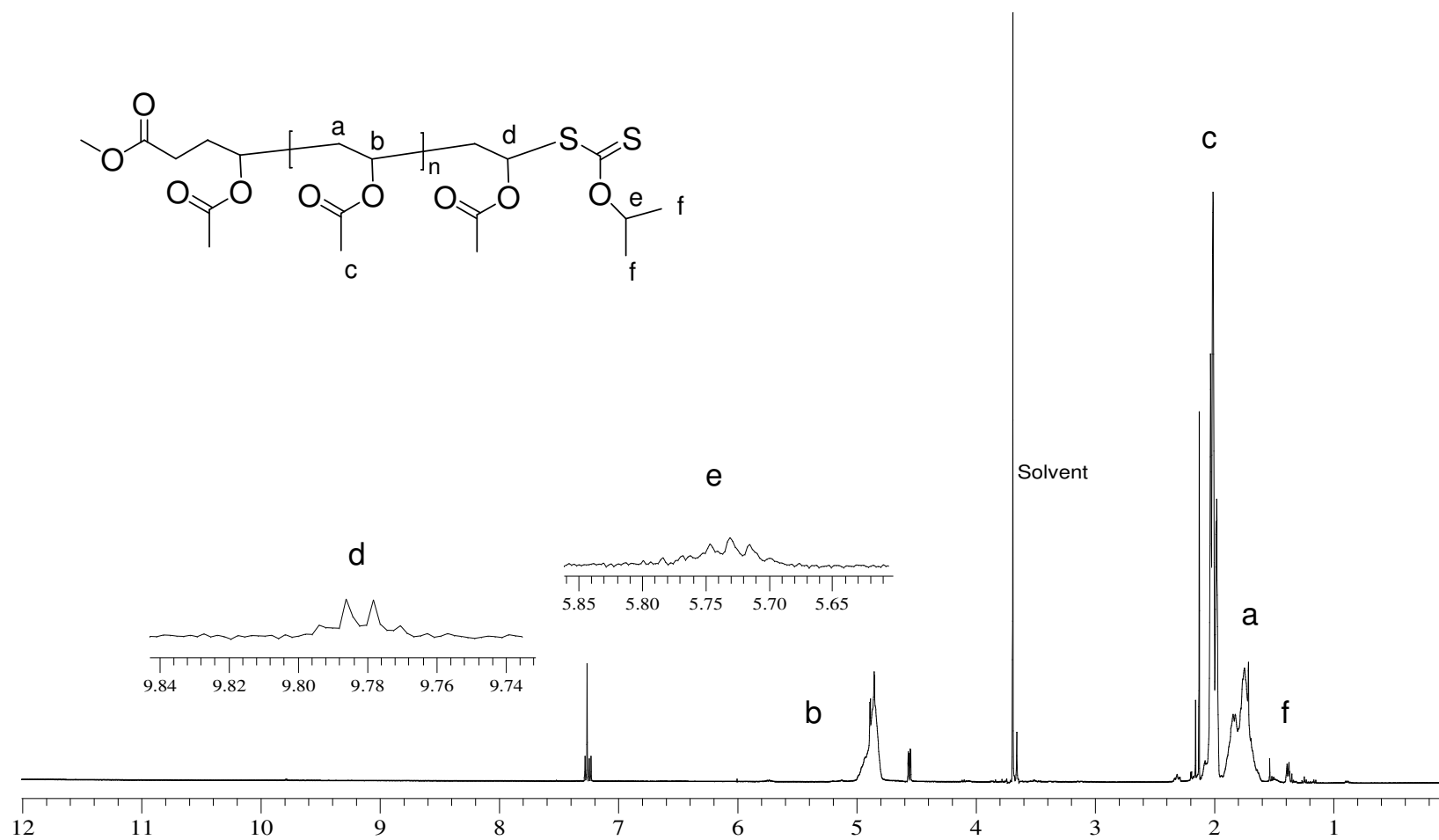


Figure 4.7.  $^1\text{H}$  NMR spectrum of C-PVA2

### 4.2.3. SEC Analysis of C-PVA1 and C-PVA2

Figure 4.8 shows the SEC data of C-PVA1, with the  $M_n$  and  $M_w/M_n$  values indicated in Table 4.1. The SEC analysis shows bimodal distribution, with the presence of a second small peak at lower molecular weight region. This may be attributed to be due to low decomposition rate of AIBN at 60 °C or partial termination of active chain end during the reaction.

Table 4.1. SEC analysis data of C-PVA1 and C-PVA2

Name	$M_n$ NMR	$M_n$	$M_w$	$M_w/M_n$
C-PVA1	12188	5557	13041	2.35
C-PVA2	10773	11365	14908	1.31

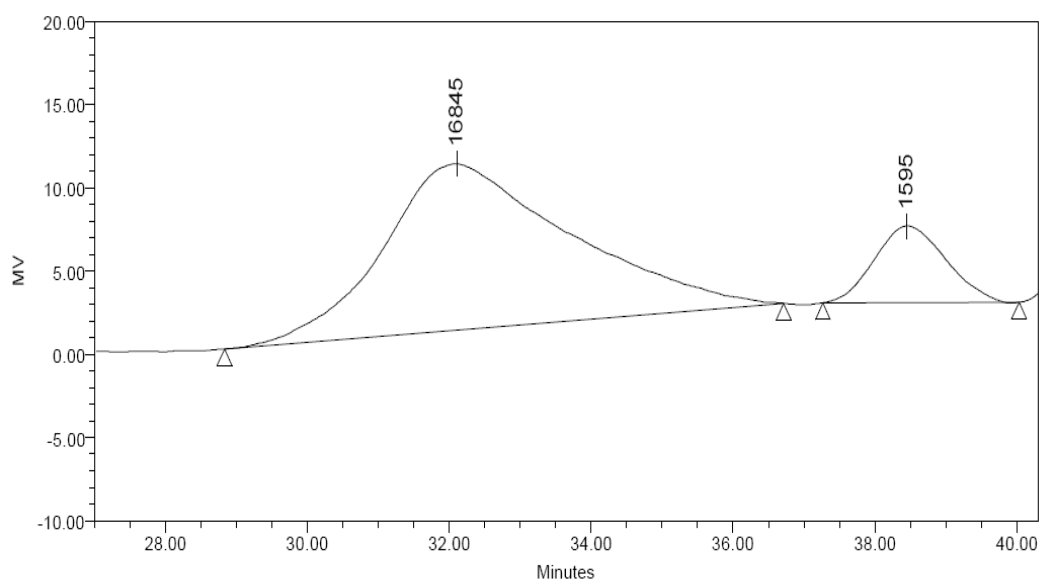


Figure 4.8. SEC curve of C-PVA1

Figure 4.9 shows the SEC data of C-PVA2, which presents unimodal molecular weight distribution. Elevation of the reaction temperature from 60 to 65 °C may be regarded as the reason of this behavior, due to the improvement on the rate of radical formation.

The higher decomposition rate constant of initiator at high temperature may result in the initiation of more chains and more polymer chains derived from initiator.

On the other hand, the increase of temperature may also lead to a larger increase of the fragmentation rate constant than of the other rate constants due to its higher activation energy. This would result in a minimization of the intermediate radical lifetime and thus in a minimization of both the retardation and the side reactions on these intermediate radicals [47].

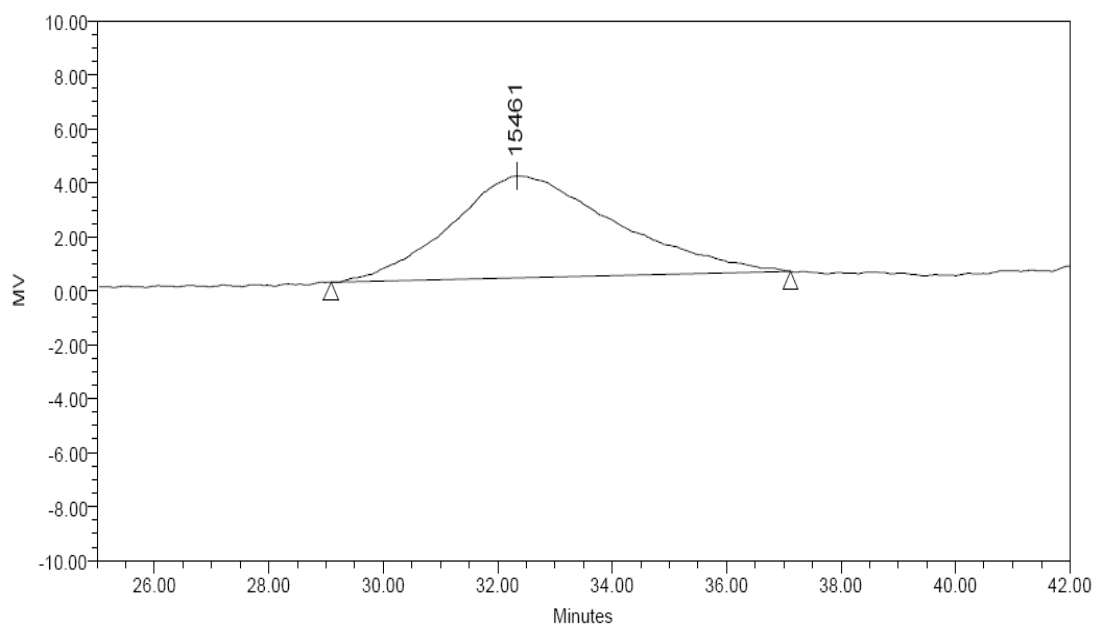


Figure 4.9. SEC curve of C-PVA2

The molecular weights of C-PVA1 and C-PVA2 were also calculated from the  $^1\text{H}$  NMR data shown in Figure 4.5 and Figure 4.6, respectively. The values are given in Table 4.1, as  $M_{n \text{ NMR}}$ . The relative intensities of specific peaks belonging to PVA (methine proton at 4.8-5.0 ppm) and CTA attached to PVA (methine proton at 9.78 ppm) were used in order to calculate the number average molecular weights. For C-PVA2, well agreement with the SEC analysis data is observed (Table 4.1), whereas the presence of bimodal distribution and low molecular weight products in C-PVA1 create divergence between the calculated and obtained number average molecular weights.

### 4.3. RAFT Polymerization of NIPAM by Using MIPCTSA as Chain Transfer Agent

NIPAM was polymerized via RAFT process by using MIPCTSA chain transfer agent, as indicated in Figure 4.10.

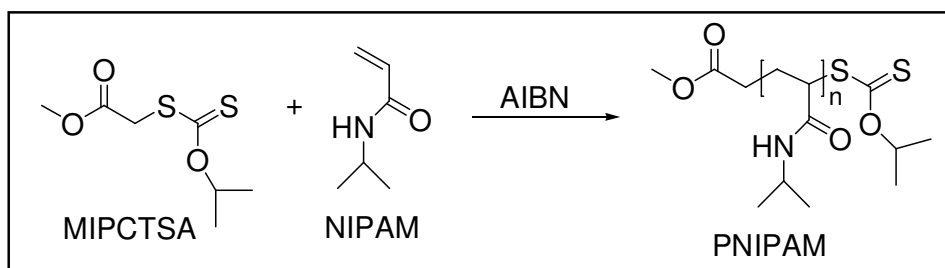


Figure 4.10. Polymerization of NIPAM via RAFT process

The  $^1\text{H}$  NMR spectrum (Figure 4.11) shows methyl protons of isopropyl group at 1.1 ppm, methylene protons between 1.6 and 1.9 ppm, methine proton at 2.3 ppm and methine proton of the isopropyl group at 4.0 ppm. The peak around 3.46 ppm belongs to the methine proton of the terminal NIPAM unit of the polymer chain, which is attached to the sulfur atom of the chain transfer agent. Termination of the chain ends with the chain transfer agent would enable the polymer to be used in further reactions to yield block copolymers.

In the FTIR spectrum of the PNIPAM (Figure 4.12), N-H stretching appears at 3293.45, the amide I band (C=O stretch) at 1638.80  $\text{cm}^{-1}$ , the amide II band (N-H vibration) at 1541.92  $\text{cm}^{-1}$  and the methyl groups in isopropyl group at 2971.54 and 1386.50-1366.58  $\text{cm}^{-1}$ .

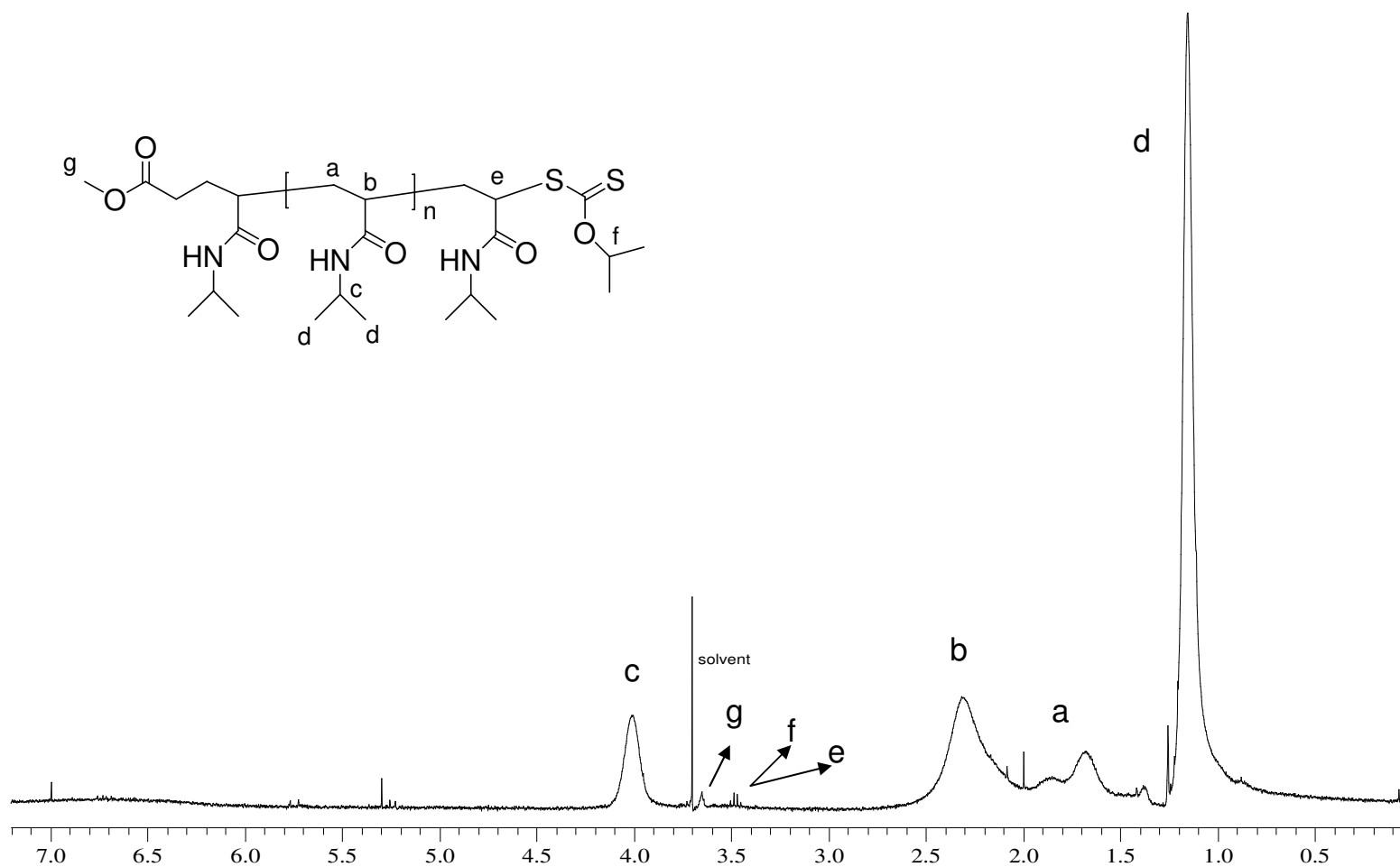


Figure 4.11.  $^1\text{H}$  NMR spectrum of C-PNIPAM

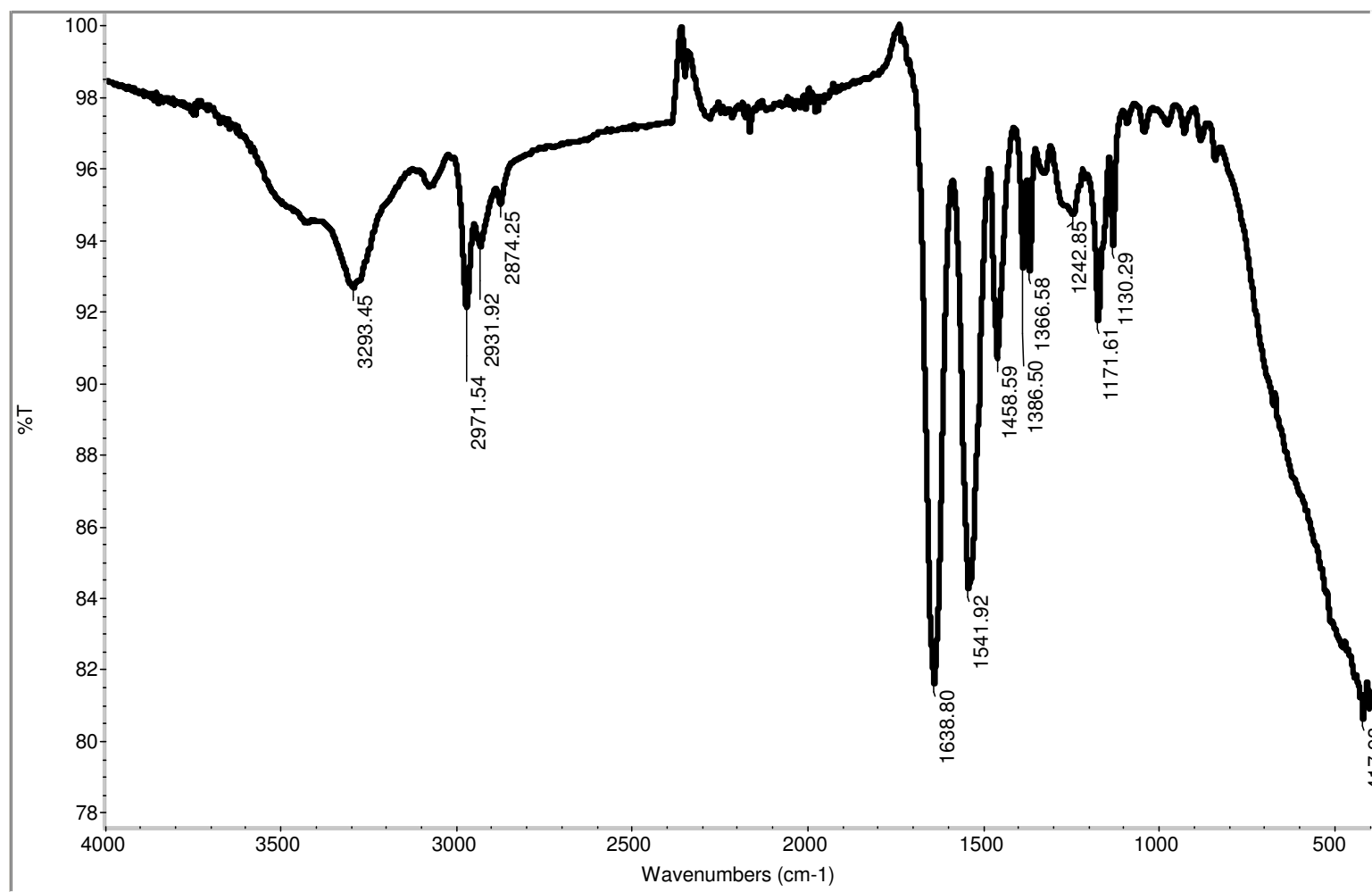


Figure 4.12. FTIR spectrum of C-PNIPAM

#### 4.4. Block Copolymerization of MIPCTSA End Functionalized PVA with NIPAM

MIPCTSA end functionalized PVA was used as macro chain transfer agent and the polymerization of NIPAM was performed by RAFT process as shown in Figure 4.13. Poly(vinyl acetate)-b-poly(NIPAM) diblock copolymers were synthesized in different compositions.

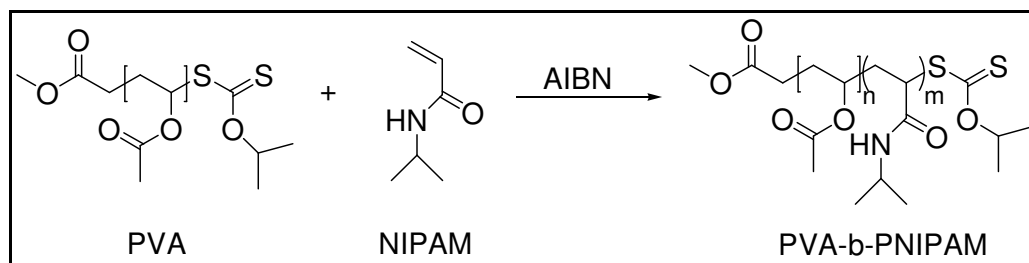


Figure 4.13. Block copolymerization of MIPCTSA end functionalized PVA with NIPAM

##### 4.4.1. Synthesis of C-AN1

In the first synthesis, 1:1 molar ratio of PVA macro-CTA (C-PVA1) and NIPAM monomer were introduced. The reaction medium contained 1,4-dioxane as solvent, therefore the product was in viscous liquid form. Precipitation into appropriate nonsolvent was chosen as purification method. Diethyl ether was selected as the nonsolvent, since it is known to be suitable for both polymers individually. However, the process was not quite efficient in this case, as phase separation was observed during precipitation. Thus, the products of the latter reactions were purified by freeze-dry technique.

In the  $^1\text{H}$  NMR spectra shown in Figure 4.14, the spectrum of the MIPCTSA end functionalized PVA (I), MIPCTSA end functionalized PNIPAM (II) and the expected copolymer (III) are included. The peaks b and f were chosen especially to investigate the presence of both PVA and PNIPAM units in the copolymer structure. The peak b at 4.8-5.0 ppm corresponds to the methine proton of PVA and the peak f at 4.0 ppm corresponds to the methine proton of the isopropyl group of PNIPAM.

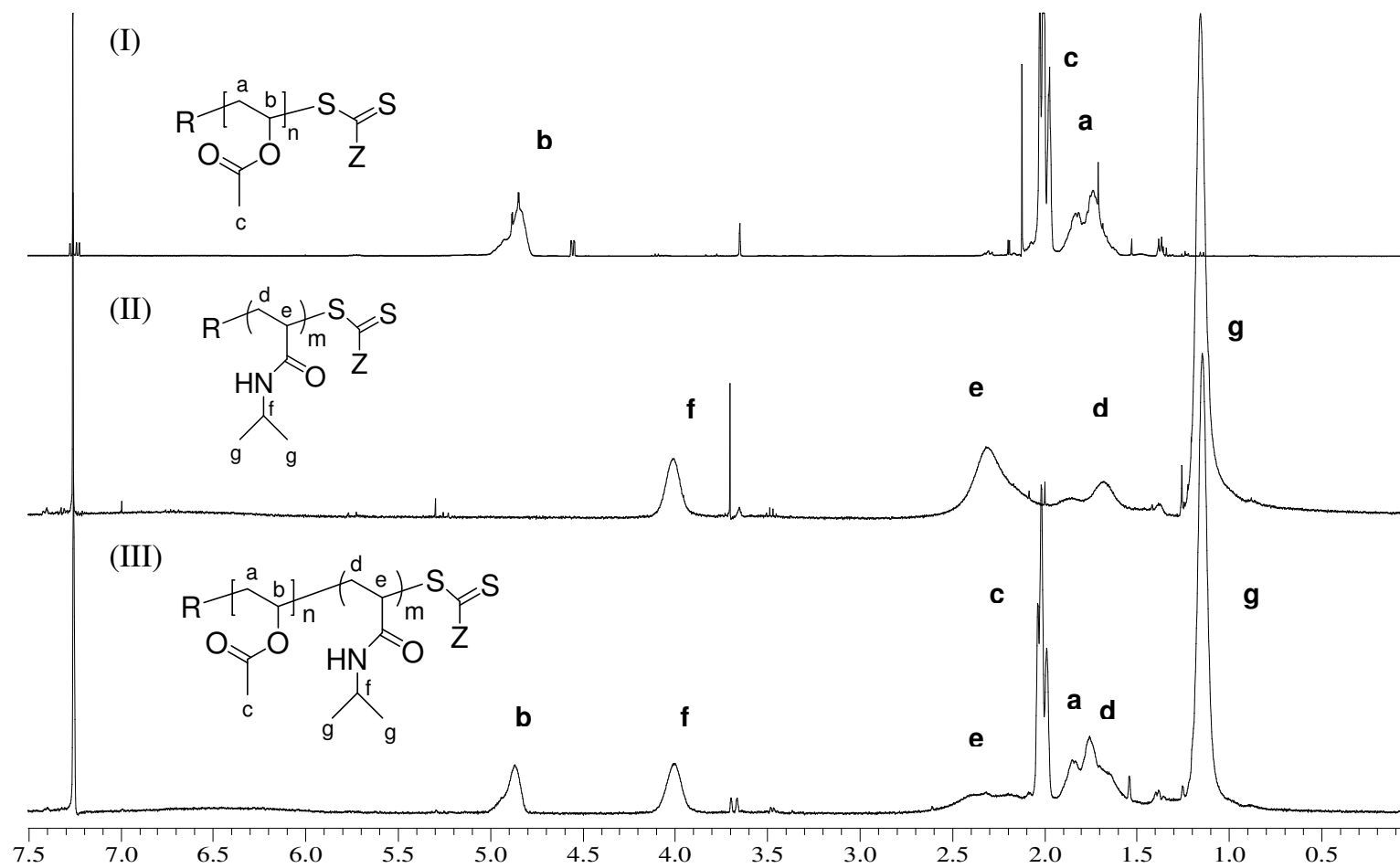


Figure 4.14.  $^1\text{H}$  NMR spectra of C-PVA1 (I), C-PNIPAM (II), C-AN1 (III)



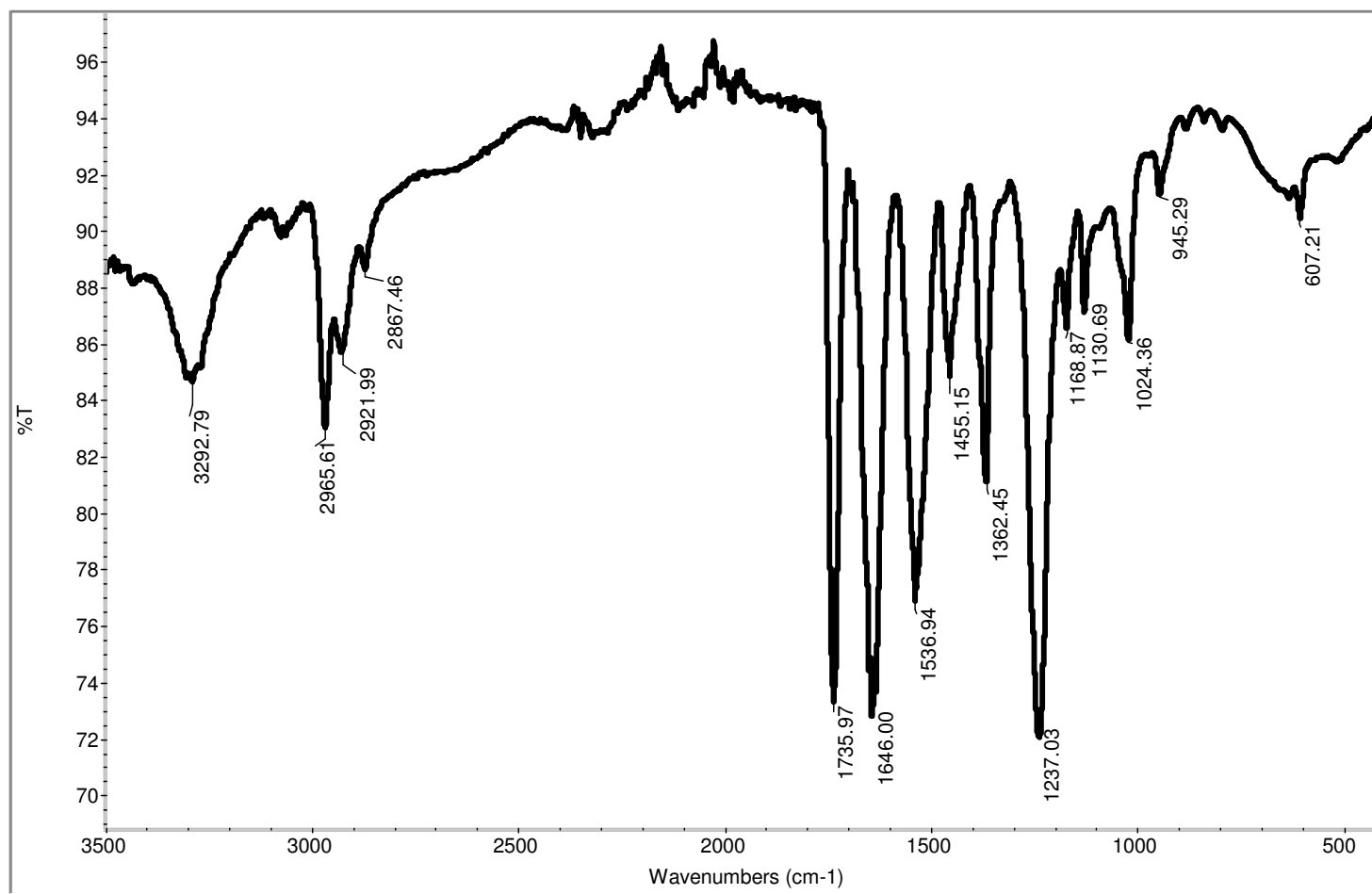


Figure 4.15. FTIR spectrum of C-AN1

When these data were compared, the presence of both peaks in the final spectrum shows the incorporation of the second monomer NIPAM in the copolymer structure, with the expected 1:1 molar ratio.

The FTIR spectrum (Figure 4.15) shows characteristic absorptions of both polymer sequences.

In the literature, the molecular weight characterizations of PVA and PNIPAM were performed with SEC analysis by using different eluents. For the characterization of PVA, tetrahydrofuran (THF) was preferred [17, 40, 45, 46]. PNIPAM polymers and copolymers were analyzed by using different solvent systems; such as N,N-dimethylformamide (DMF) [28, 32, 39], DMF with LiBr [33] and THF [5, 31, 35, 47]. Within these studies, some problems related to the SEC analysis PNIPAM samples were discussed [5, 28, 31].

Ganachaud et al. [31] reported that the SEC characterization PNIPAM in THF involved problems due to irreversible chain aggregation due to the intermolecular hydrogen-bonding, after complete drying of the polymer samples. It was emphasized that particular care was required when preparing PNIPAM samples for organic-phase GPC analysis with THF as solvent, polymer samples must be dried in the presence of water and then dissolved in THF to prevent chain aggregation. However, this procedure is not applicable in our case, due to the presence of PVA in the block copolymer structure.

Schilli et al. [5] determined the molecular weights of PNIPAM samples obtained by RAFT process by a combination of MALDI-TOF MS and SEC with THF as eluent. The problems associated with the SEC analysis of PNIPAM were reported, with experimentally obtained molecular weights considerably higher than predicted. A high-molecular weight shoulder was observed for conversions higher than 90 %. This behavior was considered to be due to combination of the growing chains, which was typical for controlled polymerizations with exchange between active and dormant species.

In the study concerning room-temperature RAFT polymerization of NIPAM [28], Convertine et al. demonstrated SEC analysis of PNIPAM samples in *N,N*-dimethylformamide (DMF) at 60 °C. It was reported that none of the previously encountered problems in the literature were observed by this method.

We performed SEC analysis by using both THF and DMF as solvent. Since THF is not a good solvent for PNIPAM and DMF for PVA, for the block copolymers we could not reach the expected SEC diagrams. The obtained results showed bimodal and broad molecular weight distributions. Figure 4.16 shows the SEC curve of C-AN1 in THF system, with the  $M_n$  and  $M_w/M_n$  values indicated in Table 4.2. The broad molecular weight distribution and the previously discussed high molecular weight shoulder could be observed.

Table 4.2. SEC analysis data of C-AN1

Name	$M_n$	$M_w$	$M_w/M_n$
C-AN1	19253	34021	1.77

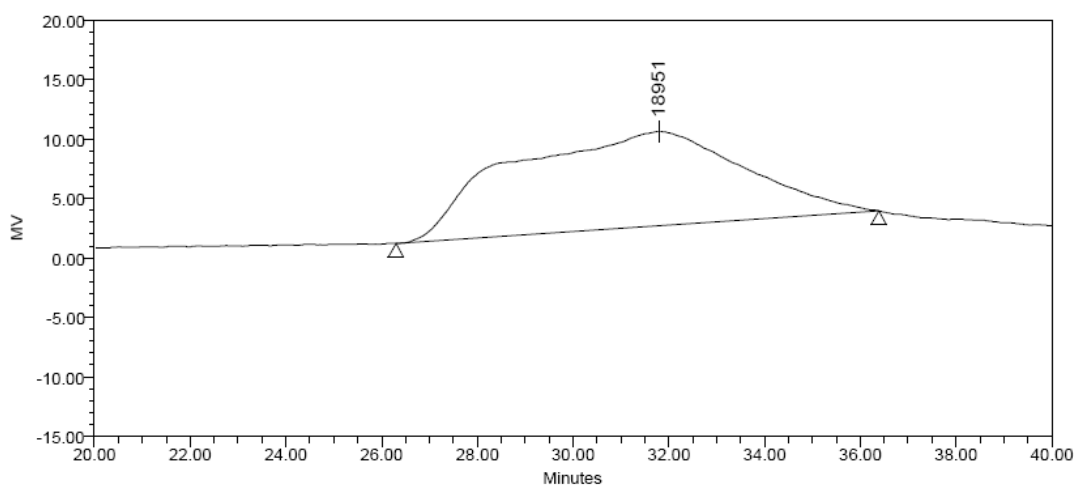


Figure 4.16. SEC curve of C-AN1

#### 4.4.2. Synthesis of C-AN2 and C-AN3

In order to examine the effect of composition, block copolymers were synthesized (Figure 4.13) with different PVA: PNIPAM ratios

4.4.2.1. Synthesis of C-AN2. PVA macro-CTA (C-PVA1) and NIPAM were introduced to the system for the synthesis of PVA-b-PNIPAM block copolymer, with the calculated molar ratio of PVA:PNIPAM as 2:1.

The product C-AN2 was compared physically with C-AN1, which contained 1:1 composition of both polymer units in its structure. It was observed that C-AN2 containing mainly PVA was a soft material with powder-like appearance.

From the  $^1\text{H}$  NMR spectrum of the block copolymer (Figure 4.17), the peak b at 4.8-5.0 ppm corresponding to the methine proton of PVA and the peak f at 4.0 ppm corresponding to the methine proton of the isopropyl group of PNIPAM were selected in order to determine the composition of both units. The integration of the peaks gave the molar ratio of PVA:PNIPAM as 2.07:1.00

4.4.2.2. Synthesis of C-AN3. PVA macro-CTA (C-PVA1) and NIPAM were introduced to the system for the synthesis of PVA-b-PNIPAM block copolymer, with the calculated molar ratio of PVA:PNIPAM as 1:2.

The product C-AN3 was observed to be rigid in comparison to C-AN1. This property may be attributed to the high PNIPAM content of the block copolymer.

To investigate the composition of the block copolymer, the peaks b and f from the  $^1\text{H}$  NMR spectrum (Figure 4.18) were chosen again, corresponding to methine proton of PVA and methine proton of the isopropyl group of PNIPAM, respectively. The integration of the peaks gave the molar ratio of PVA:PNIPAM as 1.00:2.02.

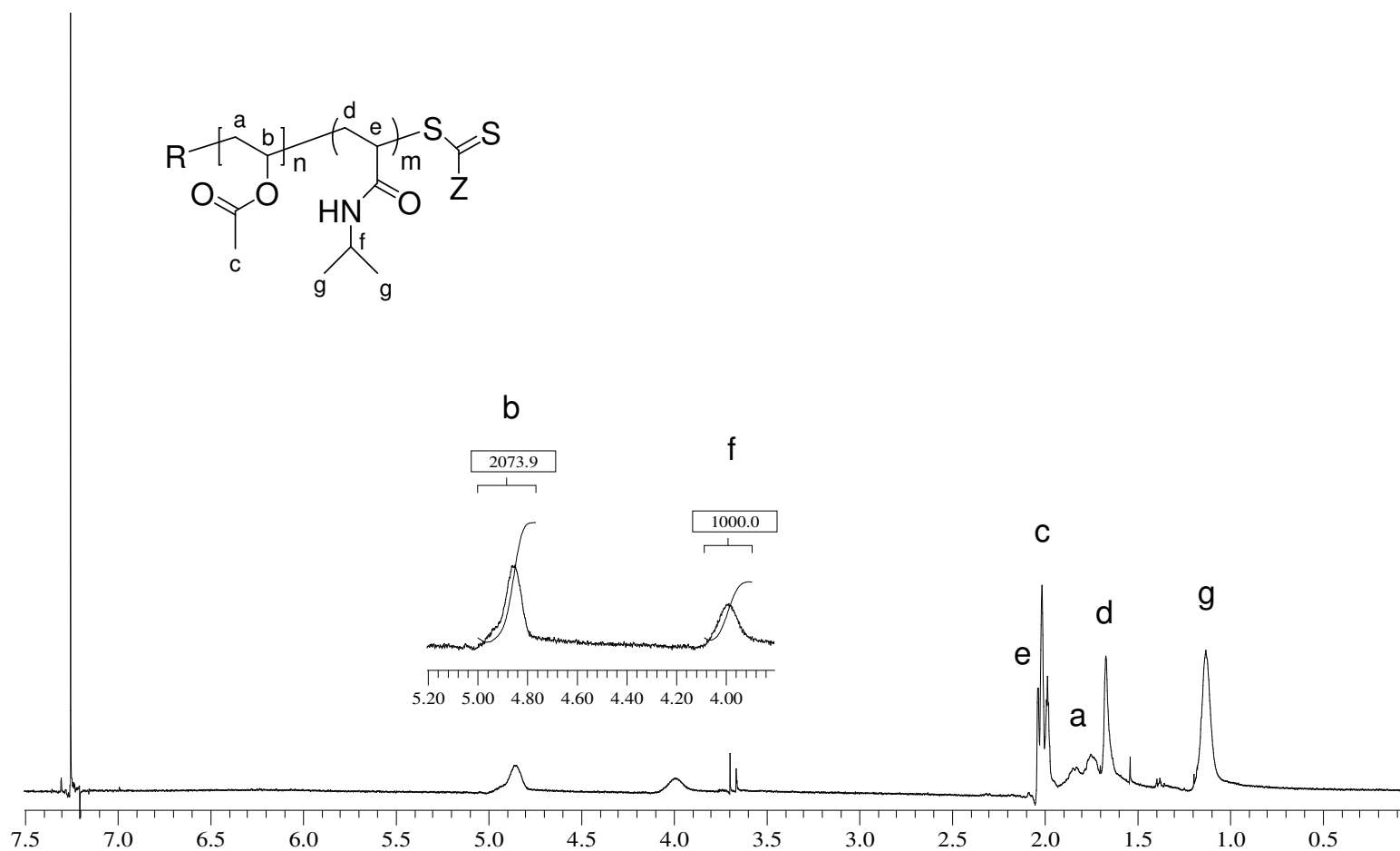


Figure 4.17.  $^1\text{H}$  NMR spectrum of C-AN2

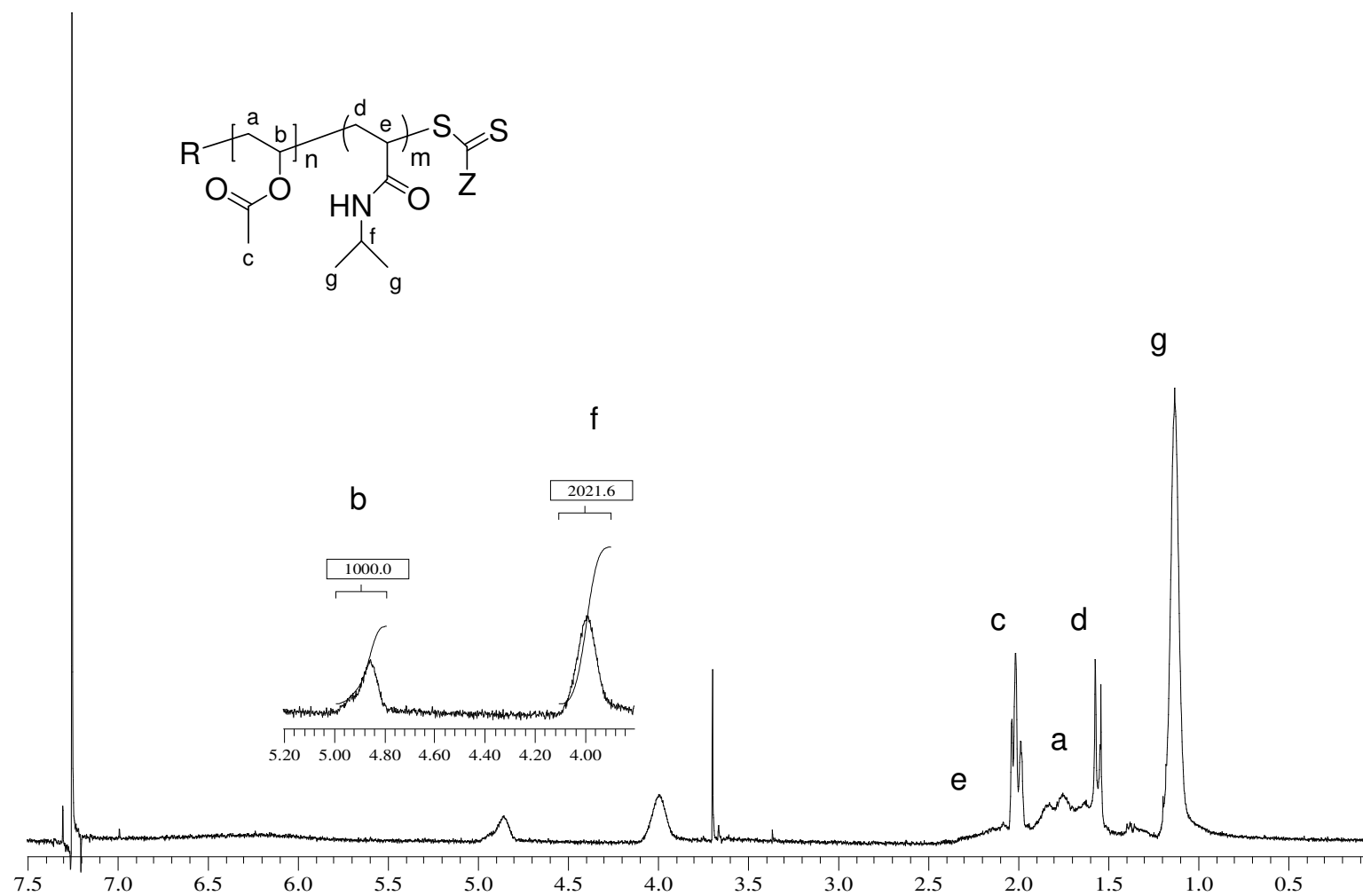


Figure 4.18.  $^1\text{H}$  NMR spectrum of C-AN3

#### 4.4.3. Synthesis of C-AN4 and C-AN5

In the previous polymerization reactions for the synthesis of block copolymers, the molar ratio of CTA and initiator AIBN was kept constant, with CTA:AIBN as 1.00:0.83. In order to examine the effect of this ratio on chain length and molecular weight distribution, two reaction sets were prepared, with the ratios of CTA:AIBN as shown in Table 4.3.

Table 4.3. The ratio of CTA and initiator

Name	CTA : AIBN
C-AN4	1.00 : 0.85
C-AN5	1.00 : 0.43

The products were designed to be block copolymers with the ratio of PVA:PNIPAM as 1:1. The reactions were carried out as shown in Figure 4.13. Since the CTA amount was fixed for the given PVA macro-CTA, different ratios of CTA to AIBN were obtained by the variation of the AIBN amount in the reaction media. C-PVA2 was used as the macro-CTA for both reactions, which was synthesized as discussed in section 4.2.2. C-AN4 had the same CTA:AIBN ratio as in the initially synthesized block copolymers C-AN1 to C-AN3. C-AN5 was designed for the first time.

$^1\text{H}$  NMR spectra of the products C-AN4 and C-AN5 showed the same peaks as the initially synthesized 1:1 block copolymer C-AN1, as described in section 4.4.1.

Figure 4.19 and Figure 4.20 shows SEC analysis of the samples, yielding broad and bimodal molecular weight distribution as in C-AN1, which was discussed in section 4.4.1. A small peak at the low molecular weight region is observed, which was considered to be due to termination reactions leading to formation of low molecular weight products.

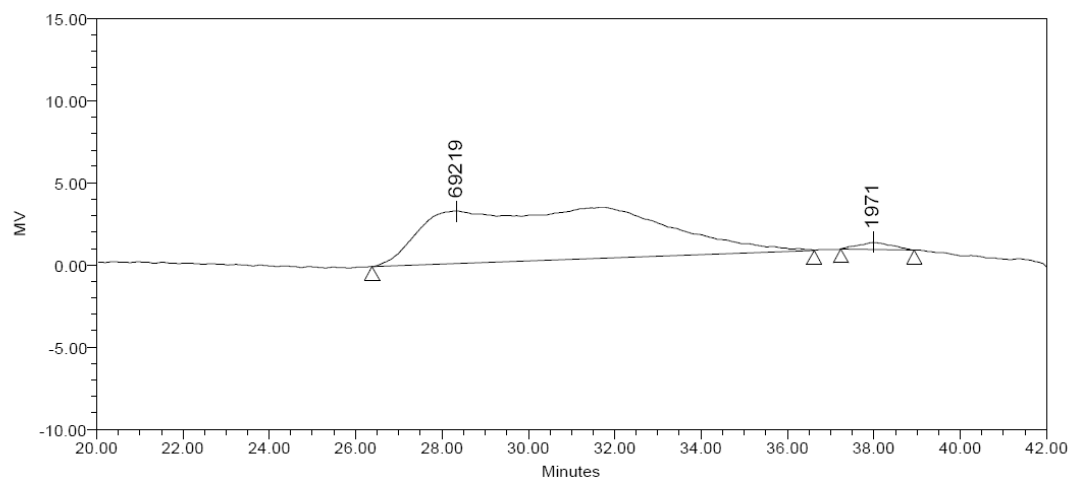


Figure 4.19. SEC curve of C-AN4

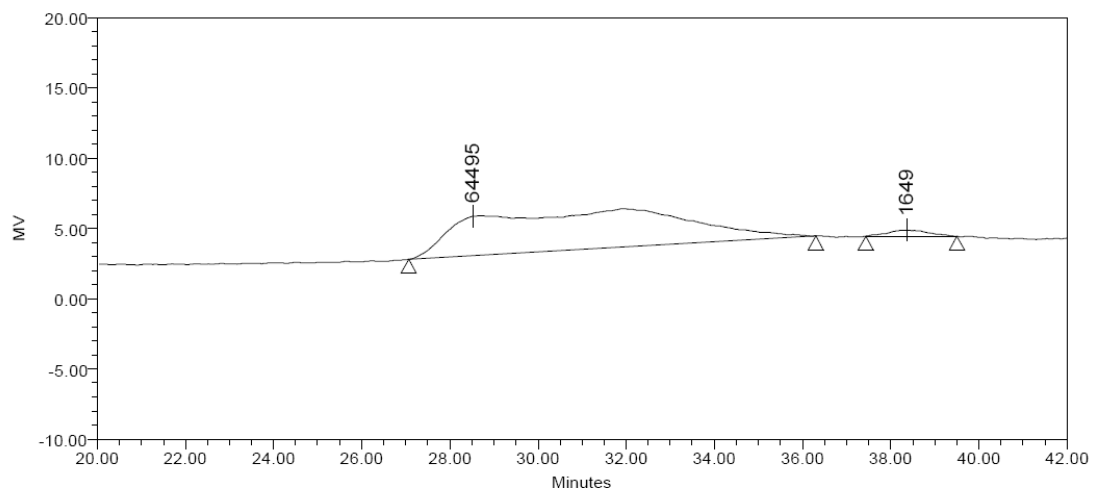


Figure 4.20. SEC curve of C-AN5



Table 4.4. SEC analysis data of C-AN4 and C-AN5

Name	$M_n$	$M_w$	$M_w/M_n$
C-AN4	21380	39139	1.83
C-AN5	19813	33649	1.70

The sample C-AN4 with the CTA:AIBN ratio of 1.00:0.85 shows higher  $M_n$  and  $M_w/M_n$  values with respect to C-AN5, as presented in Table 4.4. With the higher amount of AIBN in the system, the possibility of termination reactions would also be high. This would increase the possibility of the coupling reactions of the PVA macro-CTAs, which would lead to the formation of homopolymers with molecular weight values similar to that of the expected block copolymer. Thus, the amount of NIPAM monomer per macro-CTA would be higher than originally intended, increasing the probability of formation of block copolymers with high molecular weight and polydispersity [4].

As the AIBN amount is decreased to half in sample C-AN5, the termination reactions would be diminished with the lowering of the AIBN amount and hence the decrease of the radical amount in the system. In this case, the occurrence of coupling reactions would be lessened. As a result, the relatively smaller difference in the amount of NIPAM monomer per macro-CTA would lead to synthesis of block copolymers with lower molecular weight and polydispersity [4].

#### 4.4.4. Synthesis of C-AN6 and C-AN7

Two additional sets of reactions with the varying compositions of PVA and PNIPAM were prepared, mimicking the synthesis in 4.2.2. Here, CTA:AIBN ratio of 1.00:0.43 was used, and the macro-CTA was C-PVA2.

4.4.4.1. Synthesis of C-AN6. PVA macro-CTA (C-PVA2) and NIPAM were introduced to the system for the synthesis of PVA-b-PNIPAM block copolymer, with the calculated molar ratio of PVA:PNIPAM as 2:1.

The product C-AN6 resembled C-AN2 physically, with the similar powder-like appearance.

From the  $^1\text{H}$  NMR spectrum (Figure 4.21) the composition of the block copolymer was determined as PVA:PNIPAM as 2.04:1.00

4.4.4.2. Synthesis of C-AN7. PVA macro-CTA (C-PVA2) and NIPAM were introduced to the system for the synthesis of PVA-b-PNIPAM block copolymer, with the calculated molar ratio of PVA:PNIPAM as 1:2.

The product C-AN7 was physically similar to C-AN3, with the rigid structure.

From the  $^1\text{H}$  NMR spectrum (Figure 4.22) the composition of the block copolymer was determined as PVA:PNIPAM as 2.17:1.00

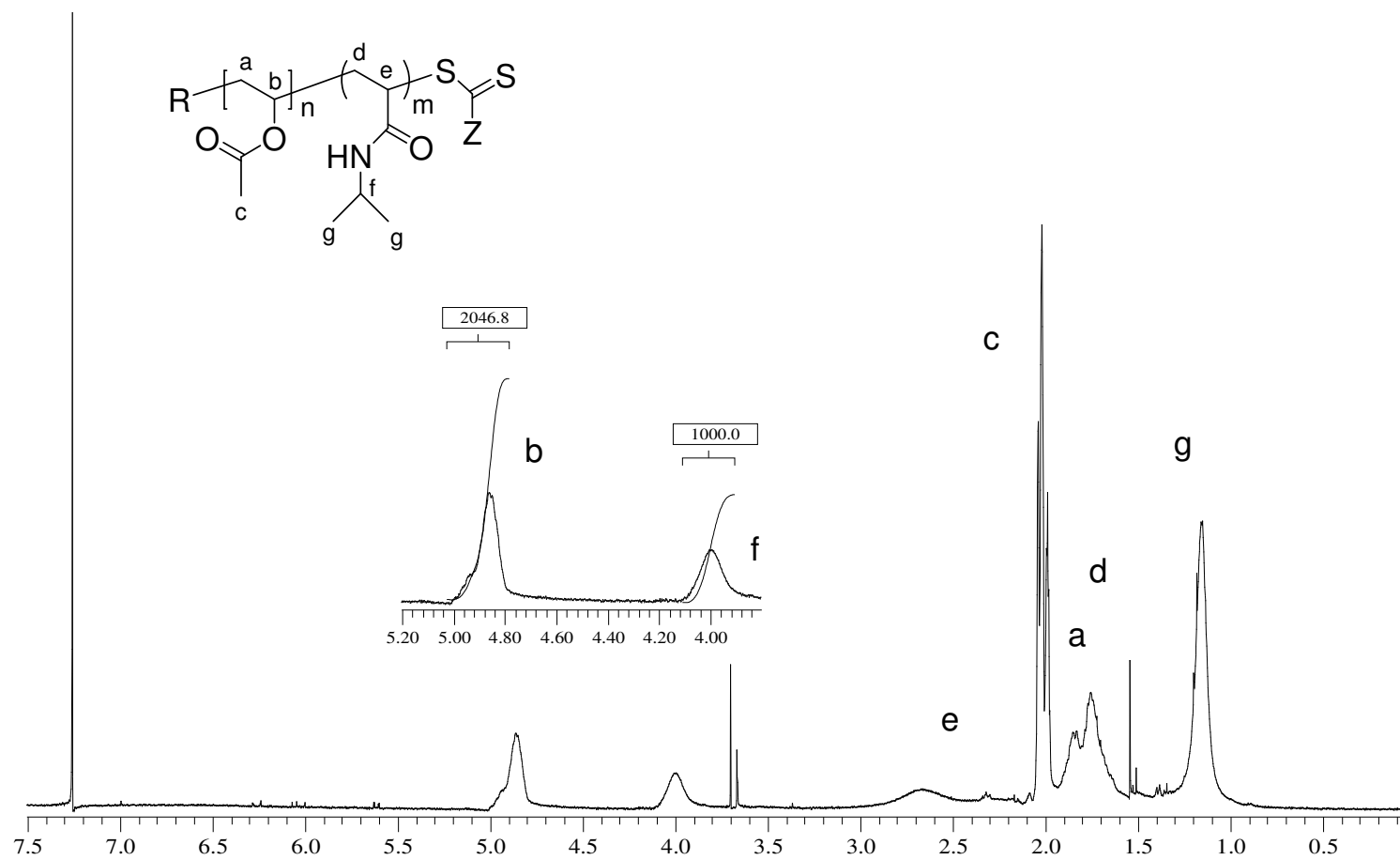


Figure 4.21.  $^1\text{H}$  NMR spectrum of C-AN6

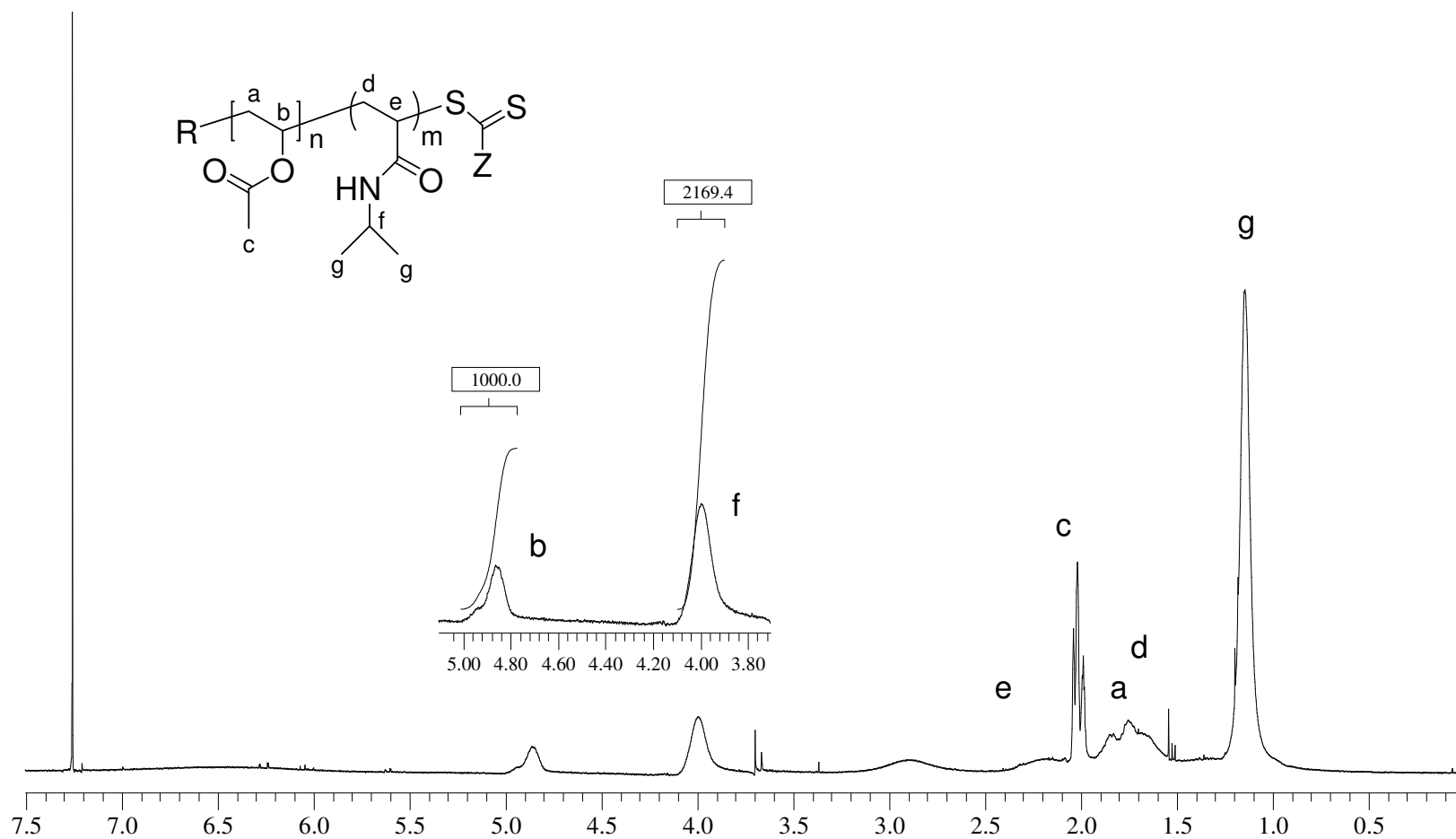


Figure 4.22.  $^1\text{H}$  NMR spectrum of C-AN7

#### 4.5. Kinetic Study

The samples taken at different time intervals during the reaction were characterized by  $^1\text{H}$  NMR spectroscopy. The per cent conversions were calculated by the comparison of relative intensities of specific peaks belonging to PVA (methine proton at 4.8-5.0 ppm), NIPAM monomer (vinyl proton at 5.6 ppm) remaining in the system and newly forming PNIPAM block (methine proton of isopropyl group at 4.0 ppm). Figure 4.23 shows the per cent conversion versus time graph, drawn from the data given at Table 4.5.

Table 4.5. Variation of conversion as function of time

Time (min)	Conversion (%)
5	2.11
10	22.66
15	35.01
20	42.46
30	59.54
60	68.80
120	83.26
240	97.15
324	98.29

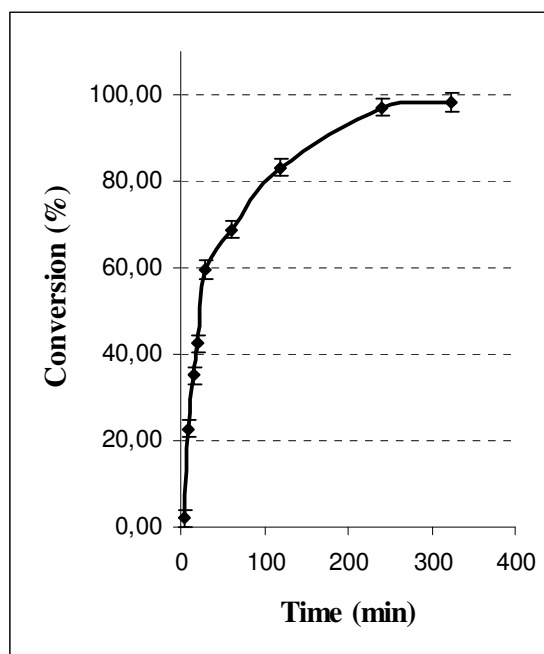


Figure 4.23. Variation of conversion as function of time

The results showed that the polymerization proceeded very quickly, even at early stages of the reaction. A linear relationship between conversion and reaction time was observed. The conversion reached to 60 % within 40 minutes. Almost complete conversion was attained at 250 minutes.

#### 4.6. Thermal Characterization

The polymer samples were subjected to thermal characterization by DSC analysis in order to examine the glass transition temperatures ( $T_g$ ). The average glass transition temperatures of the synthesized diblock copolymers of PVA-b-PNIPAM are collected in Table 4.6, as well as the  $T_g$  values obtained from PVA and PNIPAM homopolymers.

Table 4.6. Glass transition temperatures of obtained polymers

Sample	$T_{g1}$ -[PVA block] ( $^{\circ}\text{C}$ )	$T_{g2}$ -[PNIPAM block] ( $^{\circ}\text{C}$ )
C-PVA	35.67	-
C-PNIPAM	-	136.27
1 PVA : 1 PNIPAM	36.31	131.47
2 PVA : 1 PNIPAM	36.04	132.19
1 PVA : 2 PNIPAM	41.28	137.63

The obtained block copolymers polymers, as expected, exhibit two different  $T_g$  values.

Figure 4.24 shows the DSC curves of block copolymer C-AN1 (1 PVA:1 PNIPAM) and homopolymers C-PVA and C-PNIPAM. The block copolymer clearly exhibits the two  $T_g$  values belonging to PVA and PNIPAM blocks. These average  $T_g$  values are closer to each other with respect to the original values of PVA and PNIPAM homopolymers. This indicates that both polymer sequences are well distributed in each other. The  $T_g$  of PVA is higher in the block copolymers compared to that of pure PVA, due to the motional restrictions imposed by PNIPAM.

The DSC curves of three block copolymer samples with different compositions are shown in Figure 4.25. It is observed that the sample with 2 PVA:1 PNIPAM molar ratio shows smaller  $T_g$  for PNIPAM block than pure homopolymer. The presence of longer PVA segments in the block copolymer structure is considered to be the reason of the lowering of  $T_g$ , as the larger PVA segment inflicted motional ease.

The sample with 1 PVA:2 PNIPAM molar ratio shows greater  $T_g$  values for PVA and PNIPAM blocks than pure homopolymers. The occurrence of higher  $T_g$  values is regarded to be due to motional restrictions imposed by PNIPAM, arising from its greater content in the block copolymer structure.



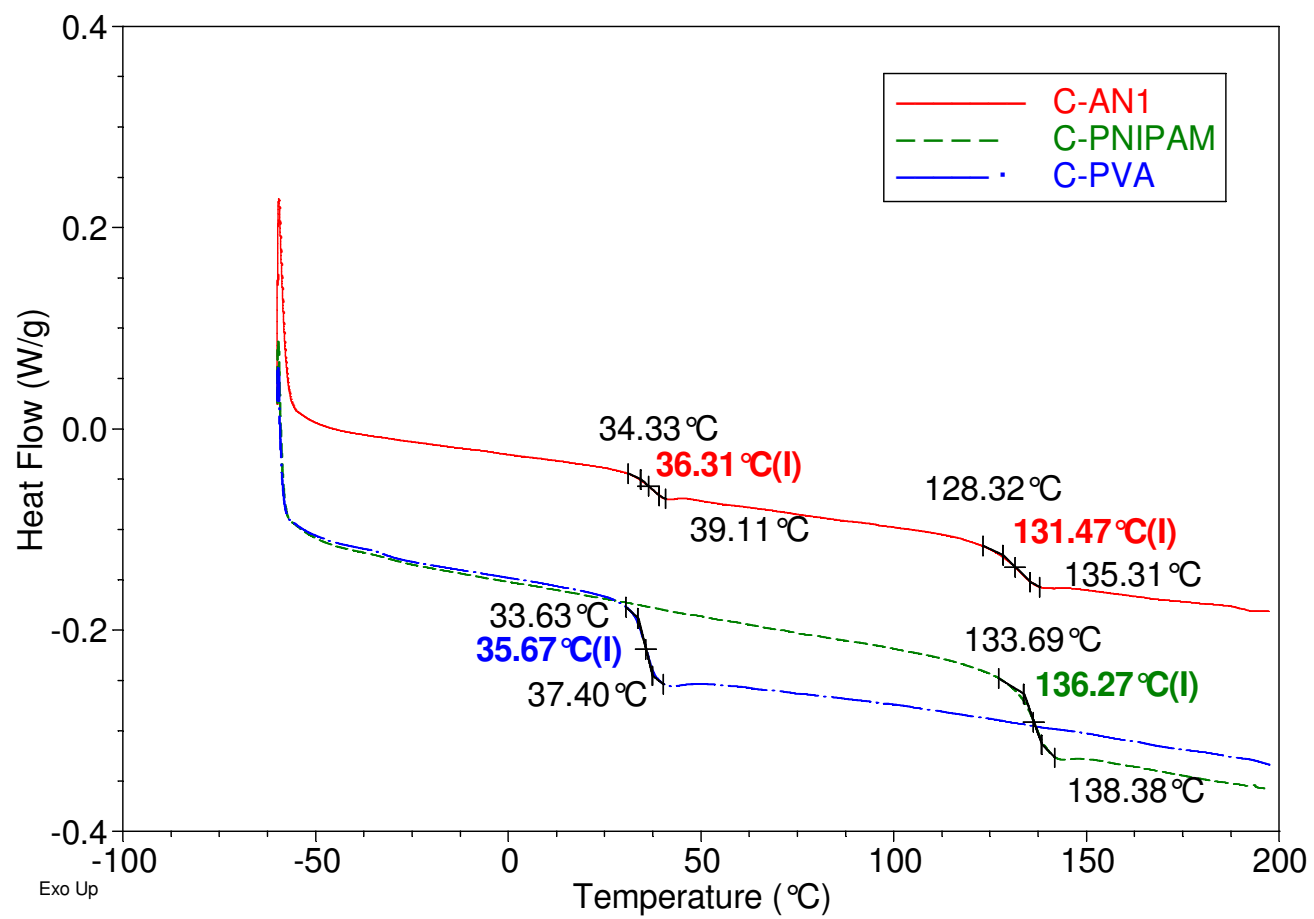


Figure 4.24. DSC curves of C-AN1, C-PNIPAM and C-PVA

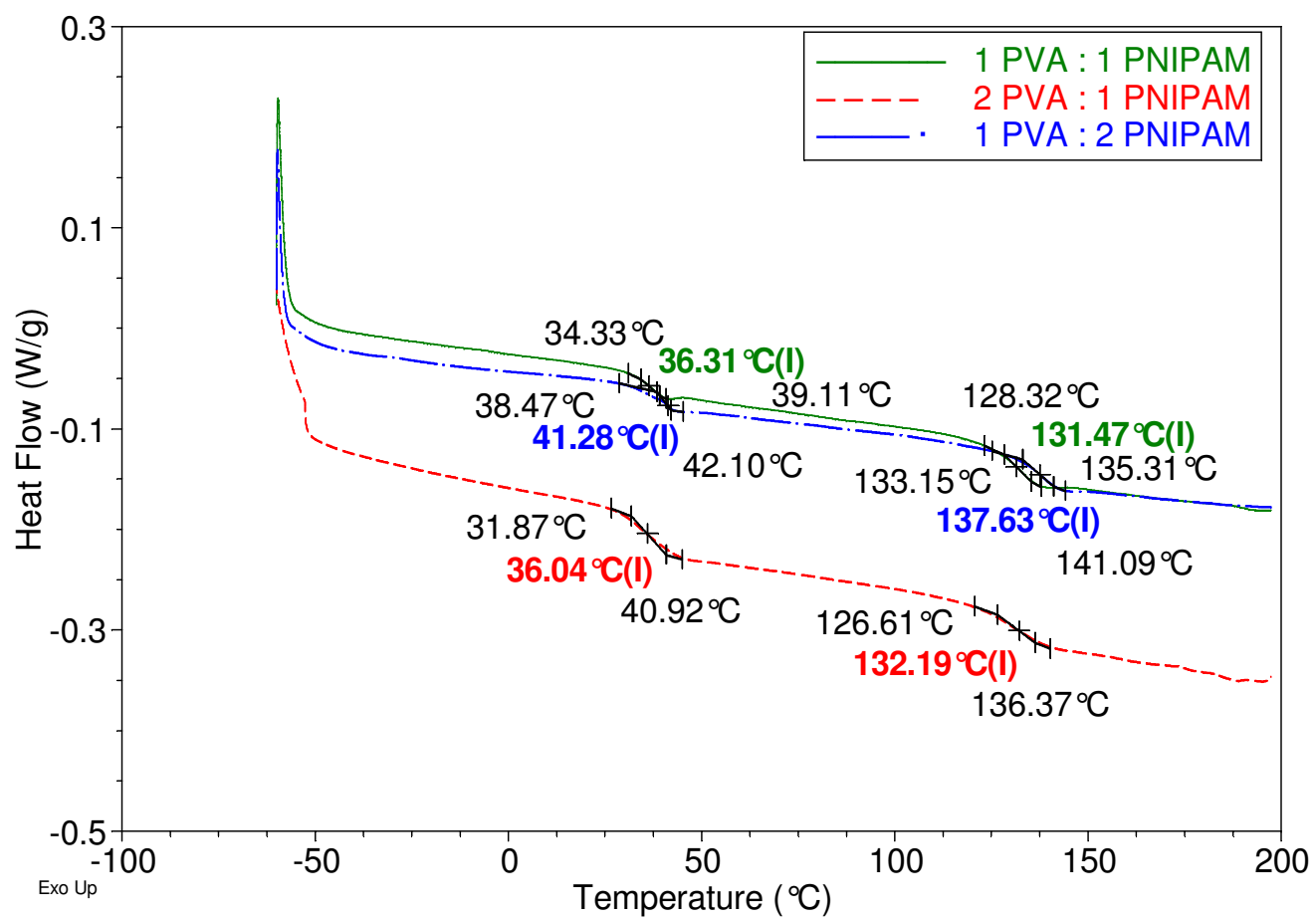


Figure 4.25. DSC curves of (1 PVA:1 PNIPAM), (2 PVA:1 PNIPAM) and (1 PVA:2 PNIPAM)

## 4.7. Morphological Analysis

### 4.7.1. ESEM Analysis

Block copolymers with three different compositions were examined by ESEM, as listed in Table 4.7. The samples were taken from the previously freeze-dried polymers.

Table 4.7. Composition of samples for morphological analysis

Name	PVA : PNIPAM
C-AN1	1.00 : 1.00
C-AN2	2.07 : 1.00
C-AN3	1.00 : 2.02

When the three samples are compared, as shown in Figure 4.26, three different morphologies could be observed.

The block copolymer with the high PVA content (Figure 4.26a) displays a discrete and rough structure, large porous matrix remains. The presence of mostly PVA in the matrix leads to weak interaction between polymer chains, most probably due to scantiness of hydrogen bonding.

For C-AN1 with 1:1 composition, more interaction between polymer chains are observed, due to hydrogen bonding arising from NIPAM units. The ESEM image (Figure 4.26b) exhibits a smoother surface as a result of enhanced chain interactions.

The sample with high PNIPAM content displays stronger interactions between chains. The overall surface is smoother with respect to the other samples and the pore size is smaller (Figure 4.26c)

These results show that the composition influence not only the morphology of copolymer matrix in terms of phase separation, but also the density of the polymer.

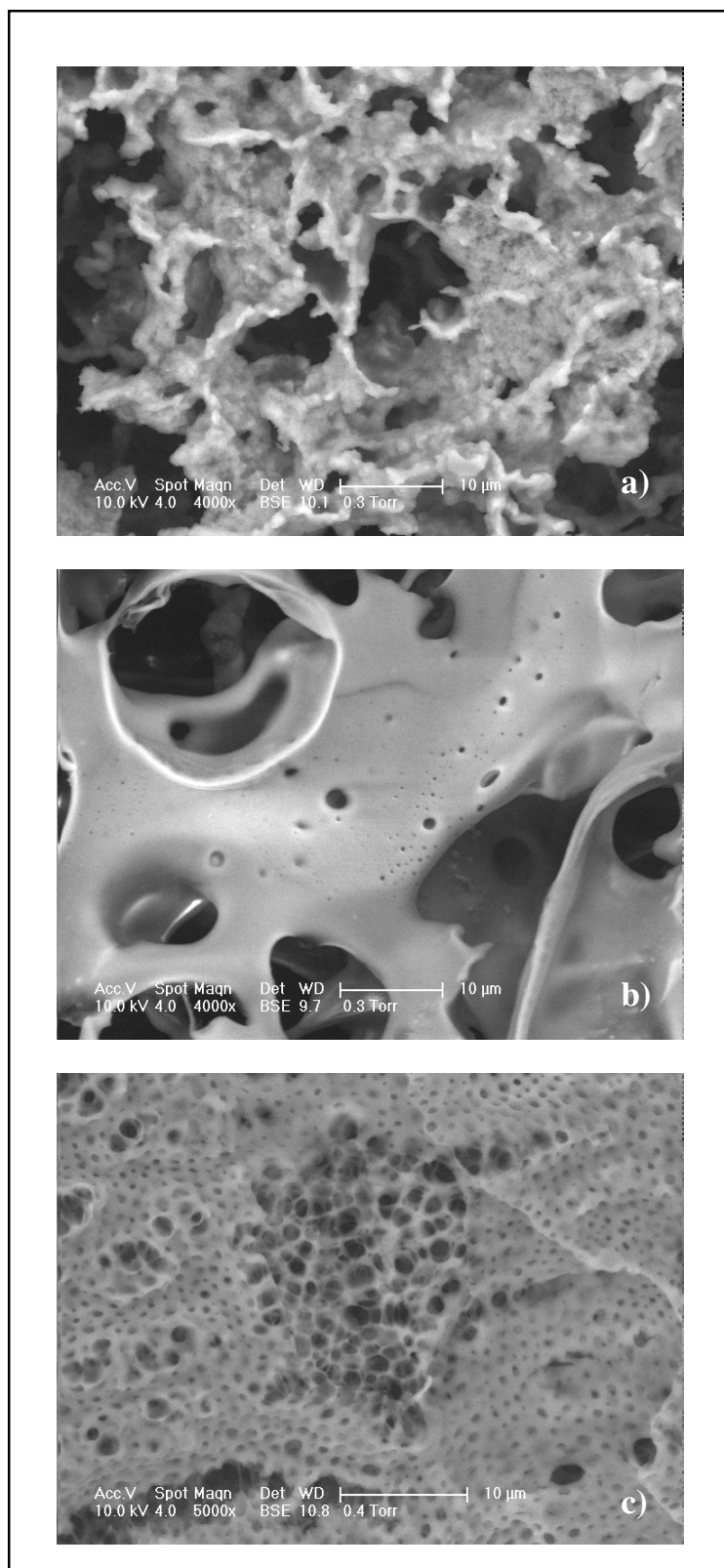


Figure 4.26. High magnification SEM images of (a) C-AN2, (b) C-AN1 and (c) C-AN3

#### 4.7.2. AFM Analysis

Block copolymers with three different compositions were examined by AFM, as listed in Table 4.7. The samples were dissolved in chloroform and then cast onto glass surface by spin coating to obtain thin films. The tapping mode AFM images of the block copolymers at scan size of 5  $\mu\text{m}$  are shown in Figure and Figure, as 3D-wave images and 2D-phase images respectively.

Among the two polymer segments, PVA is more selective for chloroform, although both PVA and PNIPAM could be dissolved in it. Therefore, as chloroform was evaporated during the spin-coating, PNIPAM block was considered to be the first to collapse on the glass surface. The affinity of NIPAM units to the polar glass surface would also be a driving force for this behavior. PVA block was deposited on top of this layer. Thus, the light colored “hill” or “island” type of appearance is regarded to be arising from PVA block and the darker colored “valleys” are composed of PNIPAM phase.

In the sample with high PVA content, shown in Figure 4.28a, the surface is highly occupied by PVA and the dark regions corresponding to very narrow valleys of PNIPAM could be observed between PVA islands. The phase image in Figure 4.29a also shows the mentioned occupation of PVA phase.

Figure 4.28b shows the AFM image of 1:1 PVA:PNIPAM sample. It is observed that both phases belonging to the two blocks of the copolymer are evenly distributed throughout the matrix, with large domain sizes. The distinction of the different regions could be observed in the phase image also (Figure 4.29b).

In the case of PNIPAM-rich block copolymer, shown in Figure 4.28c, broad and continuous PNIPAM valleys and well distributed small PVA islands could be observed. The phase image in Figure 4.29c also shows the darker regions of PNIPAM in the matrix.

The models proposed for the morphologies of the three different composition samples are given in Figure 4.27.

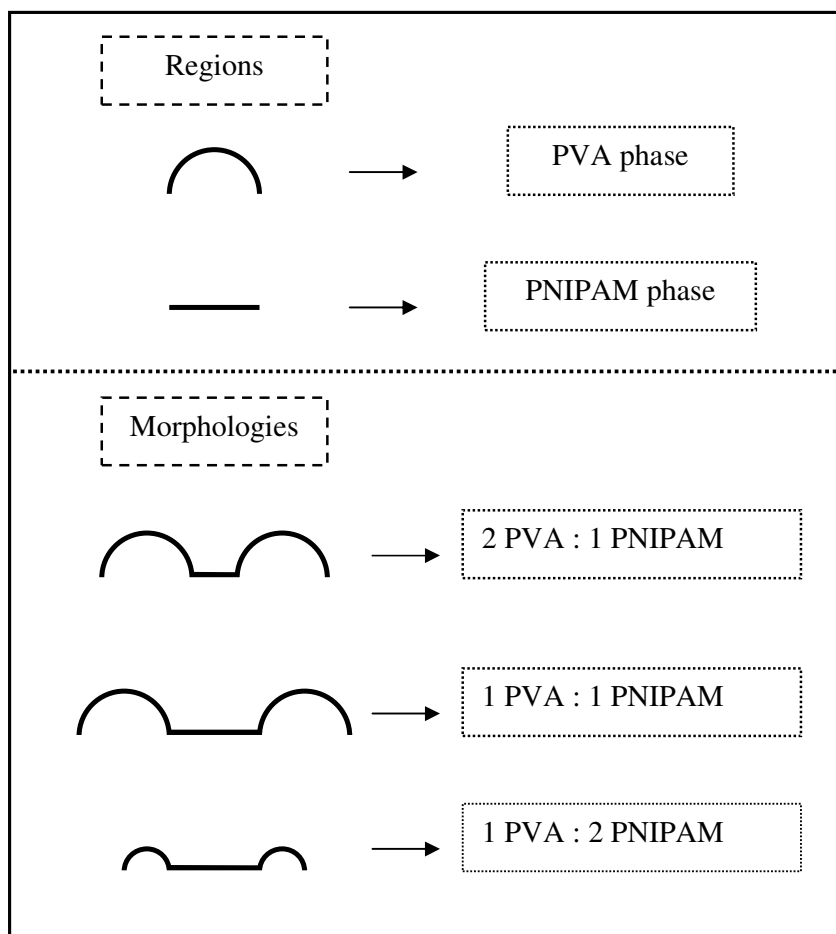


Figure 4.27. Proposed model for morphologies of polymer samples

All three examined cases show homogeneously distributed phases, which is a very good indication of the block copolymer structure. It is noticed that the solvent and the surface properties of the substrate used in casting application could influence the morphology of the samples.

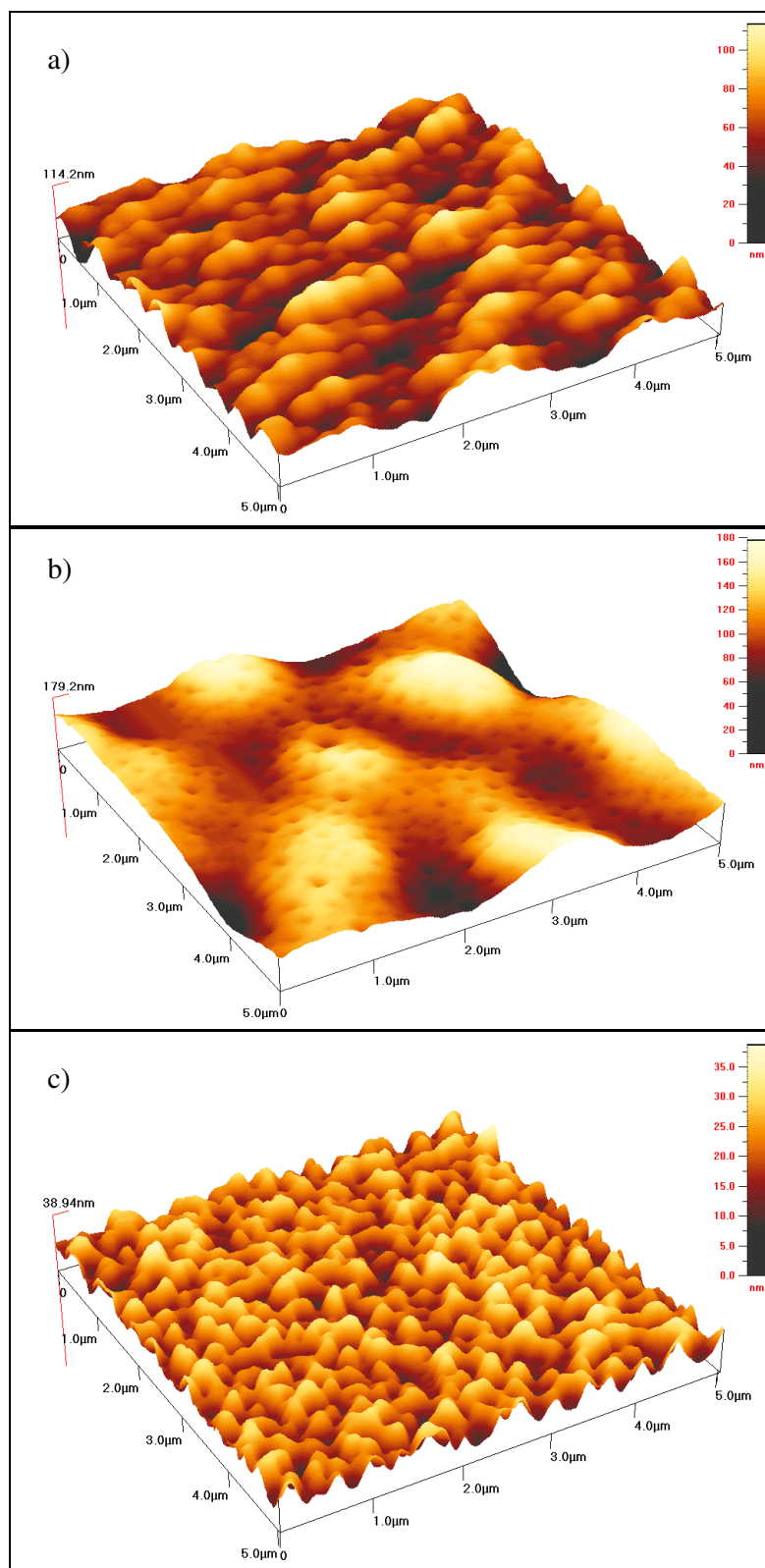


Figure 4.28. AFM 3D-wave images of (a) C-AN2, (b) C-AN1 and (c) C-AN3

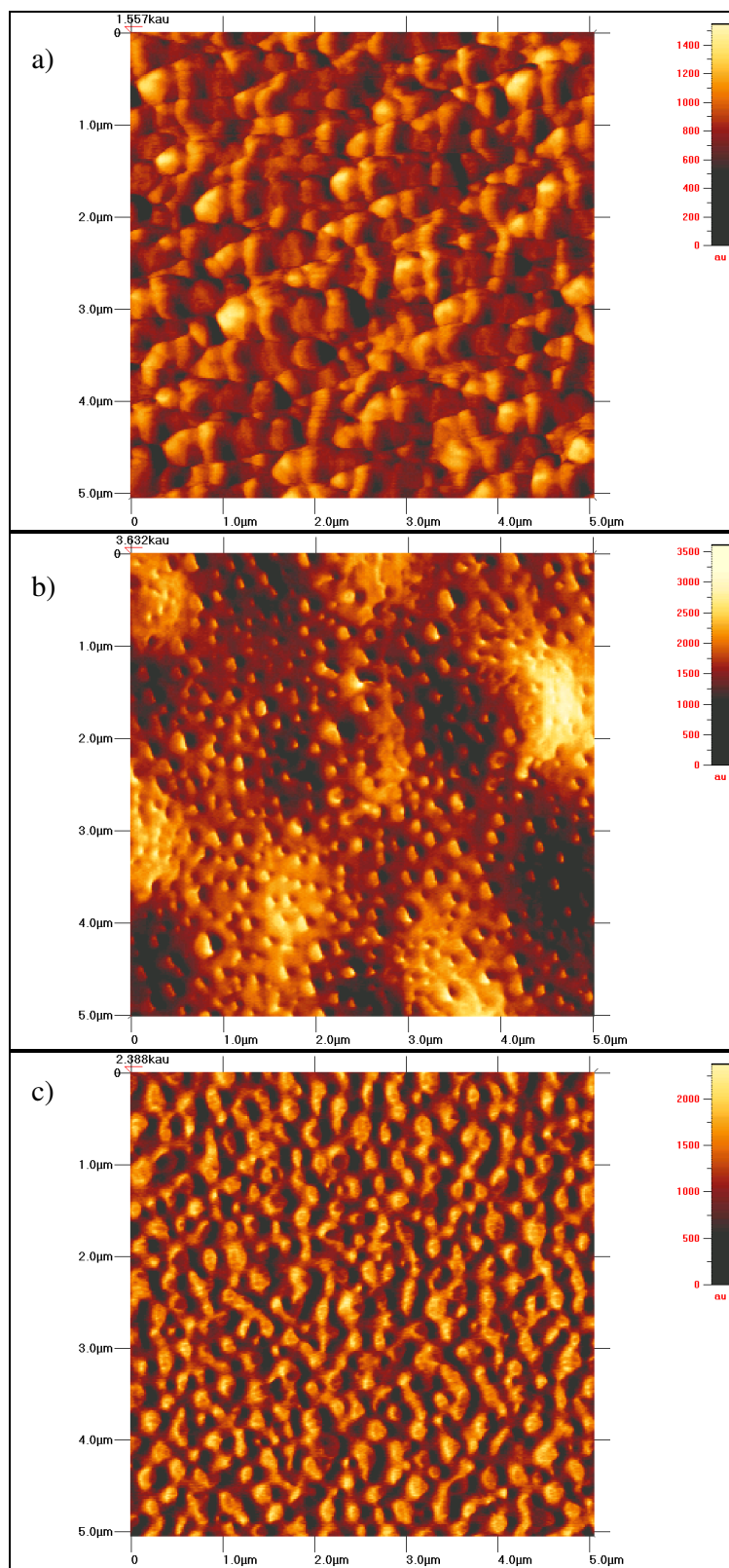


Figure 4.29. AFM 2D-phase images of (a) C-AN2, (b) C-AN1 and (c) C-AN3



## 5. CONCLUSIONS

PVA-b-PNIPAM block copolymers were successfully prepared for the first time via MADIX process, using MIPCTSA as chain transfer agent.

The presence of both blocks in the copolymer structure was confirmed and properties of block copolymers were investigated by using  $^1\text{H}$  NMR, FTIR, SEC, DSC, ESEM and AFM techniques.

The  $^1\text{H}$  NMR data showed the incorporation of both polymers in the block copolymer structure with the expected composition based on the feed ratio.  $^1\text{H}$  NMR characterization of the samples obtained from kinetic study showed that the polymerization proceeded very quickly, even at early stages of the reaction. A linear relationship between conversion and reaction time was observed. Within 40 minutes, the conversion reached to 60 % and at 250 minutes almost complete conversion was attained.

FTIR spectra showed the characteristic absorptions of both polymer sequences.

The problems arising in the SEC characterization of PNIPAM were discussed in literature. Apart from these, the usage of polystyrene standards in the calibration of the instruments also affects the results. In view of these circumstances, the deviations in the obtained molecular weight values and molecular weight distributions are expected. On the other hand, the SEC data were investigated as relative values in the presentation of this thesis, so that the variations in molecular weight can be considered to be quite similar to that of actual molecular weight.

The DSC analysis showed the two  $T_g$  values belonging to PVA and PNIPAM blocks in the copolymer structure. The  $T_g$  values were closer to each other with respect to the original values of homopolymers, which indicated that both polymer sequences were well distributed in each other. The increase in  $T_g$  of PVA was considered to be due to the motional restrictions imposed by PNIPAM.

ESEM characterization showed that the composition of the samples influenced the general morphology and density of the block copolymers.

AFM results showed homogeneously distributed phases, which was a very good indication of the block copolymer structure. The influence of the surface properties of the substrate and the solvent used in casting application on the morphology of the samples were observed.

## REFERENCES

1. Matyjaszewski, K., "Controlled/Living Radical Polymerization: State of the Art in 2002", *ACS Symposium Series*, Vol. 854, pp. 2-9, 2003.
2. Russum, J. P., "Controlled Radical Polymerizations in Miniemulsions: Advances in the Use of RAFT", Ph.D. Thesis, Georgia Institute of Technology, 2005.
3. Patten, T. E. and K. Matyjaszewski, "Atom Transfer Radical Polymerization and the Synthesis of Polymeric Materials", *Advanced Materials*, Vol. 10, No. 12, pp. 901-915, 1998.
4. Perrier, S. and P. Takolpuckdee, "Macromolecular Design via Reversible Addition-Fragmentation Chain Transfer (RAFT)/Xanthates (MADIX) Polymerization", *Journal of Polymer Science: Part A: Polymer Chemistry*, Vol. 43, pp. 5347-5393, 2005.
5. Schilli, C., M. G. Lanzendörfer and A. H. E. Müller, "Benzyl and Cumyl Dithiocarbamates as Chain Transfer Agents in the RAFT Polymerization of N-Isopropylacrylamide. In Situ FT-NIR and MALDI-TOF MS Investigation", *Macromolecules*, Vol. 35, No. 18, pp. 6819-6827, 2002.
6. Chong, Y. K., T. P. T. Le, G. Moad, E. Rizzardo and S. H. Thang, "A More Versatile Route to Block Copolymers and Other Polymers of Complex Architecture by Living Radical Polymerization: The RAFT Process", *Macromolecules*, Vol. 32, No. 6, pp. 2071-2074, 1999.
7. Mayadunne, R. T. A., E. Rizzardo, J. Chiefari, Y. K. Chong, G. Moad and S. H. Thang, "Living Radical Polymerization with Reversible Addition-Fragmentation Chain Transfer (RAFT Polymerization) Using Dithiocarbamates as Chain Transfer Agents", *Macromolecules*, Vol. 32, No. 21, pp. 6977-6980, 1999.

8. Chiefari, J., Y. K. Chong, F. Ercole, J. Krstina, J. Jeffery, T. P. T. Le, R. T. A. Mayadunne, G. F. Meijs, C. L. Moad, G. Moad, E. Rizzardo and S. H. Thang, "Living Free-Radical Polymerization by Reversible Addition-Fragmentation Chain Transfer: The RAFT Process", *Macromolecules*, Vol. 31, No. 16, pp. 5559-5562, 1998.
9. Barner-Kowollik, C., T. P. Davis, J. P. A. Heuts, M. H. Stenzel, P. Vana and M. J. Whittaker, "RAFTing Down Under: Tales of Missing Radicals, Fancy Architectures, and Mysterious Holes", *Journal of Polymer Science: Part A: Polymer Chemistry*, Vol. 41, pp. 365-375, 2003.
10. Moad, G., J. Chiefari, Y. K. Chong, J. Krstina, R. T. A. Mayadunne, A. Postma, E. Rizzardo and S. H. Thang, "Living free radical polymerization with reversible addition – fragmentation chain transfer (the life of RAFT)" *Polymer International*, Vol. 49, pp. 993-1001, 2000.
11. Hawthorne, D. G., G. Moad, E. Rizzardo and S. H. Thang, "Living Radical Polymerization with Reversible Addition-Fragmentation Chain Transfer (RAFT): Direct ESR Observation of Intermediate Radicals" *Macromolecules*, Vol. 32, No. 16, pp. 5457-5459, 1999.
12. Alberti, A., M. Benaglia, M. Laus, D. Macciantelli and K. Sparnacci, "Direct ESR Detection of Free Radicals in the RAFT Polymerization of Styrene" *Macromolecules*, Vol. 36, No. 3, pp. 736-740, 2003.
13. Chernikova, E., A. Morozov, E. Leonova, E. Garina, V. Golubev, C. Bui and B. Charleux, "Controlled Free-Radical Polymerization of n-Butyl Acrylate by Reversible Addition-Fragmentation Chain Transfer in the Presence of tert-Butyl Dithiobenzoate. A Kinetic Study", *Macromolecules*, Vol. 37, No. 17, pp. 6329-6339, 2004.
14. Calitz, F. M., M. P. Tonge and R. D. Sanderson, "Electron Spin Resonance Studies of Reversible Addition-Fragmentation Transfer Polymerization", *Macromolecular Symposia*, Vol. 193, pp. 277-288, 2003.

15. Ren, Y., Z. Zhu and J. Huang, "Radical Copolymerization of Maleimide with Ethyl  $\alpha$  - Ethylacrylate and  $\alpha$  -Ethylacrylic Acid via RAFT", *Journal of Polymer Science: Part A: Polymer Chemistry*, Vol. 42, pp. 3828-3835, 2004.
16. Perrier, S., P. Takolpuckdee, J. Westwood, and D. M. Lewis, "Versatile Chain Transfer Agents for Reversible Addition Fragmentation Chain Transfer (RAFT) Polymerization to Synthesize Functional Polymeric Architectures", *Macromolecules*, Vol. 37, No. 8, pp. 2709-2717, 2004.
17. Destarac, M., D. Charmot, X. Franck and S. Z. Zard, "Dithiocarbamates as universal reversible additionfragmentation chain transfer agents", *Macromolecular Rapid Communications*, Vol. 21, No. 15, pp. 1035-1039, 2000.
18. Destarac, M., W. Bzducha, D. Taton, I. Gauthier-Gillaizeau and S. Z. Zard, "Xanthates as Chain-Transfer Agents in Controlled Radical Polymerization (MADIX): Structural Effect of the *O*-Alkyl Group", *Macromolecular Rapid Communications*, Vol. 23, No. 17, pp. 1049–1054, 2002.
19. Chiefari, J., R. T. A. Mayadunne, C. L. Moad, G. Moad, E. Rizzardo, A. Postma, M. A. Skidmore and S. H. Thang, "Thiocarbonylthio Compounds ( $S=C(Z)S-R$ ) in Free Radical Polymerization with Reversible Addition-Fragmentation Chain Transfer (RAFT Polymerization). Effect of the Activating Group *Z*", *Macromolecules*, Vol. 36, No. 7, pp. 2273-2283, 2003.
20. Davis, T. P., C. Barner-Kowollik, T. L. U. Nguyen, M H. Stenzel, M, J. F. Quinn and P. Vana, "Influences of the Structural Design of RAFT Agents on Living Radical Polymerization Kinetics", *ACS Symposium Series*, Vol. 854, pp. 551-569, 2003.
21. Destarac, M., C. Brochon, J. M. Catala, A. Wilczewska and S. Z. Zard, "Macromolecular Design via the Interchange of Xanthates (MADIX): Polymerization of Styrene with *O*-Ethyl Xanthates as Controlling Agents", *Macromolecular Chemistry and Physics*, Vol. 203, No. 16, pp. 2281-2289, 2002.

22. Barner-Kowollik, C., J. F. Quinn, T. L. U. Nguyen, J. P. A. Heuts and T. P. Davis, "Kinetic Investigations of Reversible Addition Fragmentation Chain Transfer Polymerizations: Cumyl Phenylthioacetate Mediated Homopolymerizations of Styrene and Methyl Methacrylate", *Macromolecules*, Vol. 34, No. 22, pp. 7849-7857, 2001.
23. Coote, M. L. and D. J. Henry, "Effect of Substituents on Radical Stability in Reversible Addition Fragmentation Chain Transfer Polymerization: An ab Initio Study", *Macromolecules*, Vol. 38, No. 4, pp. 1415-1433, 2005.
24. Chong, Y. K., J. Krystina, T. P. T. Le, G. Moad, A. Postma, E. Rizzardo and S. H. Thang, "Thiocarbonylthio Compounds ( $S=C(Ph)S-R$ ) in Free Radical Polymerization with Reversible Addition-Fragmentation Chain Transfer (RAFT Polymerization). Role of the Free Radical Leaving Group (R)", *Macromolecules*, Vol. 36, No. 7, pp. 2256-2272, 2003.
25. Perrier, S., C. Barner-Kowollik, J. F. Quinn, P. Vana and T. P. Davis, "Origin of Inhibition Effects in the Reversible Addition Fragmentation Chain Transfer (RAFT) Polymerization of Methyl Acrylate", *Macromolecules*, Vol. 35, No. 22, pp. 8300-8306, 2002.
26. Donovan, M. S., A. B. Lowe, B. S. Sumerlin and C. L. McCormick, "RAFT Polymerization of N,N-Dimethylacrylamide Utilizing Novel Chain Transfer Agents Tailored for High Reinitiation Efficiency and Structural Control", *Macromolecules*, Vol. 35, No. 10, pp. 4123-4132, 2002.
27. Taton, D., A.-Z. Wilczewska and M. Destarac, "Direct Synthesis of Double Hydrophilic Statistical Di and Triblock Copolymers Comprised of Acrylamide and Acrylic Acid Units via the MADIX Process" *Macromolecular Rapid Communications*, Vol. 22, No. 18, 1497-1503, 2001.

28. Convertine, A. J., N. Ayres, C. W. Scales, A. B. Lowe and C. L. McCormick, "Facile, Controlled, Room-Temperature RAFT Polymerization of N-Isopropylacrylamide" *Biomacromolecules*, Vol. 5, No. 4, pp. 1177-1180, 2004.
29. Grosberg, A. Y. and A. R. Khokhlov, *Giant Molecules*, Academic Press, New York, 1997.
30. Plummer, R., D. J. T. Hill and A. K. Whittaker, "Solution Properties of Star and Linear Poly(N-isopropylacrylamide)", *Macromolecules*, Vol. 39, No. 24, pp. 8379-8388, 2006.
31. Ganachaud, F., M. J. Monteiro, R. G. Gilbert, M. A. Dourges, S. H. Thang and E. Rizzardo, "Molecular Weight Characterization of Poly(N-isopropylacrylamide) Prepared by Living Free-Radical Polymerization", *Macromolecules*, Vol. 33, No. 18, pp. 6738-6745, 2000.
32. You, Y. Z. and D. Oupicky, "Synthesis of Temperature-Responsive Heterobifunctional Block Copolymers of Poly(ethylene glycol) and Poly(N-isopropylacrylamide)", *Biomacromolecules*, Vol. 8, No. 1, pp. 98-105, 2007.
33. Schilli, C. M., M. Zhang, E. Rizzardo, S. H. Thang, B. Y. K. Chong, K. Edwards, G. Karlsson and A. H. E. Müller, "A New Double-Responsive Block Copolymer Synthesized via RAFT Polymerization: Poly(N-isopropylacrylamide)-b-poly(acrylic acid)", *Macromolecules*, Vol. 37, No. 21, pp. 7861-7866, 2004.
34. Ge, Z., Y. Cai, J. Yin, Z. Zhu, J. Rao and S. Liu, "Synthesis and 'Schizophrenic' Micellization of Double Hydrophilic AB<sub>4</sub> Miktoarm Star and AB Diblock Copolymers: Structure and Kinetics of Micellization", *Langmuir*, Vol. 23, No. 3, pp. 1114-1122, 2007.
35. Boyer, C., V. Bulmus, J. Liu, T. P. Davis, M. H. Stenzel and C. Barner-Kowollik, "Well-Defined Protein-Polymer Conjugates via in Situ RAFT Polymerization", *Journal of American Chemical Society*, Vol. 129, No. 22, pp. 7145-7154, 2007.

36. Hales, M., C. Barner-Kowollik, T. P. Davis and M. H. Stenzel, "Shell-Cross-Linked Vesicles Synthesized from Block Copolymers of Poly(D,L-lactide) and Poly(N-isopropylacrylamide) as Thermoresponsive Nanocontainers" *Langmuir*, Vol. 20, No. 25, pp. 10809-10817, 2004.
37. Jeon, H. J., D. H. Go, S. Choi, K. M. Kim, J. Y. Lee, D. J. Choo, H. O. Yoo, J. M. Kim and J. Kim, "Synthesis of poly(ethylene oxide)-based thermoresponsive block copolymers by RAFT radical polymerization and their uses for preparation of gold nanoparticles" *Colloids and Surfaces A: Physicochemical and Engineering Aspects*, Vol. 317, pp. 496-503, 2008.
38. Nuopponen M. and H. Tenhu, "Gold Nanoparticles Protected with pH and Temperature Sensitive Diblock Copolymers", *Langmuir*, Vol. 23, No. 10, pp. 5352-5357, 2007.
39. Ge, Z., D. Xie, D. Chen, X. Jiang, Y. Zhang, H. Liu and S. Liu, "Stimuli-Responsive Double Hydrophilic Block Copolymer Micelles with Switchable Catalytic Activity", *Macromolecules*, Vol. 40, No. 10, pp. 3538-3546, 2007.
40. Stenzel, M. H., L. Cummins, G. E. Roberts, T. P. Davis, P. Vana and C. Barner-Kowollik, "Xanthate Mediated Living Polymerization of Vinyl Acetate: A Systematic Variation in MADIX/RAFT Agent Structure", *Macromolecular Chemistry and Physics*, Vol. 204, pp. 1160-1168, 2003.
41. Wakioka, M., K. Y. Baek, T. Ando, M. Kamigaito and M. Sawamoto, "Possibility of Living Radical Polymerization of Vinyl Acetate Catalyzed by Iron(I) Complex", *Macromolecules*, Vol. 35, No. 2, pp. 330-333, 2002.
42. Coote, M. L. and L. Radom, "Substituent Effects in Xanthate-Mediated Polymerization of Vinyl Acetate: Ab Initio Evidence for an Alternative Fragmentation Pathway", *Macromolecules*, Vol. 37, No. 2, pp. 590-596, 2004.



43. Destarac, M., D. Taton, S. Z. Zard, T. Saleh and I. Six, "On the Importance of Xanthate Substituents in the MADIX Process", *ACS Symposium Series*, Vol. 854, pp. 536-550, 2003.
44. Boschmann, D. and P. Vana, "Poly(vinyl acetate) and Poly(vinyl propionate) Star Polymers via Reversible Addition Fragmentation Chain Transfer (RAFT) Polymerization", *Polymer Bulletin*, Vol. 53, pp. 231-242, 2005.
45. Fleet, R., J. B. McLeary, V. Grumel, W. G. Weber, H. Matahwa and R. D. Sanderson, "Preparation of New Multiarmed RAFT Agents for the Mediation of Vinyl Acetate Polymerization", *Macromolecular Symposia*, Vol. 255, pp. 8-19, 2007.
46. Favier, A., C. Barner-Kowollik, T. P. Davis and M. H. Stenzel, "A Detailed On-Line FT/NIR and  $^1\text{H}$  NMR Spectroscopic Investigation into Factors Causing Inhibition in Xanthate-Mediated Vinyl Acetate Polymerization", *Macromolecular Chemistry and Physics*, Vol. 205, pp. 925-936, 2004.
47. Liu, L., C. Wu, J. Zhang, M. Zhang, Y. Liu, X. Wang and G. Fu, "Controlled Polymerization of 2-(Diethylamino)ethyl Methacrylate and its Block Copolymer with N-Isopropylacrylamide by RAFT Polymerization", *Journal of Polymer Science: Part A: Polymer Chemistry*, Vol. 46, pp. 3294-3305, 2008.